Global Banking & Markets

Quantitative Analysis

RBS The Royal Bank of Scotland

April 22, 2010

# The stochastic intrinsic currency volatility framework

## A consistent model of multiple forex rates and their volatilities

The SABR stochastic volatility model is widely used for forex option pricing. Although it is able to reproduce the market's volatility smiles and skews, it introduces inconsistencies because it fails to preserve symmetries inherent between different forex rates. This article solves that problem using concept of intrinsic currency values. To model forex volatility curves, the intrinsic currency framework is extended by allowing the volatility of each intrinsic currency value to be stochastic. This makes the framework more realistic, while preserving all the required forex market symmetries. The result is a model which can simultaneously be calibrated to the volatility smiles of all possible currency pairs under consideration. Consequently, it is more powerful than modelling the volatility curves of each currency pair individually, and offers a methodology for comparing the volatility curves of different currency pairs against each other. One potential application of this is in the pricing of forex options, such as vanilla options on less liquid currency pairs. Given the volatilities of less liquid currencies against e.g. USD, the model could then be used to calculate the volatility smiles of those currencies against all other currencies.

**Correlation of intrinsic currency volatilities with the intrinsic value of JPY**

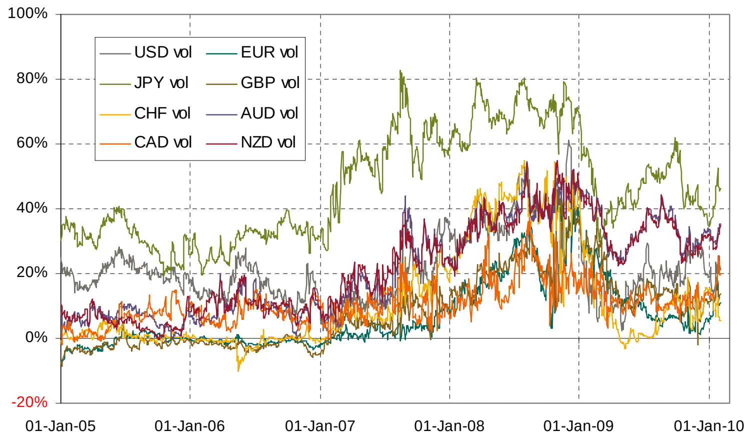


Figure 1: This graph shows that the correlation between intrinsic currency volatilities and the intrinsic value of JPY is usually positive. This means that when the JPY strengthens, all the intrinsic currency volatilities tend to rise. This effect is particularly big for JPY vs JPY volatility, and during 2008 it was significant for all other currency volatilities too.

**Paul Doust**
Global Head of
Quantitative Analysis
+44 (0)20-7085-6015
paul.doust@rbs.com

**Jian Chen**
Quantitative Analyst
+44 (0)20-7085-0135
jian.chen@rbs.com

**www.rbsm.com**

# 1 Introduction

In 2006 RBS introduced the concept of intrinsic currency values[3, 4]. The basic concept is to model forex rates $X_{ij}$ between currency $i$ and currency $j$ as ratios of the intrinsic currency values $X_i$ and $X_j$, so that

$$X_{ij} = \frac{X_i}{X_j} \quad . \tag{1}$$

The idea behind $(1)$ is that $X_i$ and $X_j$ represent the intrinsic value of the individual currencies $i$ and $j$. It is possible to give an interpretation to the intrinsic value of a currency (see e.g. [4]), and such an interpretation can be useful to aid intuition. However, the work presented here does not hinge on the correctness of any particular interpretation. Note that it is not necessary to specify the units of the $X_i$ because they cancel out in the ratio[1]. Although the $X_i$ and their volatilities $\sigma_i$ are not directly observable, various methods can be used to distill information about them from the quantities that are observable in the forex market (see e.g. [5]). The convention where each $X_i$ increases when the currency it represents becomes more valuable is adopted. This implies that $X_{ij}$ is the number of units of currency $j$ corresponding to one unit of currency $i$.

The original work on intrinsic currency values just used a simple log-normal model for the $X_i$. However such a model is naïve because it can not capture the dependence of implied volatilities on option strike. A good model of how implied forex volatilities vary for different strikes is vital to anyone who trades forex options. One approach to this is to use a stochastic volatility model, such as the SABR model which was developed by Hagan, Kumar, Lesniewski and Woodward [1]. For reasons which will be discussed below, a direct application of SABR to forex rates or to intrinsic currency variables leads to an inconsistent model. However, by modifying the SABR stochastic processes it will be shown that a consistent model is possible when applied to the intrinsic currency variables $X_i$ and their volatilities $\sigma_i$. This is the approach that is presented and analysed in this article. One of the main results of this article is a new SABR-style approximation formula for forex option volatilities, written in terms of the parameters of the intrinsic currency framework.

As with the original work on intrinsic currency volatilities[3], the idea is to calibrate the model to a snapshot of implied forex option volatilities. The original work just calibrated to the at-the-money volatilities, but so as to incorporate the full skew or smile, the aim of this article will be to calibrate to the 25-delta risk-reversals and 25-delta market strangles as well. Figure 1 on the front page illustrates the kind of results that are obtained when the model is calibrated historically to market data going back to 2005. In the forex option markets for currency pairs involving JPY, the risk-reversal is usually such that the volatility of out-of-the-money JPY calls is higher than the at-the-money volatility. Figure 1 shows that in the stochastic intrinsic currency volatility framework, the risk-reversal in favour of JPY calls manifests itself as positive correlations between the intrinsic value of JPY and all the intrinsic currency volatilities.

One possible use for the model is in the pricing of forex derivatives. With vanilla forex options on less liquid currency pairs, it can be hard to determine reliable at-the-money volatilities, and even harder to get prices for out-of-the-money options and risk-reversals. However, the methodology presented below can take whatever market data is available and produce the volatilities for all strikes and currency pairs that are most consistent with that market data. Another potential application of the model is in pricing average rate or basket options. For example, for an option on a basket of currencies against one other currency, models are typically calibrated to the volatility curves for all the currencies in the basket against the other currency. However, the stochastic intrinsic currency volatility framework also includes a calibration to the volatility curves of all the currency pairs between the currencies in the basket, so it should produce a more accurate result.

The layout of this article is as follows. Section 2 is a brief summary of the mathematics involved, including the new SABR-style approximation formula for forex option volatilities. Section 3 tests the accuracy of the new SABR-style approximation when compared to the true underlying model, which is calculated using Monte Carlo techniques. Section 4 discusses the principles behind fitting the model to market data, including a discussion of

[1] However, using the intepretation of intrinsic currency values from [4], it is possible to understand the $X_i$ as measuring currency values in 'goods'. In other words, one can imagine there exists a universal basket of goods defined implicitly by the forex market, which can be used to measure the value of currencies all over the world.

the principle of maximum information entropy that is used to help calibrate the model, and describes different ways of adapting the model parameters to achieve stable results. Section 5 shows what a typical calibration to market data looks like, discusses the quality of the fits to market data, and shows what values all the parameters have taken historically. Section 6 briefly discusses potential applications of this model, and section 7 is the conclusion.

The bulk of the mathematics is in the appendix starting on page 35. Appendix A discusses the problems encountered when applying SABR directly to the forex market, and presents a symmetrised SABR model where a forex rate and its reciprocal both follow the same stochastic process. Although this is a solution to the consistency problem for any individual forex rate, using this methodology cross rates will still follow processes with a different form. Appendix B justifies the stochastic processes of the Stochastic Intrinsic Currency Volatility Framework, which are introduced in section 2. Appendix C contains the full derivation of the new SABR-style approximation formula for forex option volatilities, which is presented in section 2. Finally, appendix D describes the details of the conjugate gradient methodology that is used to fit the model to market data, and which was used to produce the results shown in section 5.

# 2 Summary of mathematical results

The original Black-Scholes option pricing models[6, 7] introduced a volatility parameter $\sigma$ which was assumed to be constant. The model is easily extended to the case where volatility is a deterministic function of time, but market behaviour is inconsistent with deterministic volatility so in recent years models which assume that volatility is stochastic have become popular. The SABR model [1] is one such model. In the SABR model, the $\beta$ parameter controls whether changes in the quantity being modelled are normally distributed, log-normally distributed, or something in between. However, in the context of forex rates only a log-normal model makes sense, because the same kind of behaviour will be observed whether a forex rate is expressed as the value of 1 domestic currency unit or the value of 100 domestic currency units, and because the inverse forex rate provides an equally valid description of the market.

Using $F$ to denote the underlying quantity being modelled, the stochastic differential equations for the log-normal SABR model can be written

$$\frac{dF}{F} = \varepsilon\sigma dW_1 \quad , \tag{2}$$

$$\frac{d\sigma}{\sigma} = \varepsilon\upsilon dW_2 \quad , \tag{3}$$

$$dW_1 dW_2 = \rho dt \quad , \tag{4}$$

where $\varepsilon\sigma$ is the volatility of $F$, where $\varepsilon\upsilon$ is the volatility of $\sigma$, and where $\varepsilon$ is a small quantity which will be used to construct a perturbation expansion. The main result of Hagan et al [1] is an approximation formula for the implied Black-Scholes option volatilities $\sigma_B$ of the option prices that this model produces, which is derived up to and including $O\left(\varepsilon^2\right)$, assuming that $\varepsilon$ is small, and assuming that $\sigma$ and $\upsilon$ are $O\left(1\right)$. For the case of the log-normal SABR model, the approximation formula for $\sigma_B$ is

$$\sigma_B = \varepsilon\sigma \frac{z}{\tilde{x}\left(z\right)}\left(1 + \left(\frac{\rho\sigma\upsilon}{4} + \frac{2-3\rho^2}{24}\upsilon^2\right)\varepsilon^2\tau_{ex}\right) \ , \quad z = \frac{1}{\varepsilon\sigma}\ln\left(\frac{F}{K}\right) \ , \quad \tilde{x}\left(z\right) = \frac{\ln\left(\frac{\sqrt{1-2\varepsilon\rho\upsilon z+\varepsilon^2\upsilon^2 z^2}-\rho+\varepsilon\upsilon z}{1-\rho}\right)}{\varepsilon\upsilon} , \tag{5}$$

where $\tau_{ex}$ is the time to option expiry and $K$ is the strike of the option. To use $(5)$ one chooses $\varepsilon = 1$, which is justified in terms of the assumptions made to derive $(5)$ as long as $\sigma$ and $\upsilon$ are small.

When modelling any forex rate $X_{ij}$, it is important to realise that all aspects of the market could be described equally well by using the inverse forex rate $X_{ij}^{-1}$. Similarly, given two forex rates with a common currency such as EUR/GBP and GBP/USD, then their product is EUR/USD which is another forex rate. So a basic condition for any forex market model is that it should be consistent with respect to all these operations. The problem when using $(2)$-$(4)$ to model forex rates is that if $X_{ij}$ follows a SABR process then $X_{ij}^{-1}$ follows a different process, which is an inconsistency. Appendix A below discusses this in more detail, and shows that a symmetrised SABR is possible where $X_{ij}$ and $X_{ij}^{-1}$ both follow stochastic processes of the same form. However, even this symmetrised SABR is inconsistent when considering the product of forex rates such as EUR/GBP and GBP/USD, so to achieve full consistency another approach is required.

Suppose that there are $N$ currencies, so there are $N$ intrinsic currency values $X_i$ and $N$ intrinsic currency volatilities $\varepsilon\sigma_i$ where $1 \leqslant i \leqslant N$. To model the value of any financial contract then a currency must be chosen for measuring value, so without loss of generality choose currency $k$ where $1 \leqslant k \leqslant N$. With this choice of valuation currency (also known as numéraire) and its associated risk-neutral measure, appendix B then shows that the stochastic processes

$$\frac{dX_i}{X_i} = \left(\tilde{\lambda} - r_i + \varepsilon^2 \rho_{ik}\sigma_i\sigma_k\right) dt + \varepsilon\sigma_i dW_i \tag{6}$$

and
$$\frac{d\sigma_i}{\sigma_i} = \varepsilon^2 \tilde{\rho}_{ik}\upsilon_i\sigma_k dt + \varepsilon\upsilon_i dZ_i \tag{7}$$

produce the usual risk-neutral processes for all the forex rates $X_{ij}$, as well as having the right symmetries in terms of change of numéraire currency. Consequently, these processes for $X_i$ imply all the required symmetries for the forex rates $X_{ij}$ with respect to the inverse and product operations mentioned above. In $(6)$ and $(7)$, $\tilde{\lambda}$ is a variable which is the same for all the $X_i$, $r_i$ is the risk-free interest rate in currency $i$, $\varepsilon\upsilon_i$ is the volatility of $\sigma_i$, and $dW_i$ and $dZ_i$ are Weiner processes. Define the column vectors $\mathbf{dW}$ and $\mathbf{dZ}$ whose the elements are $dW_i$ and $dZ_i$. Then write the correlation matrix between the stochastic processes as

$$\begin{pmatrix} \mathbf{dW} \\ \mathbf{dZ} \end{pmatrix} \begin{pmatrix} \mathbf{dW}' & \mathbf{dZ}' \end{pmatrix} = \begin{pmatrix} \boldsymbol{\rho} & \tilde{\boldsymbol{\rho}}' \\ \tilde{\boldsymbol{\rho}} & \mathbf{r} \end{pmatrix} dt \quad , \tag{8}$$

where $'$ denotes matrix and vector transpose. Examples of this matrix involving eight currencies are shown below in tables 4 and 7. Figure 1 on the front page showed the historical values of a column from the matrix $\tilde{\boldsymbol{\rho}}$.

Looking at $(6)$-$(8)$, the stochastic intrinsic currency volatility framework has the following variables:

- $N$ intrinsic currency volatilities $\sigma_i$. These variables were present in the original work[3], however now they are stochastic quantities.
- An $N \times N$ symmetric matrix $\boldsymbol{\rho}$ of correlations between the $N$ intrinsic currency values $X_i$. Again, these correlations were present in the original work.
- $N$ volatility of volatility variables $\upsilon_i$. It turns out that there is a significant tenor dependency to the $\upsilon_i$ in the forex option market, so that the 1 month $\upsilon_i$ variables are typically around 200%-230%, with the 1 year variables around 65%-85%. This will be discussed in more detail below.
- An $N \times N$ symmetric matrix of correlations $\mathbf{r}$ between the $N$ intrinsic currency volatilities $\sigma_i$. These are typically all positive, because when there is increased or decreased uncertainty in the market in connection with one currency, that means that there is likely to be increased or decreased uncertainties in the market in connection with other currencies too.
- An $N \times N$ matrix of $\tilde{\boldsymbol{\rho}}$ between all the intrinsic currency values $X_i$ and all the intrinsic currency volatilities $\sigma_i$. As mentioned briefly above, these variables are closely connected with the risk reversals.

Given $(6)$-$(8)$, appendix C uses similar techniques to the ones used in Hagan et al [1] to solve the model up to and including $O\left(\varepsilon^2\right)$, hence producing a new formula for $\sigma_B$ in terms of the parameters of the stochastic intrinsic currency volatility framework. Although the framework is defined for multiple currencies simultaneously, forex options only relate to a pair of currencies, so to discuss the results it is sufficient to specialise to forex options between currency $i$ and currency $j$.

From the stochastic process for $X_{ij}$ (see $(38)$ in appendix B), the instantaneous volatility $\sigma_{ij}$ of $X_{ij}$ is given by

$$\sigma_{ij} = \sigma\left(\sigma_i, \sigma_j\right) = \sqrt{\sigma_i^2 - 2\rho_{ij}\sigma_i\sigma_j + \sigma_j^2} \quad . \tag{9}$$

Both $\sigma_{ij}$ and its derivatives

$$\frac{\partial\sigma_{ij}}{\partial\sigma_i} = \frac{\sigma_i - \rho_{ij}\sigma_j}{\sigma_{ij}} \quad , \quad \frac{\partial\sigma_{ij}}{\partial\sigma_j} = \frac{\sigma_j - \rho_{ij}\sigma_i}{\sigma_{ij}} \tag{10}$$

will be important in what follows. Note that there is often little advantage in substituting the expressions in $(10)$ for the derivatives of $\sigma_{ij}$, so these derivatives are usually left unexpanded.

The main result which is derived in appendix C is a formula for the vanilla forex option volatility $\sigma_B$ in terms of the parameters of the stochastic intrinsic currency volatility framework. To write down this formula, let $X_{ij}^F$ be the forward rate of the spot forex rate $X_{ij}$, and use $K$ to denote the strike of a forex option, where $K$ has the same units as $X_{ij}^F$. Then appendix C shows that the implied volatility approximation formula for the stochastic intrinsic currency volatility model defined by $(6)$-$(8)$ is given by

$$\sigma_B = \varepsilon\sigma_{ij}\frac{z}{x(z)}\frac{1}{\sqrt{1-\frac{\varepsilon^2}{12}\left(8\kappa_1+\sigma_{ij}^2\left(\frac{z}{x(z)}\right)^2\right)\tau_{ex}}} \quad , \tag{11}$$

where

$$z = \frac{1}{\varepsilon\sigma_{ij}}\ln\left(\frac{X_{ij}^F}{K}\right) \tag{12}$$

$$x(z,\sigma_i,\sigma_j) = \int_0^z \frac{d\zeta}{J(\xi,\sigma_i,\sigma_j)}$$

$$= \frac{1}{\varepsilon\sqrt{a_2+a_5}}\ln\left(\frac{\sqrt{1-2\varepsilon a_1 z+\varepsilon^2(a_2+a_5)z^2}-\frac{a_1}{\sqrt{a_2+a_5}}+\varepsilon\sqrt{a_2+a_5}z}{1-\frac{a_1}{\sqrt{a_2+a_5}}}\right)+O\left(\varepsilon^3\right) \quad , \tag{13}$$

$$J(z,\sigma_i,\sigma_j) = \sqrt{1-2\varepsilon a_1 z+\varepsilon^2(a_2+a_5)z^2+O(\varepsilon^3)} \quad , \tag{14}$$

$$\kappa_1 = \frac{1}{4}a_2-\frac{3}{8}a_1^2-\frac{1}{8}\sigma_{ij}^2+\frac{3}{4}(a_1\sigma_{ij}+2a_3+2a_4)-\frac{1}{2}a_5 \quad , \tag{15}$$

and where the functions $a_1$, $a_2$, $a_3$, $a_4$ and $a_5$ are given by

$$a_1 = a_1(\sigma_i,\sigma_j) = \frac{1}{\sigma_{ij}}\left(\sigma_i\zeta_i\frac{\partial\sigma_{ij}}{\partial\sigma_i}-\sigma_j\zeta_j\frac{\partial\sigma_{ij}}{\partial\sigma_j}\right) \quad , \tag{16}$$

$$a_2 = a_2(\sigma_i,\sigma_j) = \frac{\upsilon_i^2\sigma_i^2}{\sigma_{ij}^2}\left(\frac{\partial\sigma_{ij}}{\partial\sigma_i}\right)^2+\frac{2r_{ij}\upsilon_i\upsilon_j\sigma_i\sigma_j}{\sigma_{ij}^2}\frac{\partial\sigma_{ij}}{\partial\sigma_i}\frac{\partial\sigma_{ij}}{\partial\sigma_j}+\frac{\upsilon_j^2\sigma_j^2}{\sigma_{ij}^2}\left(\frac{\partial\sigma_{ij}}{\partial\sigma_j}\right)^2 \quad , \tag{17}$$

$$a_3 = a_3(\sigma_i,\sigma_j) = \tilde{\rho}_{ij}\frac{\upsilon_i\sigma_i\sigma_j}{\sigma_{ij}}\frac{\partial\sigma_{ij}}{\partial\sigma_i}+\tilde{\rho}_{jj}\frac{\upsilon_j\sigma_j^2}{\sigma_{ij}}\frac{\partial\sigma_{ij}}{\partial\sigma_j} \quad , \tag{18}$$

$$a_4 = a_4(\sigma_i,\sigma_j) = \frac{\sigma_i^2\sigma_j^2}{\sigma_{ij}^4}\left(1-\rho_{ij}^2\right)\left(\frac{1}{2}\upsilon_i^2-r_{ij}\upsilon_i\upsilon_j+\frac{1}{2}\upsilon_j^2\right) \tag{19}$$

$$\begin{aligned} a_5 = a_5(\sigma_i,\sigma_j) = {} & \frac{2\sigma_i^2}{\sigma_{ij}^2}\zeta_i^2-\frac{\rho_{ij}\sigma_i\sigma_j}{\sigma_{ij}^2}(\zeta_i-\zeta_j)^2+\frac{2\sigma_j^2}{\sigma_{ij}^2}\zeta_j^2-3a_1^2 \\ & +\frac{\sigma_i}{\sigma_{ij}^2}(\sigma_i\upsilon_i\tilde{\rho}_{ii}\zeta_i+\sigma_j\upsilon_i\tilde{\rho}_{ij}\zeta_j)\frac{\partial\sigma_{ij}}{\partial\sigma_i}+\frac{\sigma_j}{\sigma_{ij}^2}(\sigma_j\upsilon_j\tilde{\rho}_{jj}\zeta_j+\sigma_i\upsilon_j\tilde{\rho}_{ji}\zeta_i)\frac{\partial\sigma_{ij}}{\partial\sigma_j} \quad . \end{aligned} \tag{20}$$

where

$$\zeta_i = \frac{\upsilon_i(\tilde{\rho}_{ii}\sigma_i-\tilde{\rho}_{ij}\sigma_j)}{\sigma_{ij}} \quad , \quad \zeta_j = \frac{\upsilon_j(\tilde{\rho}_{jj}\sigma_j-\tilde{\rho}_{ji}\sigma_i)}{\sigma_{ij}} \quad . \tag{21}$$

To reduce $\sigma_B$ in $(11)$ to a form which looks more like the SABR formula $(5)$, note that

$$x = z+O(\varepsilon) \quad , \tag{22}$$

$$\frac{1}{\sqrt{1-\varepsilon^2\theta}} = 1+\frac{1}{2}\varepsilon^2\theta+O\left(\varepsilon^4\right) \quad . \tag{23}$$

Then coupled with $(15)$, it is straightforward to show that $\sigma_B$ can be written

$$\sigma_B = \varepsilon\sigma_{ij}\frac{z}{x(z)}\left(1+\varepsilon^2\left(\frac{1}{4}(a_1\sigma_{ij}+2a_3+2a_4)-\frac{1}{6}a_5+\frac{2a_2-a_1^2}{24}\right)\tau_{ex}\right) \quad . \tag{24}$$

In this form, when $\sigma_j=\upsilon_j=0$ then $a_1=\upsilon_i\tilde{\rho}_{ii}$, $a_2=\upsilon_i^2$, and $a_3=a_4=a_5=0$, which means that $(24)$ reduces to $(5)$.

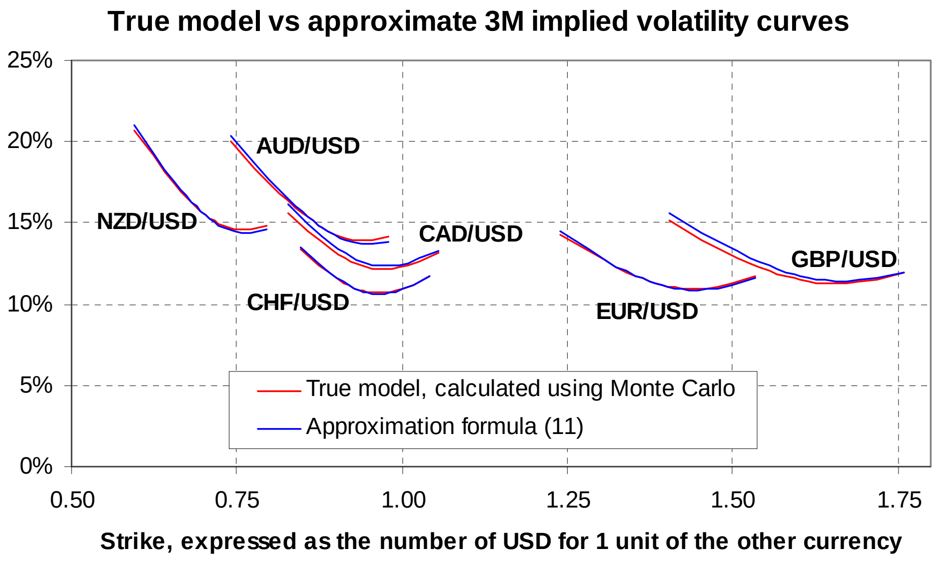


Figure 2: Comparision of the approximation formula $(11)$ to the true model $(6)$-$(8)$ for 3M options for six currencies involving USD. The values of $\sigma_i$, $\upsilon_i$, $\boldsymbol{\rho}$, $\tilde{\boldsymbol{\rho}}$ and $\mathbf{r}$ in tables 3 and 4 were used. Note that these graphs are NOT comparing the model to the market, instead they're testing the accuracy of the approximation. The root mean square error accross the 6 curves is 0.19%.

Sections 4 and 5 will discuss fitting this model to market data, and present results going back to the start of 2005. However before fitting to market data, an important question is whether $(11)$ is a good approximation to the option volatilities of the underlying model $(6)$-$(8)$, so this will be addressed in the following section.

# 3 Comparison of approximation formula $(11)$ to the underlying model $(6)$-$(8)$

Irrespective of whether the values of $\sigma_i$, $\upsilon_i$, $\boldsymbol{\rho}$, $\mathbf{r}$ and $\tilde{\boldsymbol{\rho}}$ produce implied volatility curves which match the market, given a set of these values then Monte-Carlo simulations can be done to see how closely the implied volatility curves defined by the approximation $(11)$ match the model defined by $(6)$-$(8)$. Tables 3 and 4, which will be discussed in section 5.1 below, give some typical values for the parameters $\sigma_i$, $\upsilon_i$, $\boldsymbol{\rho}$, $\mathbf{r}$ and $\tilde{\boldsymbol{\rho}}$, so for the purposes of this comparison the values from those tables were used. Figures 2, 3 and 4 compare the approximation formula $(11)$ to the implied volatility curves of the true model, calculated using Monte-Carlo simulations with 20 time steps per month and 100,000 simulations. The figures show that $(11)$ gives a reasonable fit to the underlying model. Figures 2 and 3 focus on 3M options for currency pairs involving USD and JPY, and figure 4 compares the approximation to the true model for different tenors of EUR/USD. The root mean square error across all the 3M volatility curves for the 13 currency pairs involving USD and JPY is around 0.29% in volatility. However, in the interest rate option markets for options of the same tenor, the implied volatility approximation formula of Hagan et al [1] works better when compared to the true model.

The reason that the implied volatility approximation formula of Hagan et al [1] performs better in the interest rate option markets than $(11)$ does in the forex option market is because the volatility of volatility parameters $\upsilon_i$ are much bigger in the forex option market, compared to the interest rate option markets. In the interest rate option markets, the $\upsilon_i$ are of the order of $50\%$ where in table 3 the $\upsilon_i$ for three months is $138\%$. Setting all the $\upsilon_i = 50\%$ and taking all other values from tables 3 and 4, then $(11)$ matches the Monte-Carlo results with a root mean square error of only 0.024% in volatility. This suggests that $(11)$ works as well as the implied volatility approximation formula of Hagan et al [1] when the volatility of volatility parameters are of the same order of magnitude.

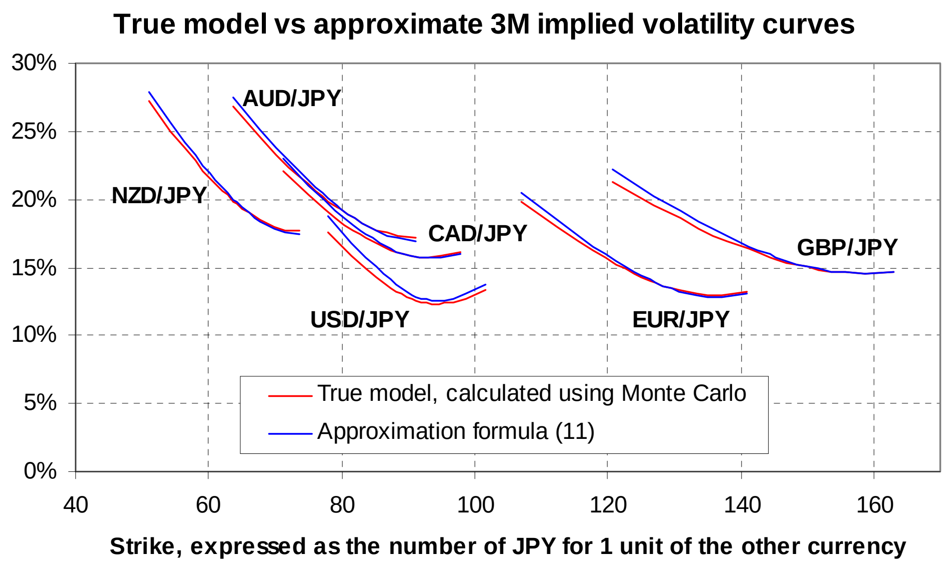


Figure 3: Comparision of the approximation formula $(11)$ to the true model $(6)$-$(8)$ for 3M options for six currencies involving JPY. The values of $\sigma_i$, $\upsilon_i$, $\boldsymbol{\rho}$, $\tilde{\boldsymbol{\rho}}$ and $\mathbf{r}$ in tables 3 and 4 were used. Note that these graphs are NOT comparing the model to the market, instead they're testing the accuracy of the approximation. The root mean square error across the 6 curves is 0.37%

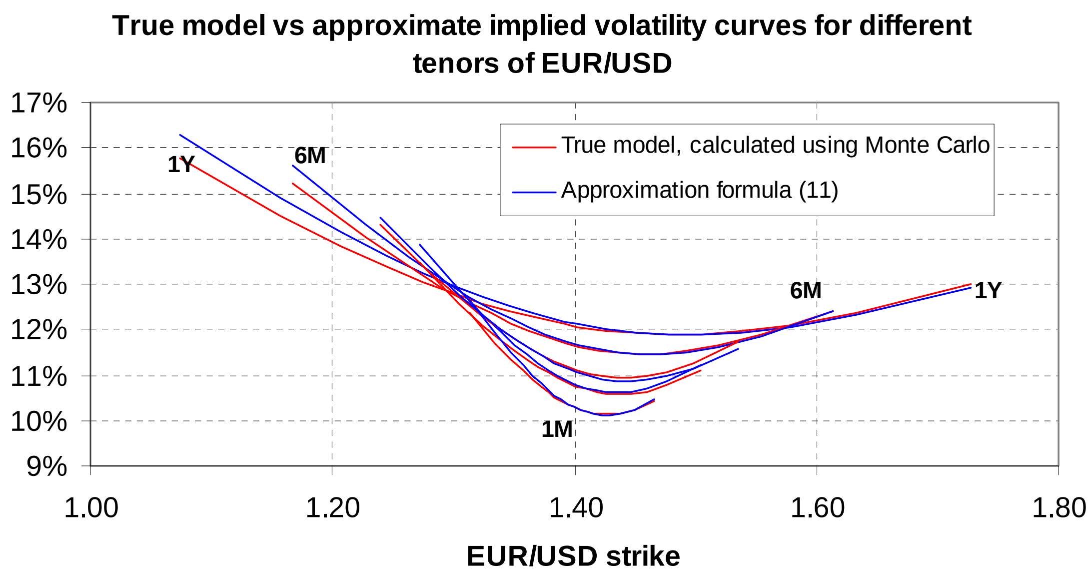


Figure 4: Comparision of the approximation formula $(11)$ to the true model $(6)$-$(8)$ for EUR/USD with tenors 1M, 2M, 3M, 6M and 1Y. The values of $\sigma_i$, $\upsilon_i$, $\boldsymbol{\rho}$, $\tilde{\boldsymbol{\rho}}$ and $\mathbf{r}$ in tables 3 and 4 were used. Note that these graphs are NOT comparing the model to the market, instead they're testing the accuracy of the approximation. The root mean square error across the 1M curve is 0.11%, and across the 1Y curve is 0.19%.

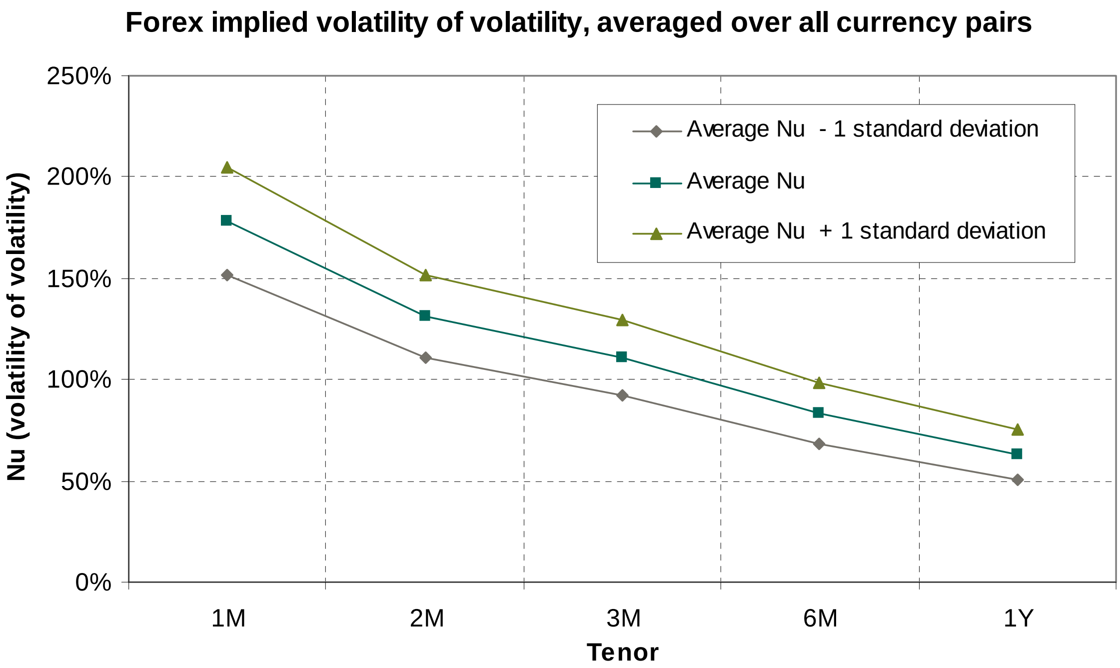


Figure 5: This figure shows that when fitting the standard SABR model $(5)$ directly to currency pair volatiltiy data, the $\upsilon$ parameter exhibits significant tenor dependency. The averages shown above, and the corresponding standard deviations, are over all currency pairs and over all days in the data set that was used in section 5.

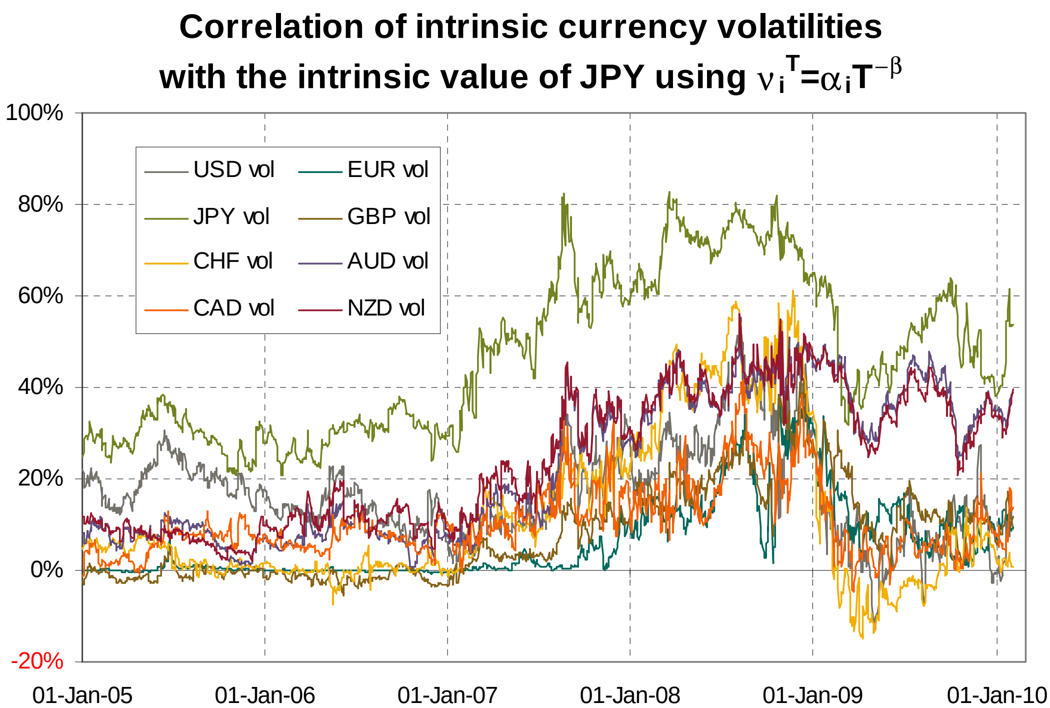


Figure 6: This graph shows the correlation between the intrinsic currency volatilities $\sigma_i$ and the intrinsic value of JPY, calculated using $\upsilon_i^T = \alpha_i T^{-\beta}$. Figure 1 shows what the results are using $\upsilon_i^T = \upsilon^T$. Qualitatively, the two graphs looks very similar.

# 4 Fitting the model to market data

As in [5], the maximum entropy principle will be used to help fit market data to the variables of the stochastic intrinsic currency volatility model, i.e. to $\sigma_i$, $\upsilon_i$, $\boldsymbol{\rho}$, $\mathbf{r}$ and $\tilde{\boldsymbol{\rho}}$, which together define the covariance matrix between all the $X_i$ and the $\sigma_i$. Using a principle like maximum entropy is necessary because the intrinsic currency framework contains an unobservable degree of freedom, which is related to the overall scale of the intrinsic currency values that can not be determined. Additionally the correlation matrix $(8)$ contains a lot of parameters, and some combinations of these parameters have a relatively small effect on the quantities that can be compared with market data, so maximum entropy helps stabilise the correlation matrix. According to information theory, if nothing is known about a distribution except that it belongs to a certain class, then the distribution with the largest information entropy should be chosen as the default. The motivation is first that maximising entropy minimises the amount of prior information built into the distribution, and second that many physical systems tend to move towards maximum entropy configurations over time. Another way of looking at this is that by choosing the distribution with the maximum entropy that is consistent with the market data, the most uninformative distribution possible is being chosen. To choose a distribution with lower entropy would be to assume information that we do not possess; and to choose one with a higher entropy would violate the constraints of the information that we do possess. Thus the maximum entropy distribution is the best choice.

The different parameters $\sigma_i$, $\upsilon_i$, $\boldsymbol{\rho}$, $\mathbf{r}$ and $\tilde{\boldsymbol{\rho}}$ were discussed above on page 4. If the objective is just to fit the model to a snapshot of market data for a single tenor, then values of $\sigma_i$, $\upsilon_i$, $\boldsymbol{\rho}$, $\mathbf{r}$ and $\tilde{\boldsymbol{\rho}}$ can usually be found so that the model fits the data almost perfectly. This is because there are more parameters to fit than market data points.

For example, suppose there are 8 currencies. There are 28 possible currency pairs involving a set of 8 currencies, and each currency pair has 3 pieces of market data, namely the at-the-money volatility, the risk reversal and the market strangle. Hence there are 84 pieces of market data for a single tenor. However there are 8 parameters $\sigma_i$, 8 parameters $\upsilon_i$, and 120 parameters in the correlation matrices $\boldsymbol{\rho}$, $\mathbf{r}$ and $\tilde{\boldsymbol{\rho}}$, making a total of 136 data points to fit. Even though there are more parameters to fit than market data, the maximum entropy concept discussed above can be used to soak up the spare degrees of freedom, so the fitting problem is still well posed. However, if the snapshot of market data contains data for multiple tenors, and if separate fits are done to the data for each tenor, then the calibration results are unstable in the sense that there are large variations in e.g. the correlation matrices from one tenor to the next and from one day to the next. In theory the model should be time-homogenous, so that each of the variables $\upsilon_i$, $\boldsymbol{\rho}$, $\mathbf{r}$ and $\tilde{\boldsymbol{\rho}}$ are fixed throughout time, and with the $\sigma_i$ evolving from their initial values leading to option prices for all strikes and tenors. Although that does not work in practice, the most plausible implementation of the model will be the one that gets as close as possible to that ideal.

In the previous work [3, 5] with the log-normal model, the fit to multiple tenors was done by allowing the $\sigma_i$ to be tenor dependent, but keeping the correlation matrix $\boldsymbol{\rho}$ tenor independent. This usually produced a reasonably good fit for the at-the-money volatilities. Having determined the tenor-independent correlation matrix, adding a small tenor dependence to the correlations allowed the model to fit the market data exactly. For the stochastic intrinsic currency volatility model, a natural extension of this methodology would be to have tenor dependent $\sigma_i$ and $\upsilon_i$, denoted $\sigma_i^T$ and $\upsilon_i^T$, and tenor independent $\boldsymbol{\rho}$, $\mathbf{r}$ and $\tilde{\boldsymbol{\rho}}$. However, it turns out that the market data doesn't have sufficiently strong traction on the $\upsilon_i^T$ to make this model stable, and if this is attempted then implausible variations in $\upsilon_i^T$ are seen from one tenor to the next and from one day to the next.

Various solutions to the problem of unstable $\upsilon_i^T$ are possible. One possibility is to make $\upsilon_i^T$ currency independent, so that for a particular tenor $T$ all currencies have the same volatility of volatility, i.e.

$$\upsilon_i^T = \upsilon^T \quad . \tag{25}$$

This choice is motivated by the fact that when the market data is fitted to the SABR model[2] $(5)$ for each currency pair individually, the $\upsilon$ parameter shows more dependence on the tenor than dependence on the currency pair.

[2] NB: the symmetrised SABR of appendix A can also be used.

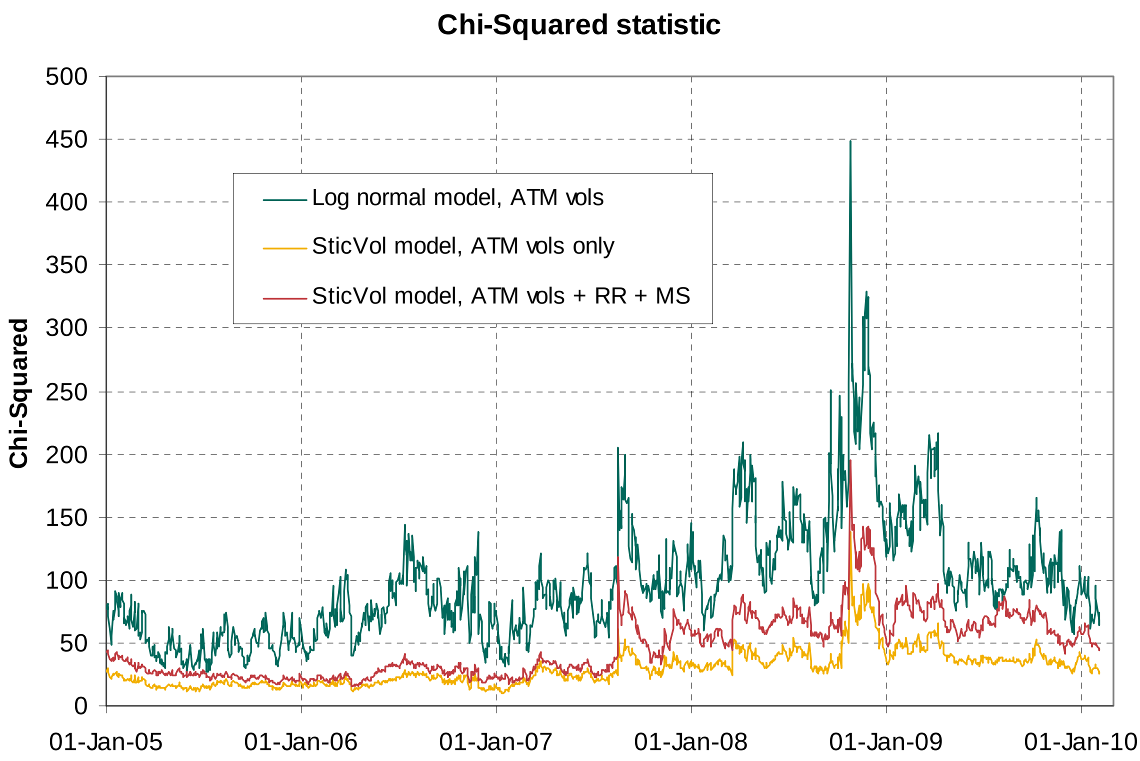


Figure 7: See sub-section 5.2. Using the fit methodology described in appendix D, the Stochastic Intrinsic Currency Volatility Model ("SticVol model") using $\upsilon_i^T = \upsilon^T$ consistently fits the at-the-money vols better than the log-normal model did in the previous work. Note that where the original model only fits the ATM vols, the SticVol model is fitting the risk reversals and market strangles as well.

This is illustrated in figure 5, which shows $\upsilon$ averaged over all currency pairs and all dates, having fitted the market data from section 5 to equation $(5)$.

Instead of $\upsilon_i^T = \upsilon^T$, another possibility is

$$\upsilon_i^T = \alpha_i T^{-\beta} \quad , \text{ or } \quad \upsilon_i^T = \alpha_i T^{-\beta_i} \tag{26}$$

so that $\upsilon_i^T$ is parameterised by currency dependent variables $\alpha_i$ and either a currency independent exponent $\beta$ or a currency dependent exponents $\beta_i$. This choice is motivated by the fact that when using the $\upsilon_i^T = \upsilon^T$ model, on each day the resulting $\upsilon^T$ can be modelled reasonably well by writing $\upsilon^T = \alpha T^{-\beta}$. This will be discussed in more detail in sub-section 5.3 in conjunction with figure 15 below. However, although both these models work reasonably well in normal market conditions, instabilities can arise when the market moves into an excited state, so this article focusses on $\upsilon_i^T = \upsilon^T$ which is more consistently reliable.

Note that a lot of the results produced by the different models are qualitatively very similar. For example, figure 1 on the front page was calculated using $\upsilon_i^T = \upsilon^T$, whereas figure 6 was calculated using $\upsilon_i^T = \alpha_i T^{-\beta}$. Both figures share many of the same characteristics.

# 5 Tables and graphs of calibration results

To analyse how this model works in practice, data was taken from the forex option market for all currency pairs that can be constructed from the 8 currencies USD, EUR, JPY, GBP, CHF, AUD, CAD, NZD. For each currency pair on each date, a snapshot of the at-the-money volatilities, risk-reversals and market strangles was taken for 1M, 2M, 3M, 6M and 1Y tenors. All the details about how the model was fitted to a snapshot of market data are

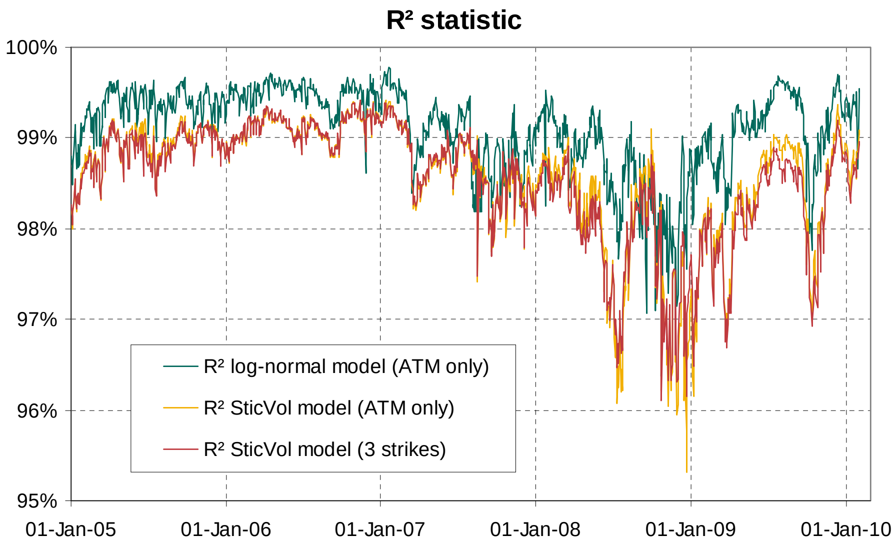


Figure 8: This figure shows the $R^2$ statistic for the fit calculated using $\upsilon_i^T = \upsilon^T$. To define a full $R^2$ statistic for the Stochastic Intrinsic Currency Volatilty ("SticVol") model, three strikes were used, namely the at-the-money strike, and the 25-delta strike on each side of at-the money. However, this 3-strike $R^2$ was virtually the same as just using the at-the-money strike on its own. The conclusion is that the $R^2$ statistic for the log-normal model in the previous work is consistently a bit better than for the SticVol model.

given in appendix D, however the basic idea is to do a least squares fit and minimise the errors between the model and market for each piece of market data. The results presented here are for the $\upsilon_i^T = \upsilon^T$ model $(25)$, which was fitted to the historical data from the start of 2005 up to early February 2010.

The previous section mentioned that with 8 currencies, each tenor contributes 84 data points, so now with 5 tenors there are 420 data points. Counting the number of model parameters, there are 40 parameters for the $\sigma_i^T$, 120 correlation parameters $\boldsymbol{\rho}$, $\mathbf{r}$ and $\tilde{\boldsymbol{\rho}}$, and 5 parameters $\upsilon^T$. Hence there are 165 parameters in total. However, because entropy maximisation is part of the fitting procedure, this means that the effective number of degrees of freedom to fit is less than this.

Even if the goal is just to fit the market data of a single tenor, doing a fit to multiple tenors is still useful because it helps to stabilise the calibration. As mentioned in the previous section, a near perfect fit is usually possible if the goal is to calibrate to a single tenor, because there are more model parameters than data points. However, calibrating to multiple tenors helps ensure that the calibrations are consistent from one tenor to the next. So a good strategy is to calculate a main fit across multiple tenors, and then as a second stage do fits to the individual tenors, using the condition that the model parameters (and in particular the correlation matrices) should be close to the average values calculated in the main fit.

The rest of this section is organised as follows. Sub-section 5.1 shows what a typical main fit looks like on a single day. Sub-section 5.2 assesses the quality of the fit for each date since the start of 2005, comparing the $\chi^2$ and $R^2$ statistics to what was achieved with the previous work[5]. Sub-section 5.3 presents graphs which show what values all the model parameters have taken since the start of 2005. Finally sub-section 5.4 calculates the volatilities and correlations of $X_i$ and $\sigma_i$ from the time series of their historical values, and compares to the values observed in sub-section 5.3.

## 5.1 Illustrative calibration results for a single day.

The market data used to illustrate what a typical fit to multiple tenors looks like was taken on 2-Feb-2010 and is shown in tables 1 and 2. Setting $\varepsilon = 1$, a best fit was done using the methodology described in appendix D to determine the intrinsic currency volatilities $\sigma_i^T$, the volatilities of volatilities $\upsilon_i^T$, and the correlation matrices $\boldsymbol{\rho}$, $\mathbf{r}$

| | Spot FX | At the money volatilities | | | | | Risk reversal (25 delta) | | | | | Market Strangle (25 delta) | | | | |
|---|---|---|---|---|---|---|---|---|---|---|---|---|---|---|---|---|
| | | 1M | 2M | 3M | 6M | 1Y | 1M | 2M | 3M | 6M | 1Y | 1M | 2M | 3M | 6M | 1Y |
| EUR/USD | 1.3948 | 10.40% | 10.85% | 11.15% | 11.80% | 12.25% | 1.22% | 1.25% | 1.28% | 1.31% | 1.37% | 0.21% | 0.25% | 0.31% | 0.38% | 0.42% |
| USD/JPY | 90.6200 | 12.30% | 12.75% | 12.95% | 13.50% | 14.00% | 1.03% | 1.36% | 1.75% | 2.07% | 2.59% | 0.25% | 0.27% | 0.28% | 0.28% | 0.23% |
| GBP/USD | 1.5941 | 10.75% | 11.35% | 11.65% | 12.50% | 13.00% | 1.28% | 1.34% | 1.50% | 1.66% | 1.81% | 0.27% | 0.29% | 0.33% | 0.41% | 0.45% |
| USD/CHF | 1.0559 | 9.90% | 10.35% | 10.65% | 11.30% | 11.75% | -0.51% | -0.50% | -0.56% | -0.61% | -0.65% | 0.23% | 0.27% | 0.34% | 0.41% | 0.45% |
| AUD/USD | 0.8824 | 14.05% | 14.50% | 14.85% | 15.35% | 15.60% | 2.08% | 2.39% | 2.70% | 2.80% | 3.00% | 0.22% | 0.29% | 0.38% | 0.50% | 0.63% |
| USD/CAD | 1.0571 | 11.45% | 12.20% | 12.55% | 13.00% | 13.25% | -1.05% | -1.07% | -1.09% | -1.11% | -1.11% | 0.27% | 0.32% | 0.40% | 0.47% | 0.55% |
| NZD/USD | 0.7081 | 14.50% | 15.25% | 15.60% | 16.30% | 16.75% | 1.74% | 2.17% | 2.61% | 2.97% | 3.26% | 0.22% | 0.31% | 0.41% | 0.55% | 0.65% |
| EUR/JPY | 126.3968 | 13.25% | 13.75% | 14.10% | 14.80% | 15.40% | 1.87% | 2.32% | 2.71% | 3.23% | 3.77% | 0.18% | 0.18% | 0.20% | 0.19% | 0.19% |
| EUR/GBP | 0.8750 | 9.25% | 9.85% | 10.10% | 10.70% | 11.05% | -0.32% | -0.47% | -0.66% | -0.80% | -0.90% | 0.19% | 0.27% | 0.32% | 0.36% | 0.43% |
| EUR/CHF | 1.4728 | 3.90% | 4.00% | 4.10% | 4.20% | 4.40% | 0.16% | 0.32% | 0.47% | 0.78% | 0.99% | 0.19% | 0.26% | 0.32% | 0.34% | 0.34% |
| EUR/AUD | 1.5807 | 10.25% | 10.80% | 11.10% | 11.60% | 12.05% | -0.80% | -1.04% | -1.26% | -1.49% | -1.58% | 0.23% | 0.29% | 0.35% | 0.44% | 0.52% |
| EUR/CAD | 1.4744 | 10.35% | 10.75% | 11.10% | 11.50% | 11.80% | 0.33% | 0.33% | 0.34% | 0.35% | 0.38% | 0.31% | 0.37% | 0.43% | 0.47% | 0.53% |
| EUR/NZD | 1.9698 | 10.30% | 10.90% | 11.25% | 12.05% | 12.50% | -1.05% | -1.36% | -1.66% | -1.95% | -2.22% | 0.26% | 0.33% | 0.39% | 0.52% | 0.60% |
| GBP/JPY | 144.4535 | 14.65% | 15.40% | 16.00% | 16.85% | 17.45% | 2.16% | 2.61% | 3.00% | 3.52% | 4.14% | 0.22% | 0.21% | 0.23% | 0.20% | 0.18% |
| CHF/JPY | 85.8207 | 12.80% | 13.40% | 13.60% | 14.10% | 14.40% | 1.81% | 2.26% | 2.39% | 2.75% | 3.21% | 0.10% | 0.10% | 0.15% | 0.15% | 0.18% |
| AUD/JPY | 79.9631 | 18.85% | 19.50% | 20.00% | 20.50% | 21.50% | 2.43% | 3.35% | 4.18% | 5.12% | 6.59% | 0.15% | 0.14% | 0.14% | 0.12% | -0.23% |
| CAD/JPY | 85.7251 | 15.75% | 16.25% | 16.50% | 17.15% | 17.75% | 1.94% | 2.42% | 2.78% | 3.31% | 3.77% | 0.22% | 0.26% | 0.26% | 0.24% | 0.24% |
| NZD/JPY | 64.1680 | 19.35% | 20.00% | 20.50% | 21.00% | 22.00% | 2.36% | 3.30% | 4.13% | 5.08% | 6.57% | 0.16% | 0.15% | 0.15% | 0.13% | -0.22% |
| GBP/CHF | 1.6832 | 9.65% | 10.27% | 10.52% | 11.12% | 11.45% | 0.55% | 0.71% | 0.91% | 1.07% | 1.21% | 0.18% | 0.25% | 0.28% | 0.31% | 0.34% |
| GBP/AUD | 1.8065 | 12.75% | 13.05% | 13.30% | 13.50% | 13.85% | -0.73% | -0.78% | -1.09% | -1.13% | -1.16% | 0.27% | 0.34% | 0.40% | 0.50% | 0.57% |
| GBP/CAD | 1.6851 | 11.85% | 12.30% | 12.65% | 13.00% | 13.30% | 0.52% | 0.53% | 0.53% | 0.55% | 0.58% | 0.35% | 0.41% | 0.46% | 0.50% | 0.56% |
| GBP/NZD | 2.2512 | 12.85% | 13.30% | 13.55% | 14.20% | 14.65% | -0.25% | -0.56% | -0.84% | -1.00% | -1.28% | 0.27% | 0.34% | 0.41% | 0.54% | 0.61% |
| AUD/CHF | 0.9317 | 10.70% | 11.30% | 11.85% | 12.85% | 13.30% | 0.74% | 1.00% | 1.22% | 1.48% | 1.92% | 0.26% | 0.30% | 0.35% | 0.39% | 0.37% |
| CAD/CHF | 0.9989 | 10.55% | 11.15% | 11.65% | 12.15% | 12.55% | -0.09% | -0.08% | -0.07% | 0.01% | 0.14% | 0.33% | 0.40% | 0.47% | 0.52% | 0.59% |
| NZD/CHF | 0.7477 | 10.80% | 11.40% | 11.85% | 13.00% | 13.60% | 1.00% | 1.32% | 1.73% | 2.59% | 3.04% | 0.31% | 0.35% | 0.38% | 0.41% | 0.36% |
| AUD/CAD | 0.9328 | 10.75% | 11.00% | 11.25% | 11.45% | 11.50% | 1.51% | 1.70% | 1.91% | 1.91% | 2.02% | 0.18% | 0.24% | 0.32% | 0.43% | 0.51% |
| AUD/NZD | 1.2462 | 7.60% | 7.65% | 7.70% | 7.90% | 8.10% | -0.09% | -0.09% | -0.12% | -0.12% | -0.14% | 0.11% | 0.13% | 0.15% | 0.19% | 0.22% |
| NZD/CAD | 0.7485 | 10.80% | 11.50% | 11.80% | 12.25% | 12.55% | 0.97% | 1.35% | 1.73% | 2.05% | 2.26% | 0.18% | 0.26% | 0.36% | 0.46% | 0.51% |

Table 1: Market data on 2-Feb-2010 for the 28 currency pairs that can be constructed from the 8 currencies USD, EUR, JPY, GBP, CHF, AUD, CAD, NZD. The risk reversals for e.g. USD/JPY are quoted as the vol of JPY calls less the vol of JPY puts. The discount factors for constructing the forward forex rates are given in table 2.

| | Discount factors for constructing forwards | | | | |
|---|---|---|---|---|---|
| | 1M | 2M | 3M | 6M | 1Y |
| AUD | 0.9967591 | 0.9933766 | 0.9899626 | 0.9787474 | 0.9527758 |
| CAD | 0.9997707 | 0.9995240 | 0.9993084 | 0.9978284 | 0.9900307 |
| CHF | 0.9999571 | 0.9999640 | 0.9998982 | 0.9992974 | 0.9950770 |
| EUR | 0.9997357 | 0.9994520 | 0.9991335 | 0.9972597 | 0.9892359 |
| GBP | 0.9995743 | 0.9991424 | 0.9987009 | 0.9966632 | 0.9885727 |
| JPY | 0.9998993 | 0.9998347 | 0.9997303 | 0.9990824 | 0.9958563 |
| NZD | 0.9977166 | 0.9953509 | 0.9929622 | 0.9843366 | 0.9609446 |
| USD | 0.9997975 | 0.9996038 | 0.9993680 | 0.9980889 | 0.9916011 |

Table 2: Discount factors on 2-Feb-2010 for USD, EUR, JPY, GBP, CHF, AUD, CAD, NZD. The data in this table was used to constuct the forward forex rates, for use in conjunction with table 1.

| | Intrinsic currency volatilities | | | | | Intrinsic currency volatility of volatiliites | | | | |
|---|---|---|---|---|---|---|---|---|---|---|
| | 1M | 2M | 3M | 6M | 1Y | 1M | 2M | 3M | 6M | 1Y |
| USD | 8.40% | 8.74% | 8.89% | 9.29% | 9.50% | 200.45% | 161.46% | 138.00% | 103.37% | 75.14% |
| EUR | 3.49% | 3.60% | 3.71% | 3.93% | 4.21% | 200.45% | 161.46% | 138.00% | 103.37% | 75.14% |
| JPY | 11.96% | 12.09% | 12.31% | 12.62% | 13.04% | 200.45% | 161.46% | 138.00% | 103.37% | 75.14% |
| GBP | 8.09% | 8.40% | 8.60% | 9.07% | 9.28% | 200.45% | 161.46% | 138.00% | 103.37% | 75.14% |
| CHF | 3.34% | 3.21% | 3.32% | 3.37% | 3.58% | 200.45% | 161.46% | 138.00% | 103.37% | 75.14% |
| AUD | 9.76% | 9.81% | 9.99% | 10.14% | 10.31% | 200.45% | 161.46% | 138.00% | 103.37% | 75.14% |
| CAD | 8.98% | 9.38% | 9.36% | 9.47% | 9.40% | 200.45% | 161.46% | 138.00% | 103.37% | 75.14% |
| NZD | 10.14% | 9.76% | 10.28% | 10.70% | 11.09% | 200.45% | 161.46% | 138.00% | 103.37% | 75.14% |

Table 3: Calibration results for the $\sigma_i^T$ and $\upsilon_i^T$ on 2-Feb-2010 using the model where $\upsilon_i^T = \upsilon^T$.

| | $X_{USD}$ | $X_{EUR}$ | $X_{JPY}$ | $X_{GBP}$ | $X_{CHF}$ | $X_{AUD}$ | $X_{CAD}$ | $X_{NZD}$ | $\sigma_{USD}$ | $\sigma_{EUR}$ | $\sigma_{JPY}$ | $\sigma_{GBP}$ | $\sigma_{CHF}$ | $\sigma_{AUD}$ | $\sigma_{CAD}$ | $\sigma_{NZD}$ |
|---|---|---|---|---|---|---|---|---|---|---|---|---|---|---|---|---|
| $X_{USD}$ | 1 | -0.31 | 0.46 | 0.28 | -0.23 | -0.10 | 0.25 | -0.17 | **0.17** | 0.18 | 0.20 | 0.07 | 0.01 | 0.26 | 0.13 | 0.23 |
| $X_{EUR}$ | -0.31 | 1 | -0.20 | -0.07 | 0.53 | -0.01 | -0.15 | 0.02 | -0.13 | **-0.36** | -0.13 | -0.05 | 0.02 | -0.11 | -0.12 | -0.08 |
| $X_{JPY}$ | 0.46 | -0.20 | 1 | 0.03 | -0.08 | -0.44 | -0.03 | -0.47 | 0.21 | 0.12 | **0.45** | 0.14 | 0.05 | 0.36 | 0.20 | 0.34 |
| $X_{GBP}$ | 0.28 | -0.07 | 0.03 | 1 | -0.20 | 0.13 | 0.19 | 0.11 | -0.07 | 0.01 | -0.07 | **-0.24** | 0.03 | 0.03 | 0.06 | 0.01 |
| $X_{CHF}$ | -0.23 | 0.53 | -0.08 | -0.20 | 1 | -0.19 | -0.25 | -0.16 | 0.04 | -0.01 | -0.05 | 0.01 | **-0.12** | -0.02 | -0.04 | 0.01 |
| $X_{AUD}$ | -0.10 | -0.01 | -0.44 | 0.13 | -0.19 | 1 | 0.46 | 0.78 | -0.21 | -0.04 | -0.30 | -0.08 | 0.01 | **-0.36** | -0.19 | -0.37 |
| $X_{CAD}$ | 0.25 | -0.15 | -0.03 | 0.19 | -0.25 | 0.46 | 1 | 0.44 | -0.06 | 0.07 | -0.11 | 0.05 | 0.05 | -0.01 | **-0.03** | -0.04 |
| $X_{NZD}$ | -0.17 | 0.02 | -0.47 | 0.11 | -0.16 | 0.78 | 0.44 | 1 | -0.20 | -0.06 | -0.30 | -0.07 | 0.00 | -0.36 | -0.18 | **-0.38** |
| $\sigma_{USD}$ | **0.17** | -0.13 | 0.21 | -0.07 | 0.04 | -0.21 | -0.06 | -0.20 | 1 | 0.09 | 0.32 | 0.20 | -0.00 | 0.23 | 0.21 | 0.22 |
| $\sigma_{EUR}$ | 0.18 | **-0.36** | 0.12 | 0.01 | -0.01 | -0.04 | 0.07 | -0.06 | 0.09 | 1 | 0.05 | 0.05 | 0.12 | 0.08 | 0.13 | 0.07 |
| $\sigma_{JPY}$ | 0.20 | -0.13 | **0.45** | -0.07 | -0.05 | -0.30 | -0.11 | -0.30 | 0.32 | 0.05 | 1 | 0.09 | -0.01 | 0.18 | 0.12 | 0.17 |
| $\sigma_{GBP}$ | 0.07 | -0.05 | 0.14 | **-0.24** | 0.01 | -0.08 | 0.05 | -0.07 | 0.20 | 0.05 | 0.09 | 1 | 0.01 | 0.12 | 0.20 | 0.12 |
| $\sigma_{CHF}$ | 0.01 | 0.02 | 0.05 | 0.03 | **-0.12** | 0.01 | 0.05 | 0.00 | -0.00 | 0.12 | -0.01 | 0.01 | 1 | 0.04 | 0.11 | 0.03 |
| $\sigma_{AUD}$ | 0.26 | -0.11 | 0.36 | 0.03 | -0.02 | **-0.36** | -0.01 | -0.36 | 0.23 | 0.08 | 0.18 | 0.12 | 0.04 | 1 | 0.30 | 0.74 |
| $\sigma_{CAD}$ | 0.13 | -0.12 | 0.20 | 0.06 | -0.04 | -0.19 | **-0.03** | -0.18 | 0.21 | 0.13 | 0.12 | 0.20 | 0.11 | 0.30 | 1 | 0.29 |
| $\sigma_{NZD}$ | 0.23 | -0.08 | 0.34 | 0.01 | 0.01 | -0.37 | -0.04 | **-0.38** | 0.22 | 0.07 | 0.17 | 0.12 | 0.03 | 0.74 | 0.29 | 1 |

Table 4: Calibration results for the correlation matrix on 2-Feb-2010 using the model where $\upsilon_i^T = \upsilon^T$. The correlation matrix is divided into four quadrants, corresponding to $\boldsymbol{\rho}$, $\tilde{\boldsymbol{\rho}}$, $\tilde{\boldsymbol{\rho}}'$ and $\mathbf{r}$ as shown in $(8)$.

| | Errors in the at-the-money volatilities | | | | | Errors in the risk reversals | | | | | Errors in the market strangles | | | | |
|---|---|---|---|---|---|---|---|---|---|---|---|---|---|---|---|
| | 1M | 2M | 3M | 6M | 1Y | 1M | 2M | 3M | 6M | 1Y | 1M | 2M | 3M | 6M | 1Y |
| EURUSD | -0.0% | 0.0% | -0.0% | -0.1% | -0.1% | -0.3% | -0.2% | -0.1% | -0.0% | -0.0% | -0.0% | -0.0% | -0.0% | -0.1% | -0.1% |
| USDJPY | -0.3% | -0.1% | 0.0% | 0.2% | 0.3% | 0.4% | 0.4% | 0.2% | 0.1% | -0.2% | 0.0% | 0.1% | 0.2% | 0.3% | 0.4% |
| GBPUSD | -0.0% | 0.1% | 0.2% | 0.1% | 0.0% | -0.2% | -0.0% | -0.1% | -0.0% | -0.1% | -0.1% | -0.0% | -0.0% | -0.1% | -0.1% |
| USDCHF | 0.2% | 0.1% | 0.1% | -0.1% | -0.2% | 0.0% | -0.1% | -0.1% | -0.1% | -0.1% | -0.0% | -0.0% | -0.0% | -0.0% | -0.0% |
| AUDUSD | -0.0% | -0.0% | -0.0% | 0.0% | 0.1% | -0.1% | -0.0% | -0.1% | -0.0% | -0.2% | -0.0% | -0.1% | -0.1% | -0.2% | -0.4% |
| USDCAD | 0.1% | 0.1% | -0.0% | 0.1% | 0.1% | 0.3% | 0.1% | 0.1% | -0.1% | -0.2% | -0.1% | -0.0% | -0.1% | -0.1% | -0.1% |
| NZDUSD | 0.2% | -0.4% | -0.2% | -0.1% | -0.0% | 0.3% | 0.1% | -0.1% | -0.2% | -0.4% | -0.0% | -0.1% | -0.1% | -0.2% | -0.4% |
| EURJPY | 0.2% | 0.0% | -0.0% | -0.2% | -0.2% | 0.4% | 0.4% | 0.2% | -0.0% | -0.4% | 0.0% | 0.1% | 0.1% | 0.2% | 0.2% |
| EURGBP | 0.1% | -0.0% | 0.0% | 0.0% | 0.1% | -0.2% | -0.2% | -0.0% | 0.0% | 0.1% | 0.0% | 0.0% | -0.0% | 0.0% | -0.0% |
| EURCHF | -0.1% | -0.1% | 0.1% | 0.2% | 0.4% | 0.1% | 0.1% | -0.0% | -0.2% | -0.3% | -0.1% | -0.1% | -0.1% | -0.1% | -0.1% |
| EURAUD | 0.5% | 0.1% | 0.1% | -0.1% | -0.3% | -0.3% | -0.3% | -0.1% | -0.0% | 0.1% | 0.0% | 0.0% | 0.0% | -0.0% | -0.1% |
| EURCAD | 0.1% | 0.3% | 0.0% | -0.1% | -0.2% | -0.1% | -0.1% | -0.1% | -0.1% | -0.0% | -0.1% | -0.1% | -0.1% | -0.1% | -0.1% |
| EURNZD | 0.7% | -0.1% | 0.1% | -0.2% | -0.1% | -0.3% | -0.1% | 0.1% | 0.2% | 0.4% | -0.0% | -0.0% | -0.0% | -0.1% | -0.1% |
| GBPJPY | 0.3% | 0.1% | -0.1% | -0.2% | -0.1% | 0.1% | 0.1% | -0.1% | -0.3% | -0.7% | -0.0% | 0.0% | 0.0% | 0.1% | 0.1% |
| CHFJPY | 0.2% | -0.2% | -0.0% | -0.1% | 0.2% | 0.4% | 0.3% | 0.4% | 0.3% | 0.0% | 0.1% | 0.2% | 0.2% | 0.2% | 0.2% |
| AUDJPY | 0.0% | -0.3% | -0.4% | -0.4% | -0.8% | 0.9% | 0.5% | -0.0% | -0.7% | -2.0% | 0.0% | 0.1% | 0.1% | 0.1% | 0.4% |
| CADJPY | 0.1% | 0.3% | 0.3% | 0.2% | -0.0% | 0.2% | 0.1% | -0.0% | -0.2% | -0.5% | -0.0% | 0.0% | 0.1% | 0.1% | 0.1% |
| NZDJPY | 0.0% | -0.7% | -0.5% | -0.3% | -0.5% | 1.0% | 0.5% | 0.0% | -0.5% | -1.9% | 0.0% | 0.1% | 0.1% | 0.1% | 0.4% |
| GBPCHF | 0.0% | -0.3% | -0.2% | -0.3% | -0.3% | 0.1% | 0.1% | -0.1% | -0.1% | -0.2% | 0.0% | -0.0% | -0.0% | 0.0% | 0.0% |
| GBPAUD | -0.3% | -0.1% | -0.0% | 0.4% | 0.3% | -0.1% | -0.1% | 0.1% | 0.1% | 0.1% | -0.0% | 0.0% | 0.0% | -0.0% | -0.0% |
| GBPCAD | -0.2% | 0.1% | -0.1% | 0.2% | 0.0% | -0.2% | -0.2% | -0.1% | -0.0% | -0.0% | -0.1% | -0.1% | -0.1% | -0.1% | -0.1% |
| GBPNZD | 0.1% | -0.2% | 0.1% | 0.2% | 0.3% | -0.6% | -0.3% | -0.2% | -0.1% | 0.1% | -0.0% | 0.0% | 0.0% | -0.0% | -0.1% |
| AUDCHF | 0.5% | -0.0% | -0.3% | -1.1% | -1.3% | 0.5% | 0.4% | 0.3% | 0.1% | -0.3% | -0.0% | -0.0% | -0.0% | -0.1% | -0.0% |
| CADCHF | 0.1% | -0.0% | -0.5% | -0.7% | -1.0% | 0.1% | 0.1% | 0.1% | -0.0% | -0.2% | -0.1% | -0.1% | -0.1% | -0.1% | -0.2% |
| NZDCHF | 0.7% | -0.3% | -0.1% | -0.8% | -0.9% | 0.4% | 0.2% | -0.0% | -0.7% | -1.1% | -0.1% | -0.1% | -0.1% | -0.1% | -0.0% |
| AUDCAD | -0.0% | 0.3% | 0.4% | 0.6% | 0.7% | -0.2% | -0.2% | -0.2% | -0.0% | -0.1% | 0.0% | 0.1% | 0.0% | -0.0% | -0.1% |
| AUDNZD | -0.2% | -0.1% | 0.3% | 0.5% | 0.6% | 0.0% | 0.1% | 0.0% | -0.0% | -0.1% | 0.1% | 0.2% | 0.2% | 0.3% | 0.2% |
| NZDCAD | 0.3% | -0.0% | 0.2% | 0.3% | 0.3% | 0.3% | 0.1% | -0.1% | -0.1% | -0.2% | 0.0% | 0.0% | -0.0% | -0.1% | -0.1% |

Table 5: This table show how well formula $(11)$ with the values of $\sigma_i$, $\upsilon_i$, $\boldsymbol{\rho}$, $\tilde{\boldsymbol{\rho}}$ and $\mathbf{r}$ from tables 3 and 4 match the at-the-money volatilities, risk reversals and market strangles shown in table 1. All entries in the above table are "Market value" $-$ "Model value".

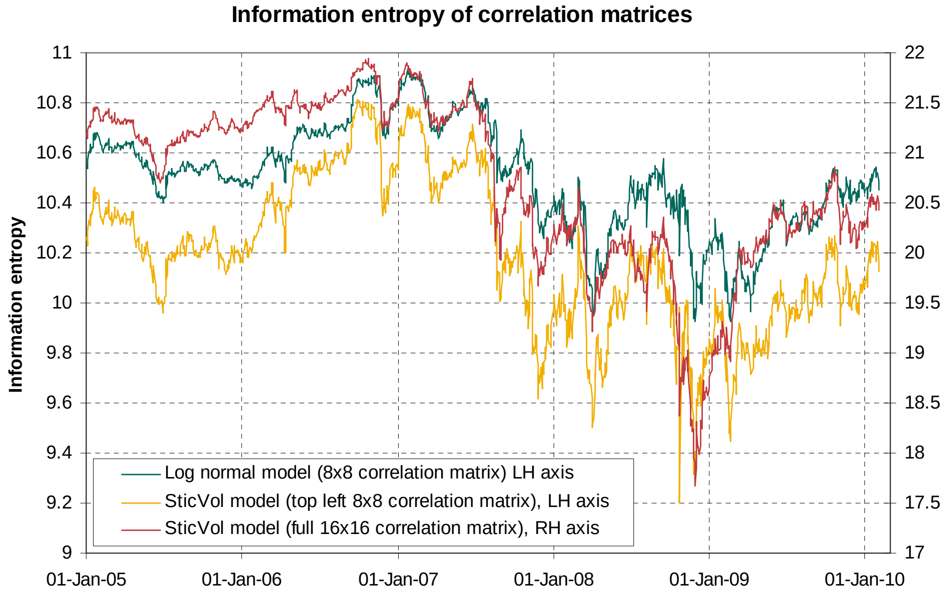


Figure 9: Information entropy for a correlation matrix $\mathbf{\Omega}$ is defined by $\log\left(\sqrt{(2\pi e)^d\,|\mathbf{\Omega}|}\right)$, where $d$ is the number of dimenstions. Just looking at the entropy in the $8 \times 8$ correlation matrices, it's clear that the Stochastic Intrinsic Currency Volatilty ("SticVol") model has slightly less entropy and hence more information than the log-normal model. As with figures 7 and 8, all lines have the same shape, in terms of where their major peaks and troughs are.

and $\tilde{\boldsymbol{\rho}}$. The calibration results are shown in tables 3 and 4. Table 5 shows the residual errors between the model values and market values.

The correlation matrix shown in table 4 has several interesting characteristics. The correlation matrix $\rho_{ij}$ in the top left hand corner looks very much like the intrinsic currency correlation matrices calculated in the previous work [3, 4, 5]. For example there are positive correlations between EUR and CHF, and between AUD and NZD. Similarly, the familiar carry-trade picture is present, because JPY is negatively correlated with AUD and NZD. The bottom right hand corner of the correlation matrix shown in table 4 contains the correlation matrix $\mathbf{r}$ between the $\sigma_i$, and apart from the slightly negative correlations between $\sigma_{CHF}$ and $\sigma_{USD}$ and between $\sigma_{CHF}$ and $\sigma_{JPY}$, all other correlations are positive. This has the intuitive interpretation that changes in volatility are mostly positively correlated, so that if one volatility moves up the rest are likely to move up too, and similarly when one volatility moves down. Regarding the correlations in matrix $\tilde{\boldsymbol{\rho}}$ between the $X_i$ and the $\sigma_i$, these tend to reflect the market data for risk reversals. Figure 1 on the front page showed how these correlations imply that volatilities rise with JPY strength, and the corresponding $\tilde{\boldsymbol{\rho}}$ in table 4 were part of that figure.

The conclusion is that the stochastic intrinsic currency volatility model can be calibrated simultaneously to the implied volatility curves seen in the forex option market for all currency pairs based on this set of eight currencies, across a range of tenors.

## 5.2 Assessing the quality of the fit to the market data

The same exercise that was discussed in detail in the previous sub-section for 2-Feb-2010 was repeated for every day in the data set, i.e. using $\varepsilon = 1$ and the methodology described in appendix D, best fits were done to historical snapshots of market data starting at the beginning of January 2005. To assess the quality of the fits, figures 7 and 8 show the $\chi^2$ and $R^2$ statistics, where the corresponding statistics are also shown for the fits achieved with the log-normal model discussed in the previous work[5]. Additionally, figure 9 shows the information entropy of the correlation matrices, again with a comparison to the previous work[5]. All three figures show two lines for the stochastic intrinsic currency model ("SticVol model"), to allow a cleaner

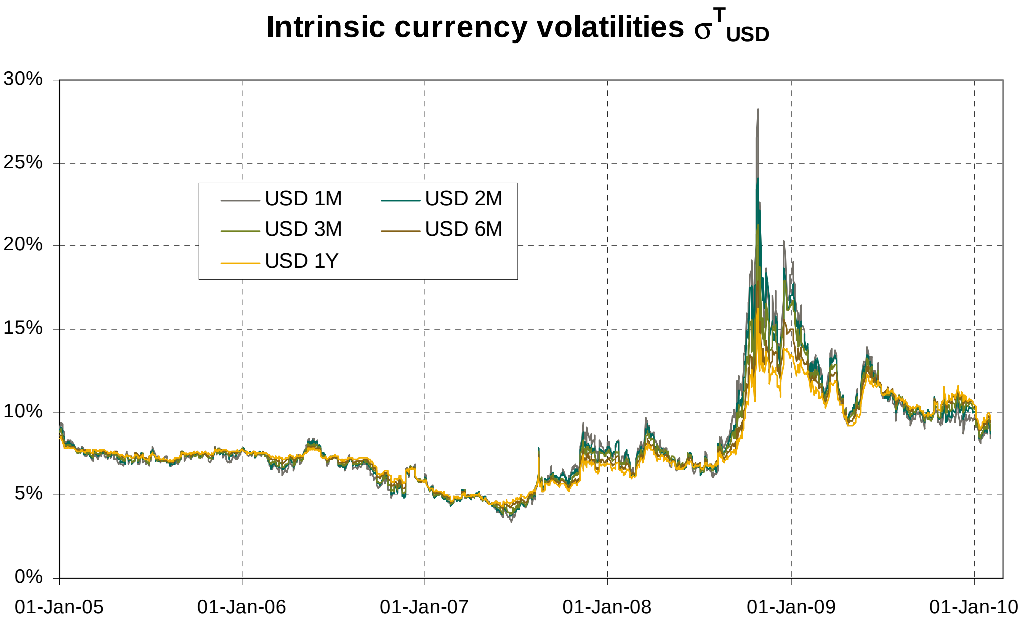


Figure 10: This graph shows that intrinsic currency USD volatilities of different tenors all move around together. The graphs for $\sigma^T_{EUR}$ and $\sigma^T_{CHF}$ are shown in figures 11 and 12. All the intrinsic currency volatilities look qualitatively similar to these graphs.

comparison with the previous work. For example, with figure 7 the full definition of the $\chi^2$ statistic given by formula $(167)$ in appendix D.3 is shown, however the first term $\chi^2_{ATM}$ defined by $(168)$ is also shown, because $\chi^2_{ATM}$ is more directly comparable with the previous work.

Whereas the original log-normal intrinsic currency volatility model just fitted the at-the-money volatilities, the SticVol model also fits the risk reversals and market strangles. Nonetheless, the figures show that using the $\chi^2$ statistic to measure the quality of the fit, the stochastic intrinsic currency volatility model gives a better fit to the data than the purely log-normal model. However the $R^2$ statistic for the log-normal model looks a bit better than the $R^2$ statistic for the stochastic intrinsic currency volatility model. Overall the result is that the new model gives a good fit to the market data, of similar quality to what was achieved in the previous work, but now with good fits to the risk reversals and market strangles.

## 5.3 Historical calibration results

This sub-section presents the historical values that $\sigma_i$, $\upsilon_i$, $\boldsymbol{\rho}$, $\mathbf{r}$ and $\tilde{\boldsymbol{\rho}}$ have taken, given the methodologies described in section 4 and in appendix D. The important features of the methodologies are that the intrinsic currency volatilities $\sigma^T_i$ depend on both currency and tenor, the volatility of volatilities are given by $\upsilon^T_i = \upsilon^T$, and the correlation matrices $\boldsymbol{\rho}$, $\mathbf{r}$ and $\tilde{\boldsymbol{\rho}}$ are tenor independent.

Starting with the volatilities $\sigma^T_i$, figures 10-12 shows how the historical values of $\sigma^T_{USD}$, $\sigma^T_{EUR}$ and $\sigma^T_{CHF}$ have varied for all five tenors in the data set. This shows that the different tenors largely all move around in sync with each other. Figure 13 shows the 1M intrinsic currency volatilities for all eight currencies in the data set. As was seen in the earlier work [3, 5], EUR typically has the lowest intrinsic currency volatility.

Figure 14 shows the how the volatilities of volatilities $\upsilon^T$ have varied since the start of 2005. The $\upsilon^T$ exhibit a strong dependence on tenor. A reasonable model for this tenor dependence is $\upsilon^T = \alpha T^{-\beta}$. This is analysed in figure 15, which shows $\alpha$, $\beta$, as well as the root mean square of the residual errors $\left(\alpha T^{-\beta} - \upsilon^T\right)$. The average value of $\beta$ is around $0.43$, which means that the variance of the volatility grows as $T^{0.14}$. This is the idea behind the alternative models of $\upsilon^T_i$ suggested in $(26)$.

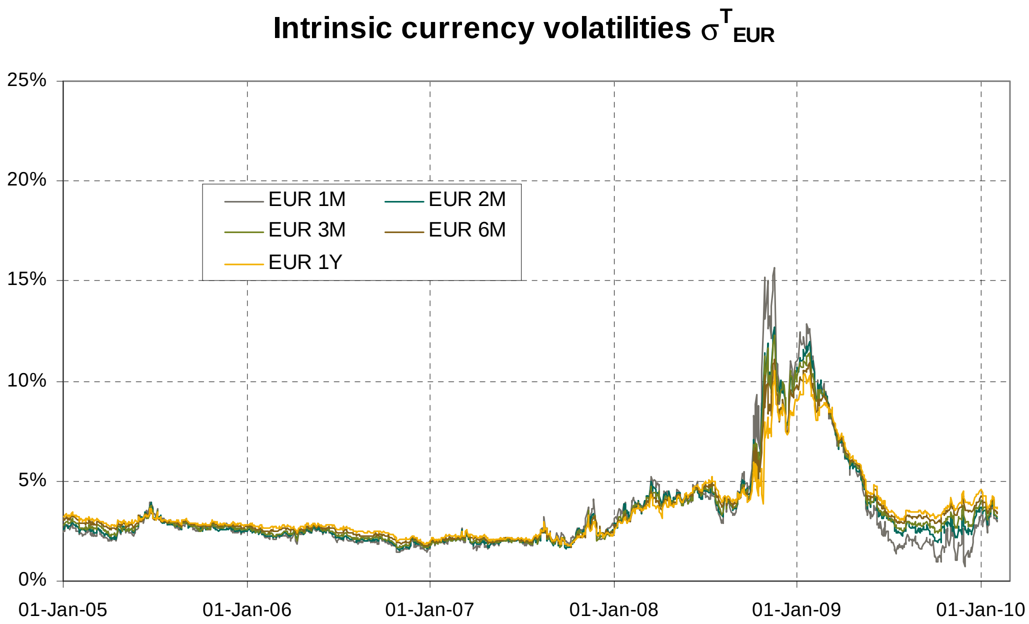


Figure 11: This graph shows that intrinsic currency EUR volatilities of different tenors all move around together, apart from a period in 2009 when there are some gaps between the volatilities of different tenors. Apart from this period in 2009, these graphs look qualitatively similar to the graphs of USD and CHF intrinsic currency volatilities shown in figures 10 and 12 respectively.

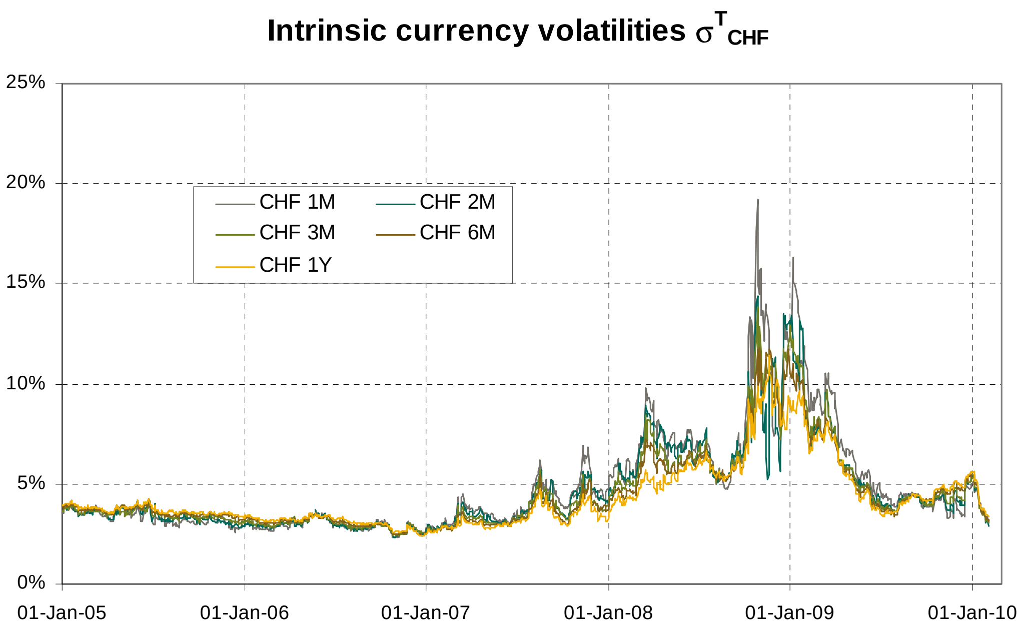


Figure 12: This graph shows that the intrinsic currency CHF volatilities of different tenors mostly all moved around together. Qualitatively, these graphs look like the graphs of USD and EUR intrinsic currency volatilities shown in figures 10 and 11 respectively.

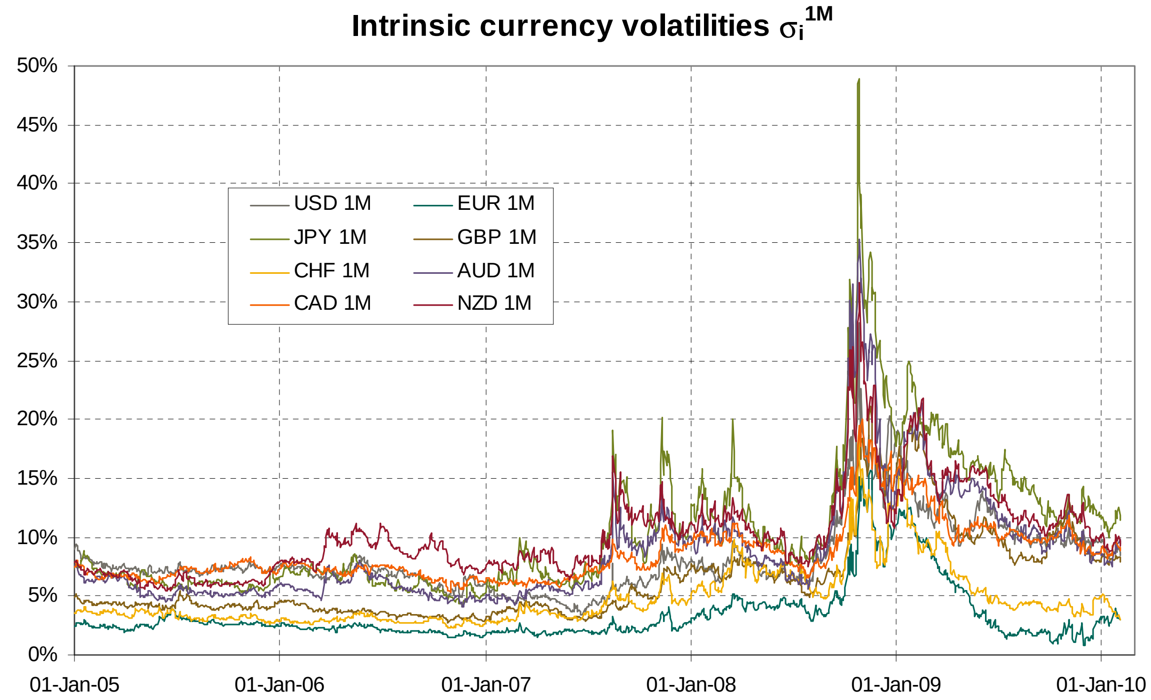


Figure 13: The 1M intrinsic currency volatilities for all 8 currencies in the data set. This shows that the intrinsic currency volatilities of EUR are consistenly lower than all other intrinsic currency volatilities, with CHF being the second least volatilite currency.

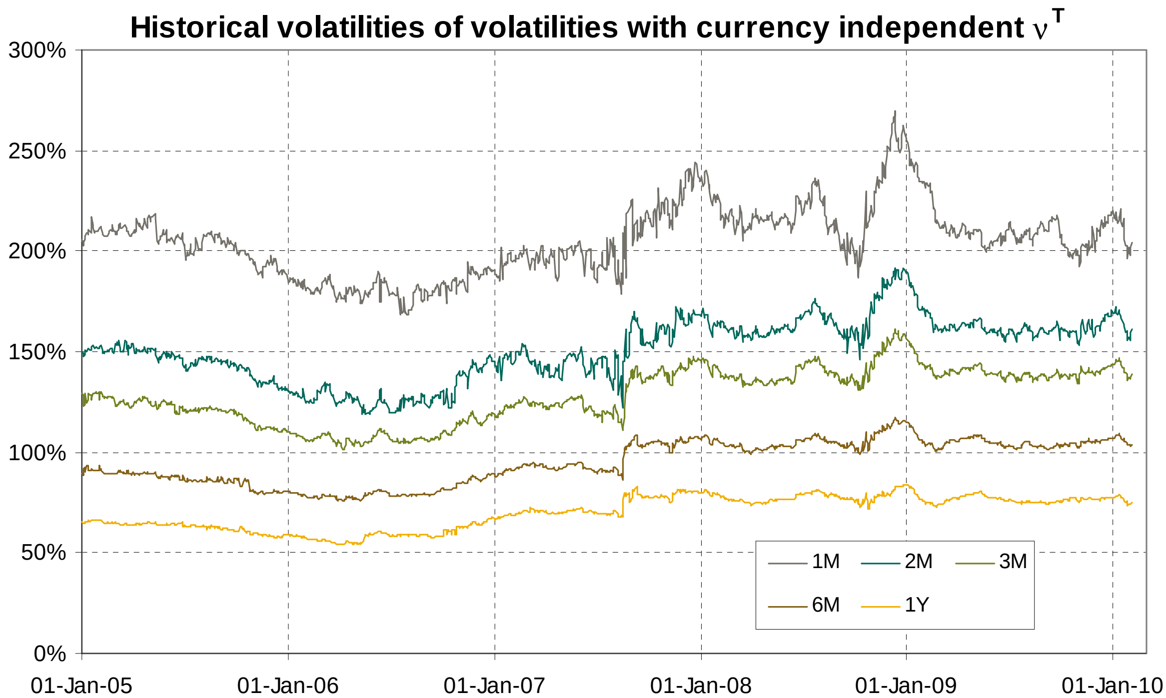


Figure 14: This figure shows that the values taken by $\upsilon^T$ when $\upsilon_i^T = \upsilon^T$ have significant tenor dependence. Figure 15 shows that a good model for this tenor dependence is given by $\upsilon^T = \alpha T^{-\beta}$.

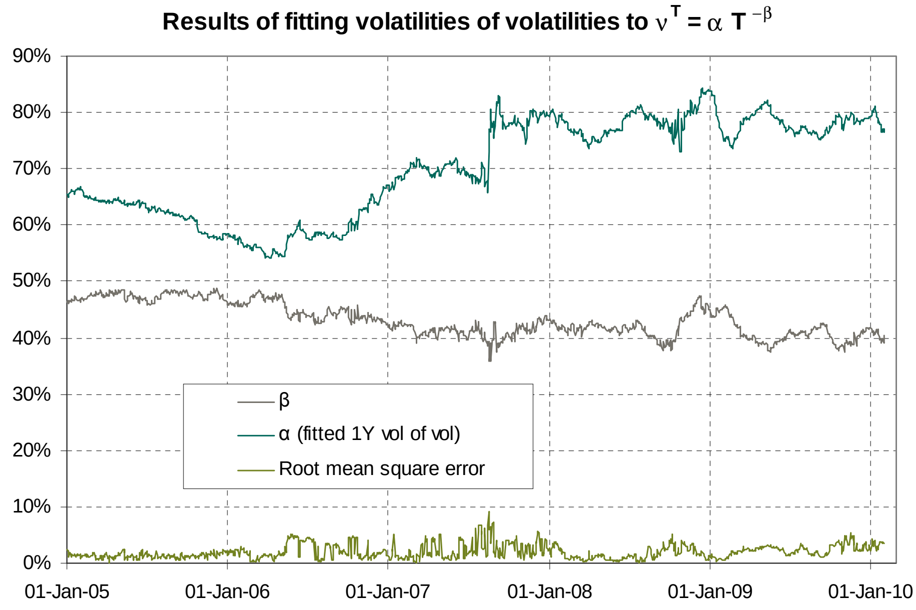


Figure 15: This graph shows that for the $\upsilon_i^T = \upsilon^T$ model, the tenor dependence of $\upsilon^T$ shown in figure 14 can be modelled reasonably well by $\upsilon^T = \alpha T^{-\beta}$. In this graph, the average $\beta$ is $0.43$, so on average the volatility variance $\left(\upsilon^T\right)^2 T$ grows as $\tau^{0.14}$.

Figures 16 to 19 show how some of the parameters of the intrinsic currency correlation matrix $\boldsymbol{\rho}$ have varied over the period under consideration. These graphs are very similar to the correlation graphs that were found in the previous work [3, 5]. For example, there are significant EUR-CHF and AUD-NZD correlations throughout the period, exactly as seen previously.

Figures 20 to 27 show how the parameters of the correlation matrix $\mathbf{r}$ have varied, which are the correlations between the intrinsic currency volatilities $\sigma_i$. Appendix D.3 describes in connection with equation $(181)$ how these correlations are constrained to be positive, because a rise in uncertainty in the markets should mean that all volatilities tend to rise, not that some tend to rise and some tend to fall. Figures 28 to 35, coupled with figure 1 on the front page, show how the parameters of $\tilde{\boldsymbol{\rho}}$ have varied. These are the correlations between the intrinsic currency values $X_i$ and the intrinsic currency volatilities $\sigma_i$. As mentioned above, these parameters tend to reflect the risk reversals, because risk reversals describe what volatility changes are expected as forex rates move.

Lastly in this sub-section, figures 36-41 show some of the residual errors between the model values and market values. Figures 36 and 39 show the residual at-the-money error $[\varepsilon_\sigma]_{ij}^T$ defined by $(168)$ in appendix D.3, and the other graphs show the same for risk reversals and market strangles, i.e. $[\varepsilon_{RR}]_{ij}^T$ and $[\varepsilon_{MS}]_{ij}^T$ defined by $(169)$ and $(170)$ respectively. Unlike a lot of the other currency pairs, the USD/JPY errors exhibit some structure, in the sense that the errors are usually ordered by tenor. This suggests that there is some persistent tenor dependence in the correlation matrix which isn't being captured by the tenor independent assumption for $\boldsymbol{\rho}$, $\mathbf{r}$ and $\tilde{\boldsymbol{\rho}}$.

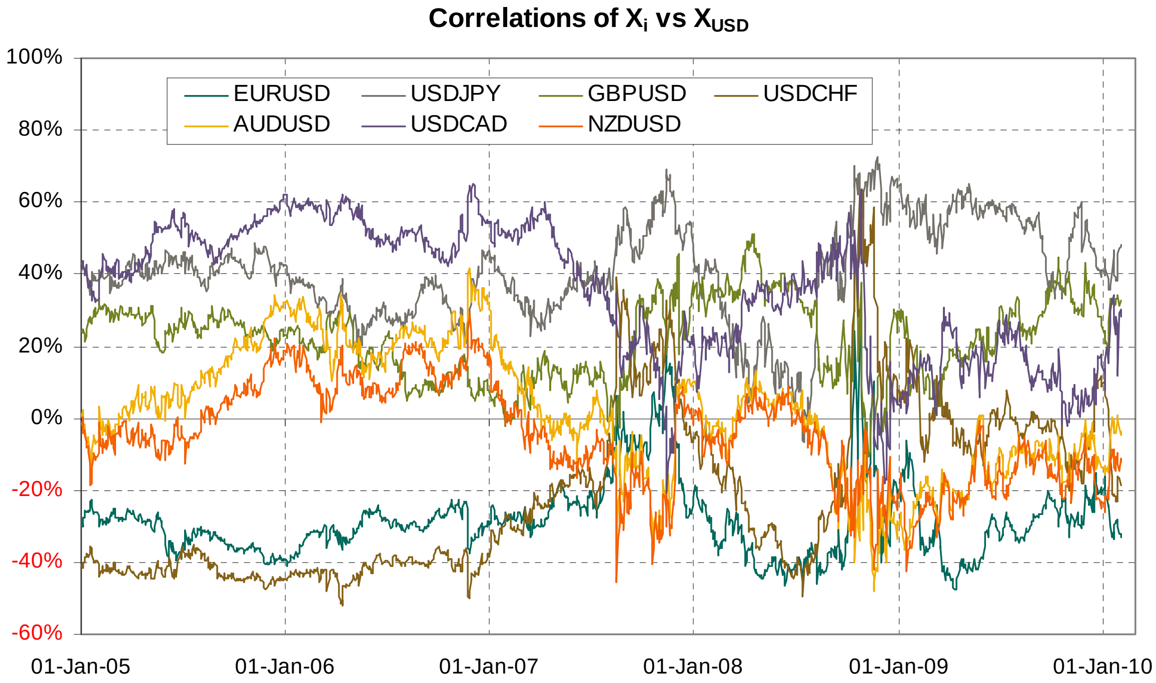


Figure 16: Historical implied correlations of $X_i$ with $X_{USD}$ for the $\upsilon_i^T = \upsilon^T$ model, from the correlation matrix $\boldsymbol{\rho}$.

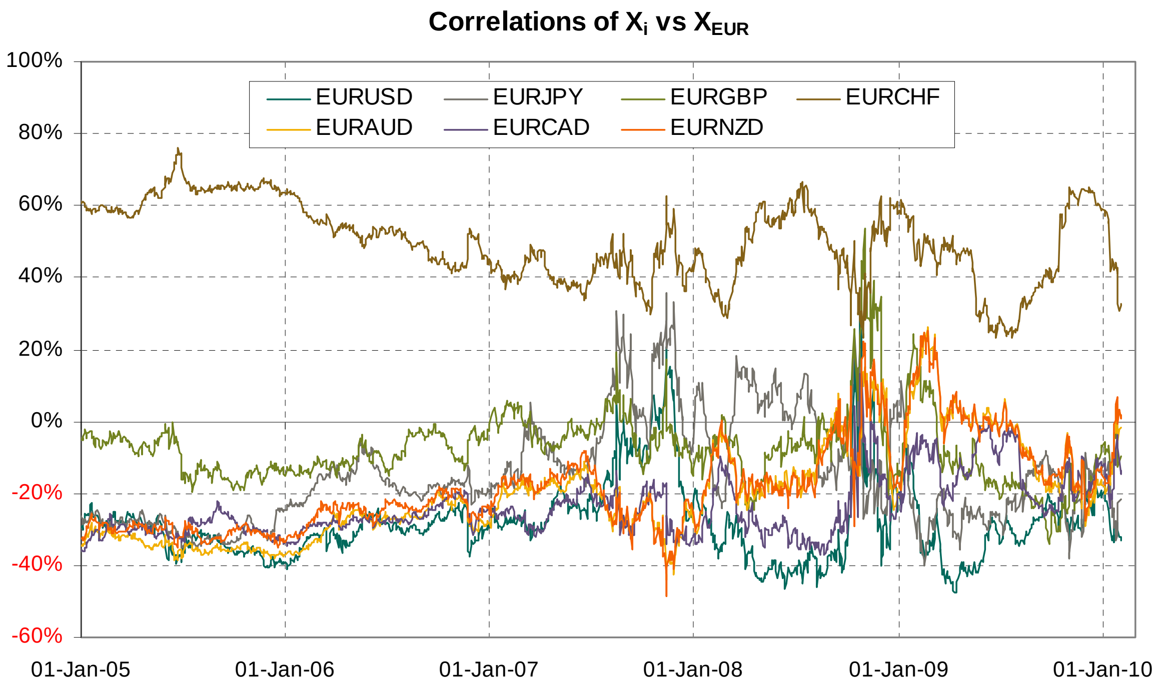


Figure 17: Historical implied correlations of $X_i$ with $X_{EUR}$ for the $\upsilon_i^T = \upsilon^T$ model, from the correlation matrix $\boldsymbol{\rho}$. The correlation of $X_{EUR}$ with $X_{CHF}$ has been consistently high.

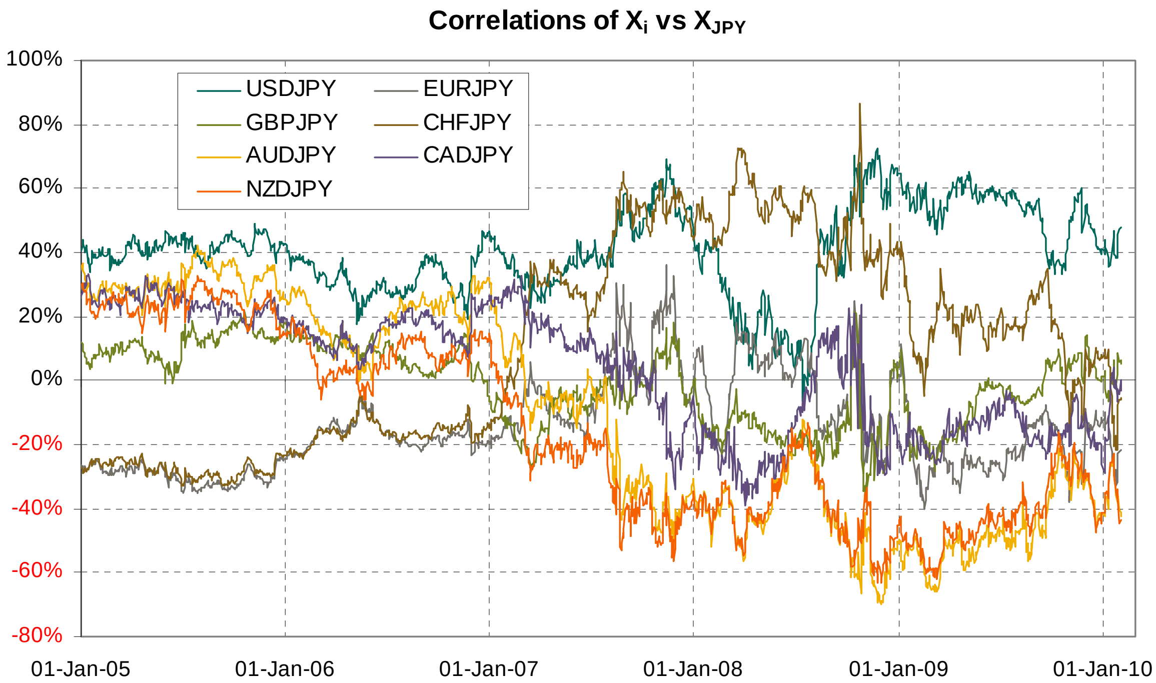


Figure 18: Historical implied correlations of $X_i$ with $X_{JPY}$ for the $\upsilon_i^T = \upsilon^T$ model, from the correlation matrix $\boldsymbol{\rho}$. The forex carry-trade is probably responsible for the fact that the correlations of $X_{JPY}$ with $X_{AUD}$ and $X_{NZD}$ has been significantly negative since mid 2007.

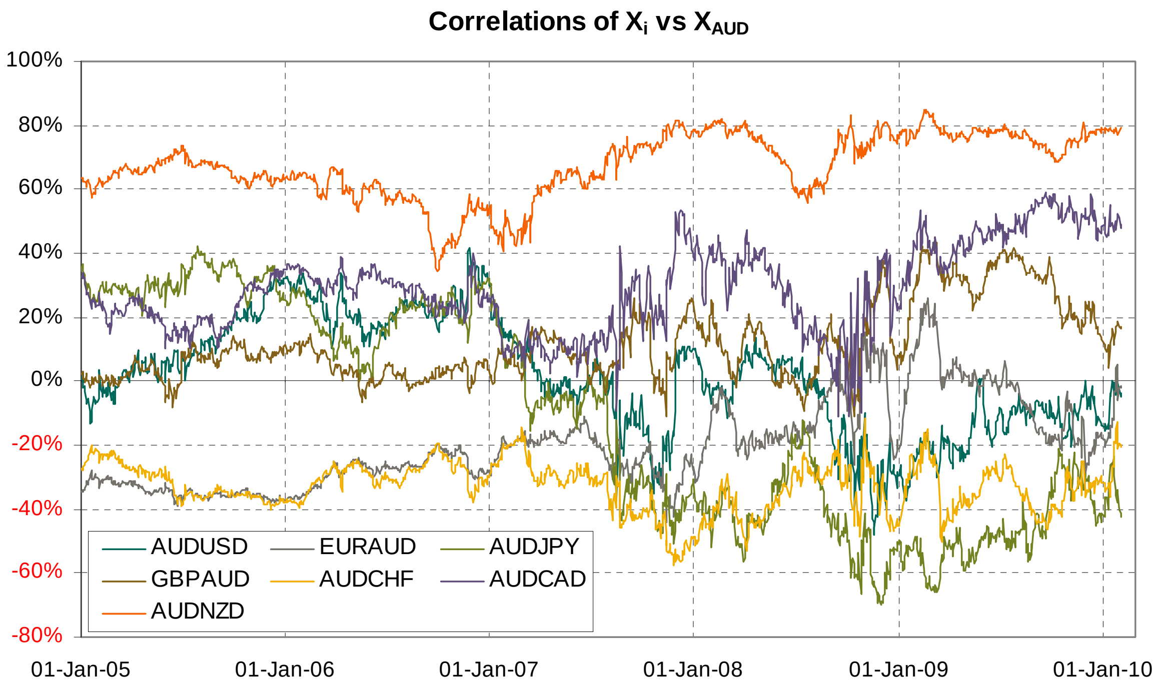


Figure 19: Historical implied correlations of $X_i$ with $X_{AUD}$ for the $\upsilon_i^T = \upsilon^T$ model, from the correlation matrix $\boldsymbol{\rho}$. The correlation of $X_{AUD}$ with $X_{NZD}$ has been consistently significantly positive.

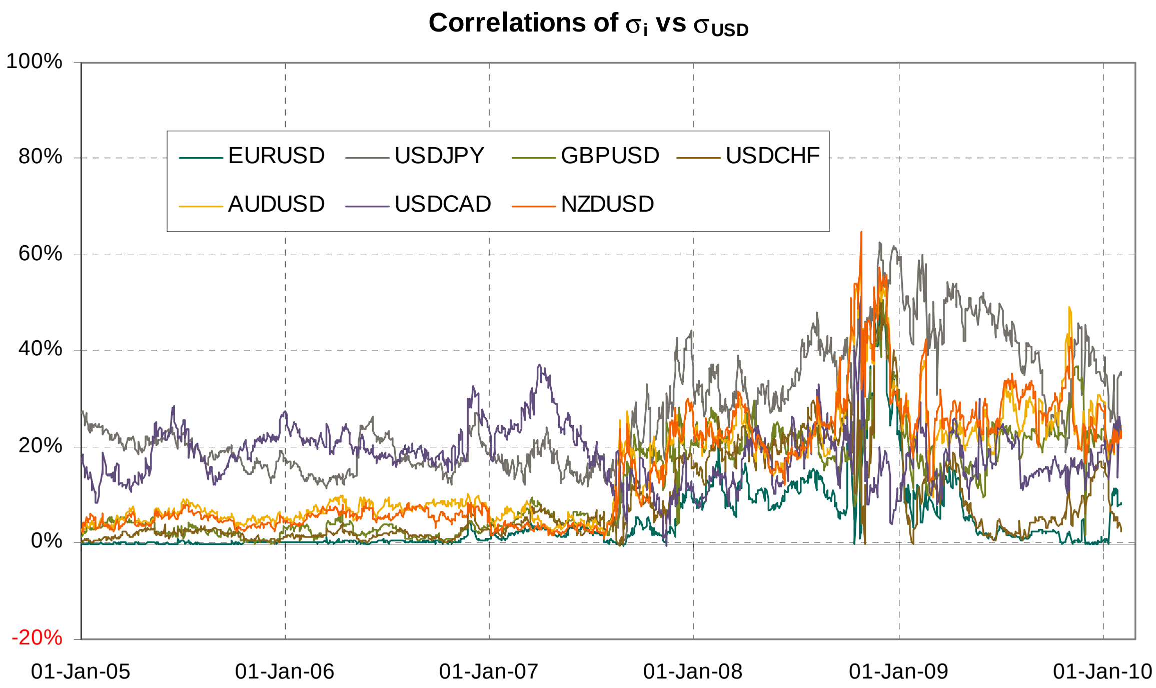


Figure 20: Historical implied correlations of $\sigma_i$ with $\sigma_{USD}$ for the $\upsilon_i^T = \upsilon^T$ model, from the correlation matrix $\mathbf{r}$.

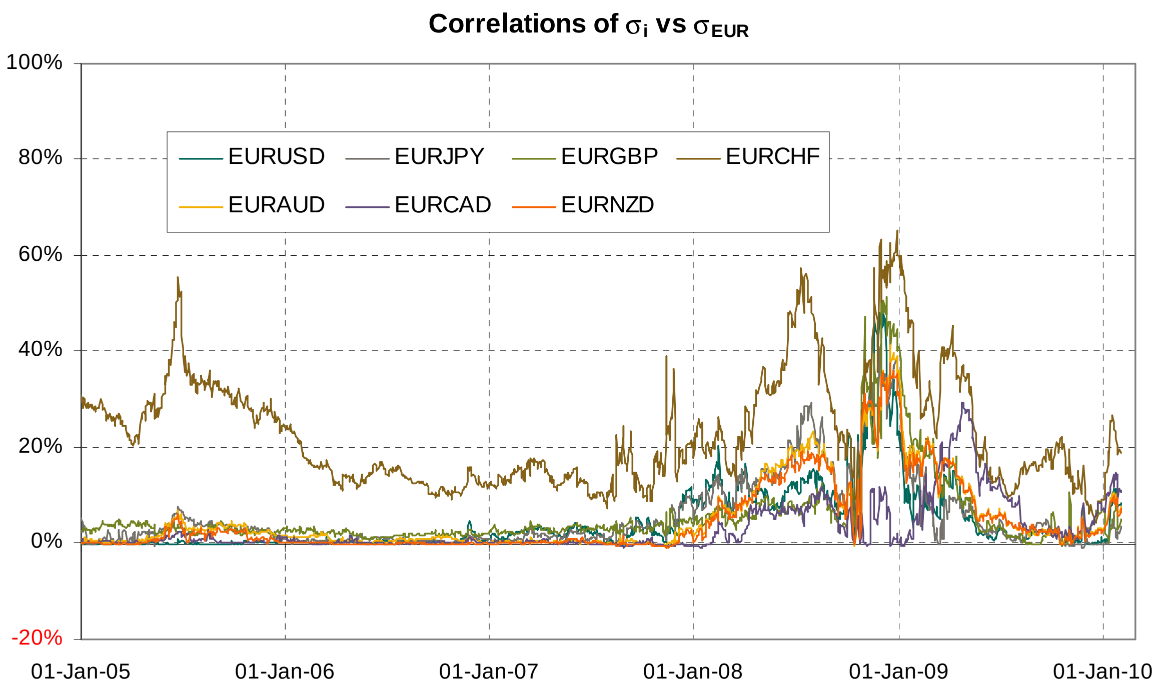


Figure 21: Historical implied correlations of $\sigma_i$ with $\sigma_{EUR}$ for the $\upsilon_i^T = \upsilon^T$ model, from the correlation matrix $\mathbf{r}$. The correlation between $\sigma_{EUR}$ and $\sigma_{CHF}$.has usually been noticably larger than the other correlations.

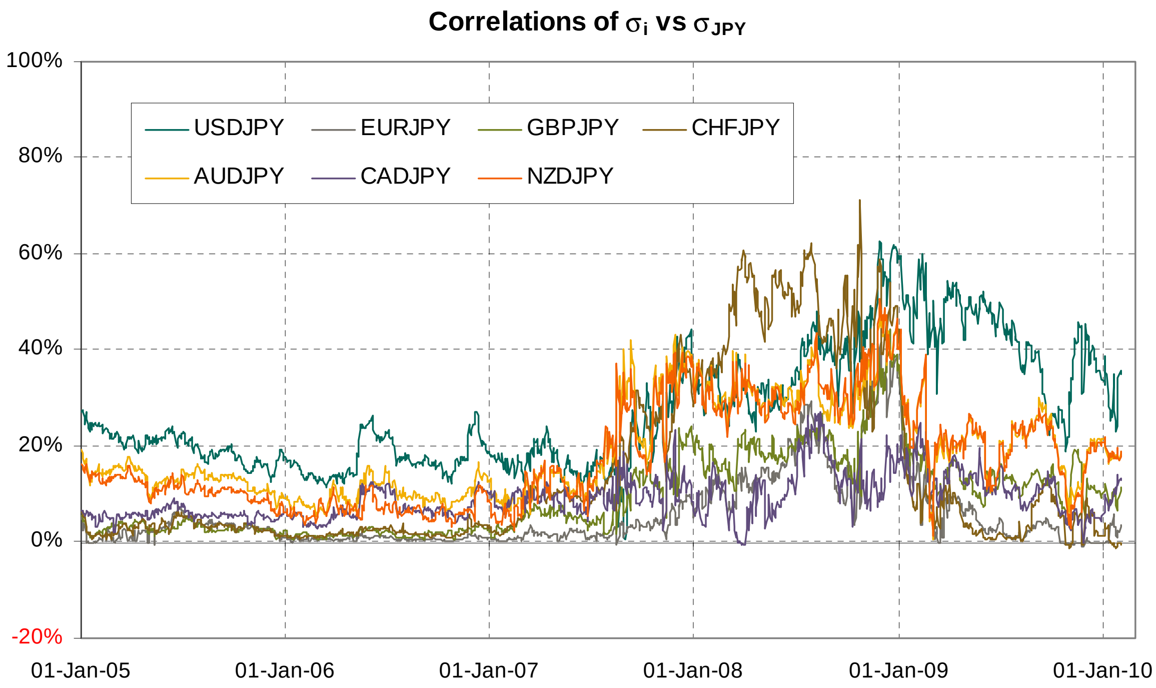


Figure 22: Historical implied correlations of $\sigma_i$ with $\sigma_{JPY}$ for the $\upsilon_i^T = \upsilon^T$ model, from the correlation matrix $\mathbf{r}$.

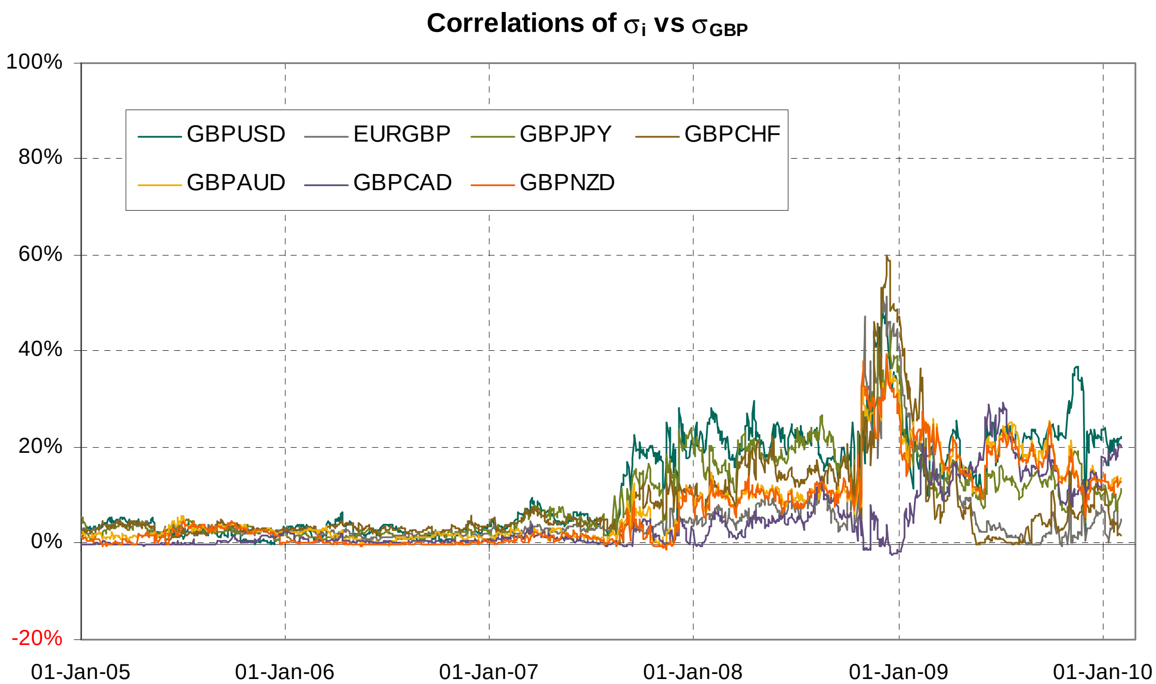


Figure 23: Historical implied correlations of $\sigma_i$ with $\sigma_{GBP}$ for the $\upsilon_i^T = \upsilon^T$ model, from the correlation matrix $\mathbf{r}$.

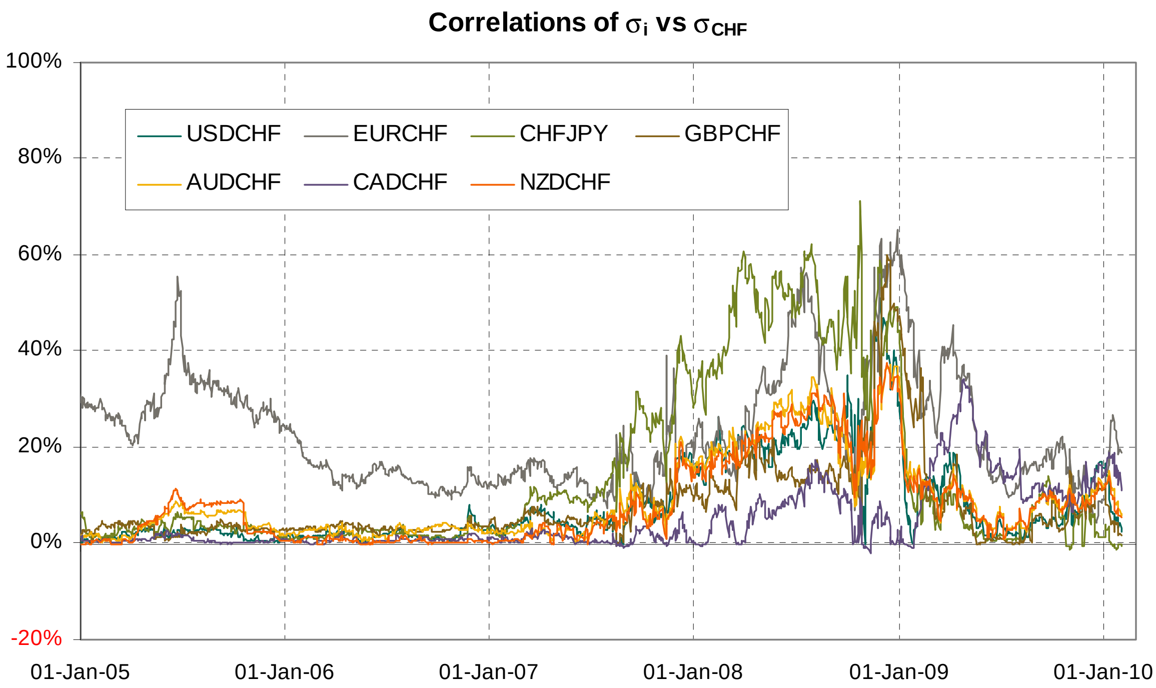


Figure 24: Historical implied correlations of $\sigma_i$ with $\sigma_{CHF}$ for the $\upsilon_i^T = \upsilon^T$ model, from the correlation matrix $\mathbf{r}$.

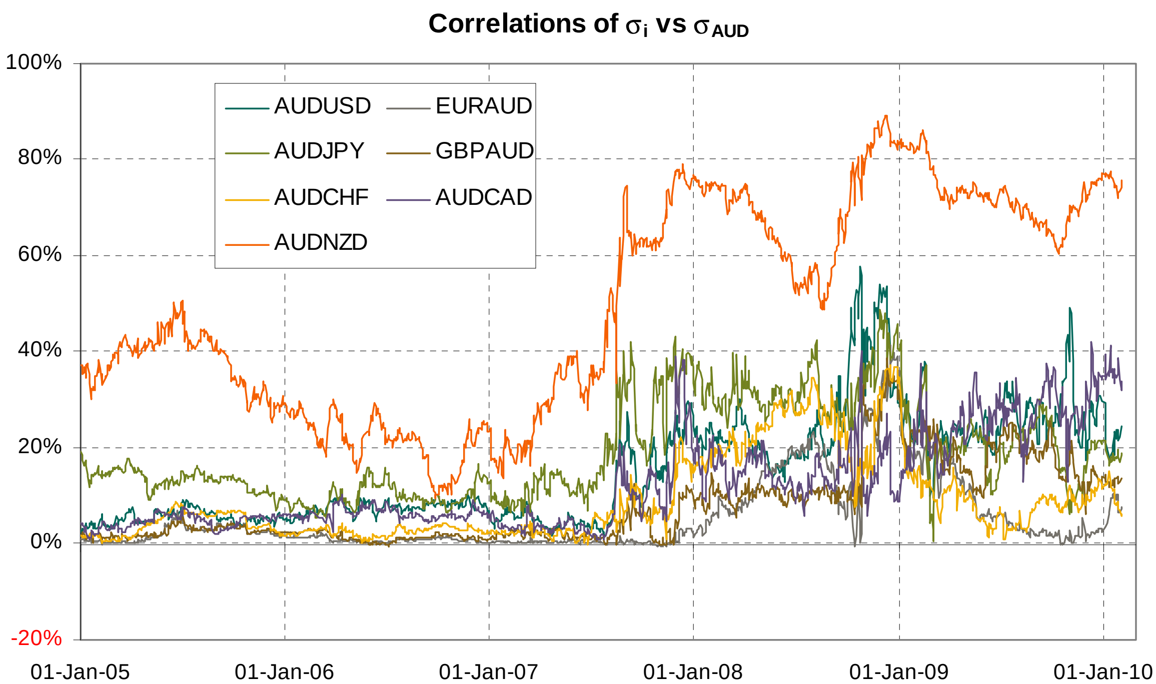


Figure 25: Historical implied correlations of $\sigma_i$ with $\sigma_{AUD}$ for the $\upsilon_i^T = \upsilon^T$ model, from the correlation matrix $\mathbf{r}$. The correlation between $\sigma_{AUD}$ and $\sigma_{NZD}$ has been consistently positive, particularly since mid 2007.

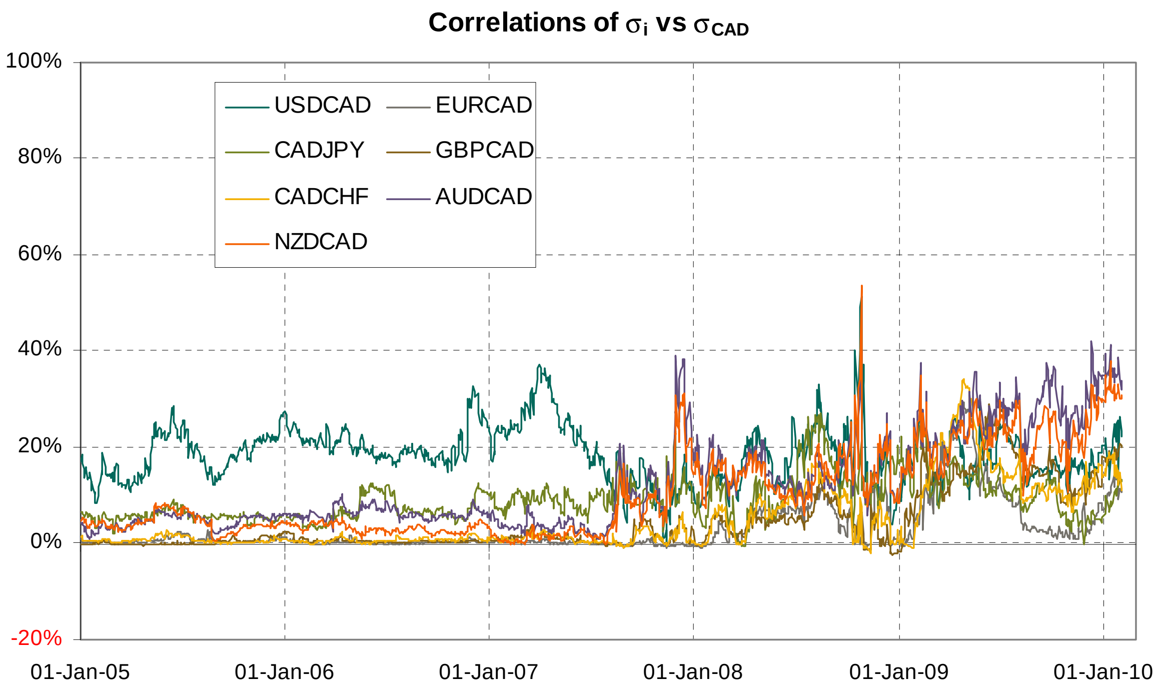


Figure 26: Historical implied correlations of $\sigma_i$ with $\sigma_{CAD}$ for the $\upsilon_i^T = \upsilon^T$ model, from the correlation matrix $\mathbf{r}$.

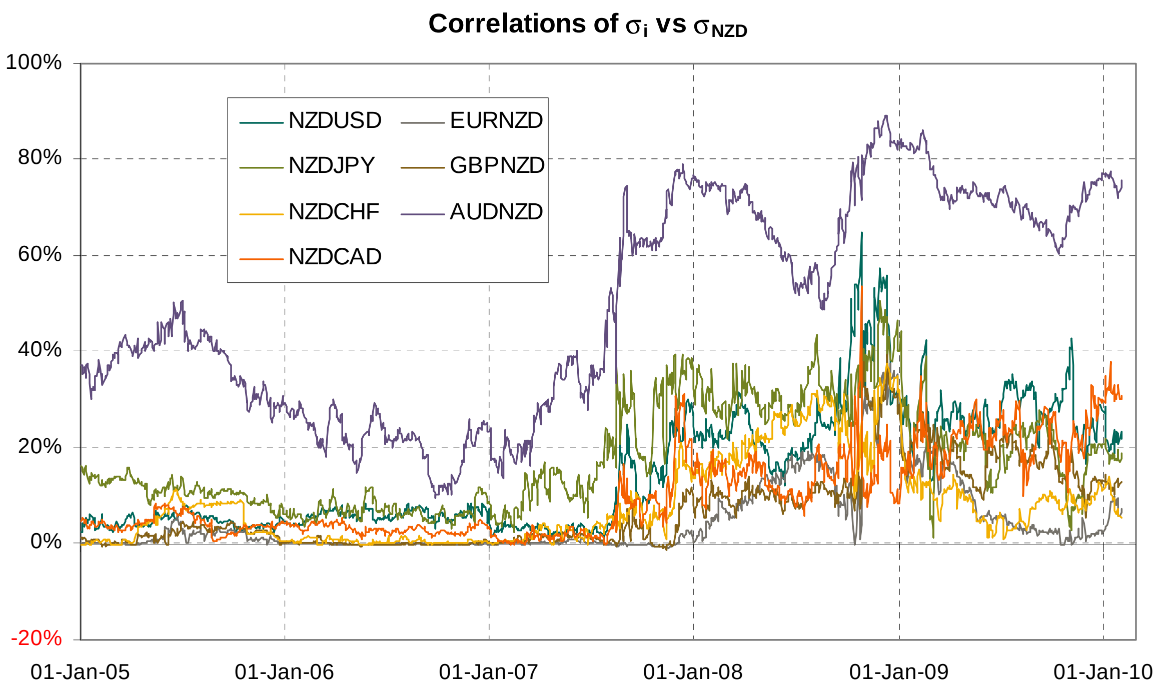


Figure 27: Historical implied correlations of $\sigma_i$ with $\sigma_{NZD}$ for the $\upsilon_i^T = \upsilon^T$ model, from the correlation matrix $\mathbf{r}$. The correlation between $\sigma_{NZD}$ and $\sigma_{AUD}$ has been consistenly positive, particularly since mid 2007.

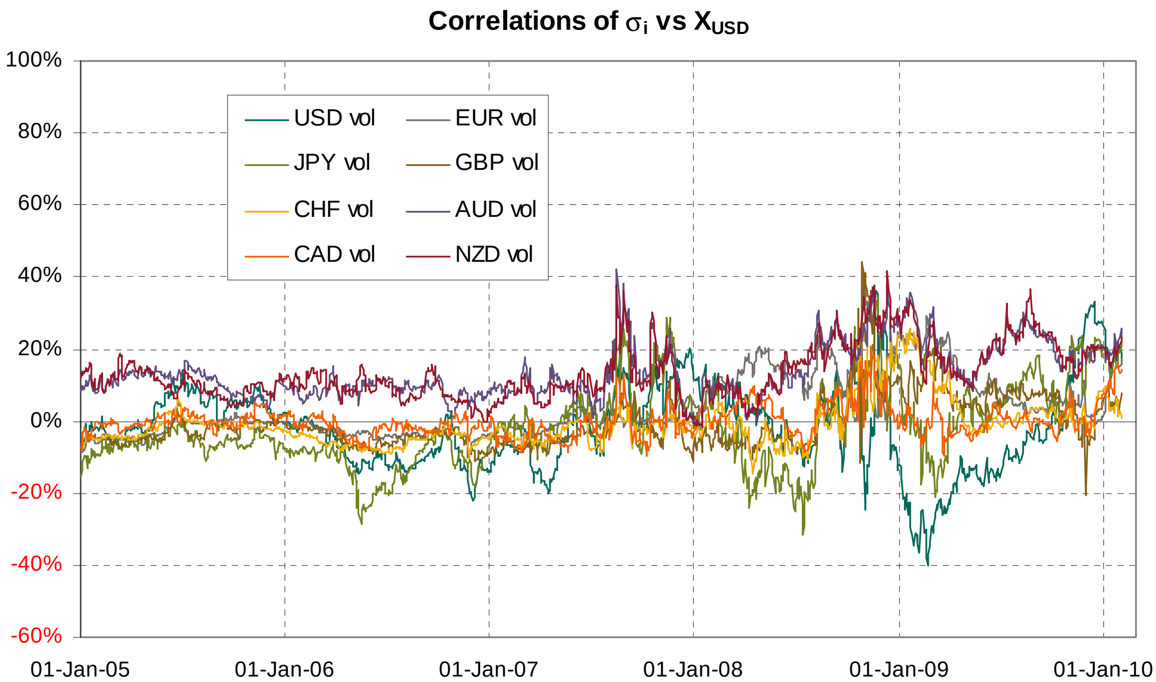


Figure 28: Historical implied correlations of $\sigma_i$ with $X_{USD}$ for the $\upsilon_i^T = \upsilon^T$ model, from the correlation matrix $\tilde{\boldsymbol{\rho}}$. The correlation of $\sigma_{AUD}$ and $\sigma_{NZD}$ with $X_{USD}$ has mostly been positive.

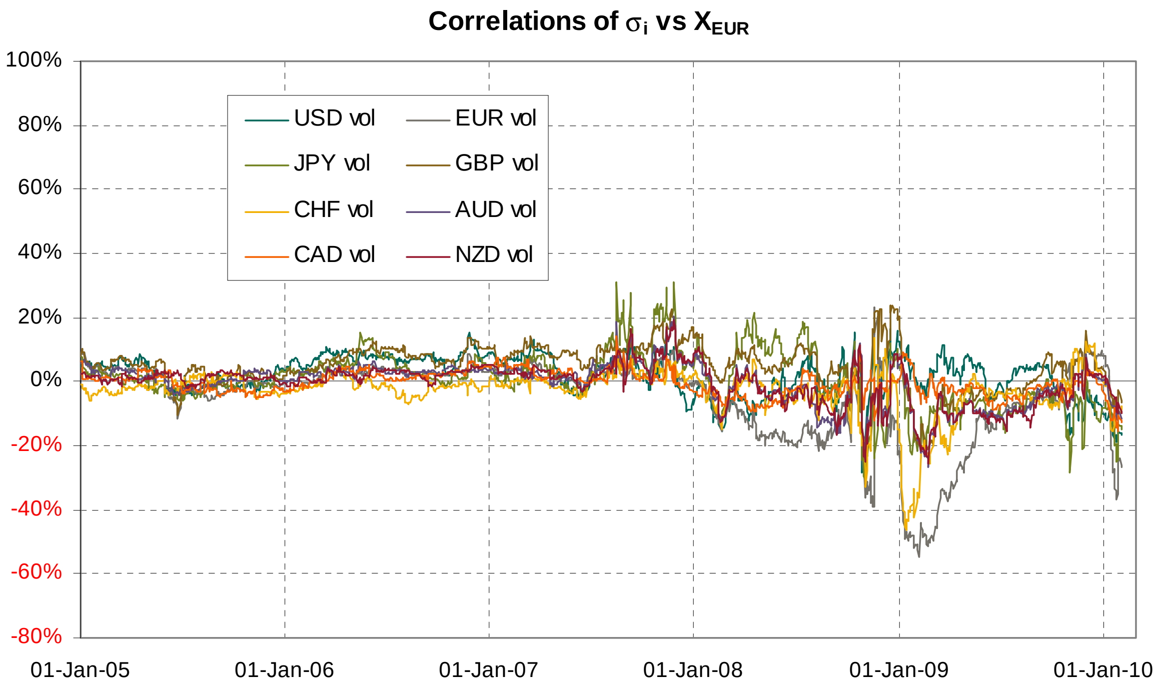


Figure 29: Historical implied correlations of $\sigma_i$ with $X_{EUR}$ for the $\upsilon_i^T = \upsilon^T$ model, from the correlation matrix $\tilde{\boldsymbol{\rho}}$. Until around the start of 2008, the correlations of all $\sigma_i$ with $X_{EUR}$ were close to zero. However, during 2009 a lot of the correlations became negative, and for a while the correlation between $\sigma_{EUR}$ and $X_{EUR}$ was significantly negative, suggesting that increases in $EUR$ volatility were coupled with $EUR$ weakness.

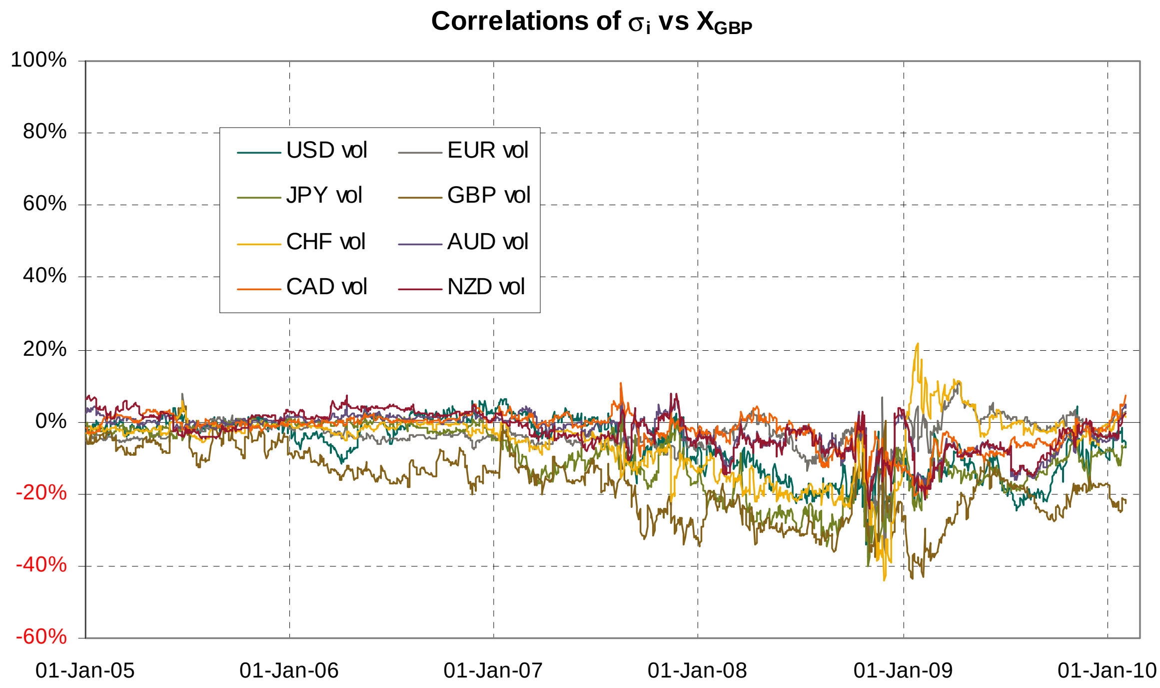


Figure 30: Historical implied correlations of $\sigma_i$ with $X_{GBP}$ for the $\upsilon_i^T = \upsilon^T$ model, from the correlation matrix $\tilde{\boldsymbol{\rho}}$. Since the start of the credit crunch in mid 2007, most correlations have been negative, so that any volatility increase is likely to be associated with $GBP$ weakness.

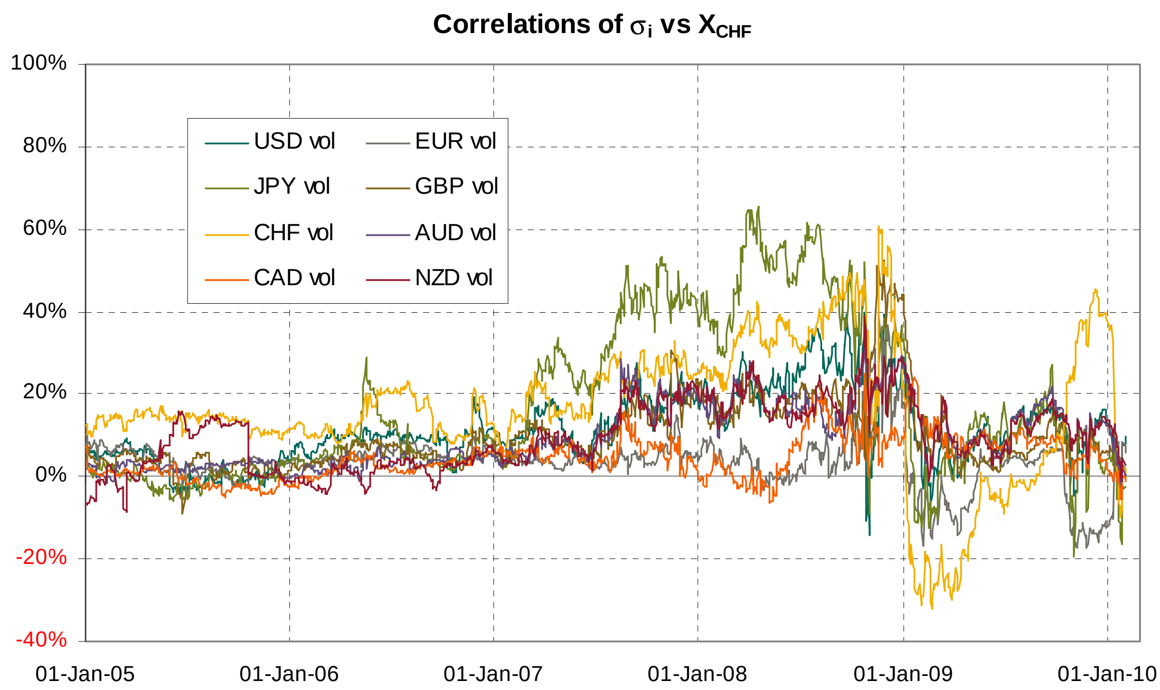


Figure 31: Historical implied correlations of $\sigma_i$ with $X_{CHF}$ for the $\upsilon_i^T = \upsilon^T$ model, from the correlation matrix $\tilde{\boldsymbol{\rho}}$. These correlations have mostly been positive, suggesting that $CHF$ is regarded as a safe haven currency, because rising volatilty is likely to be associated with $CHF$ strength.

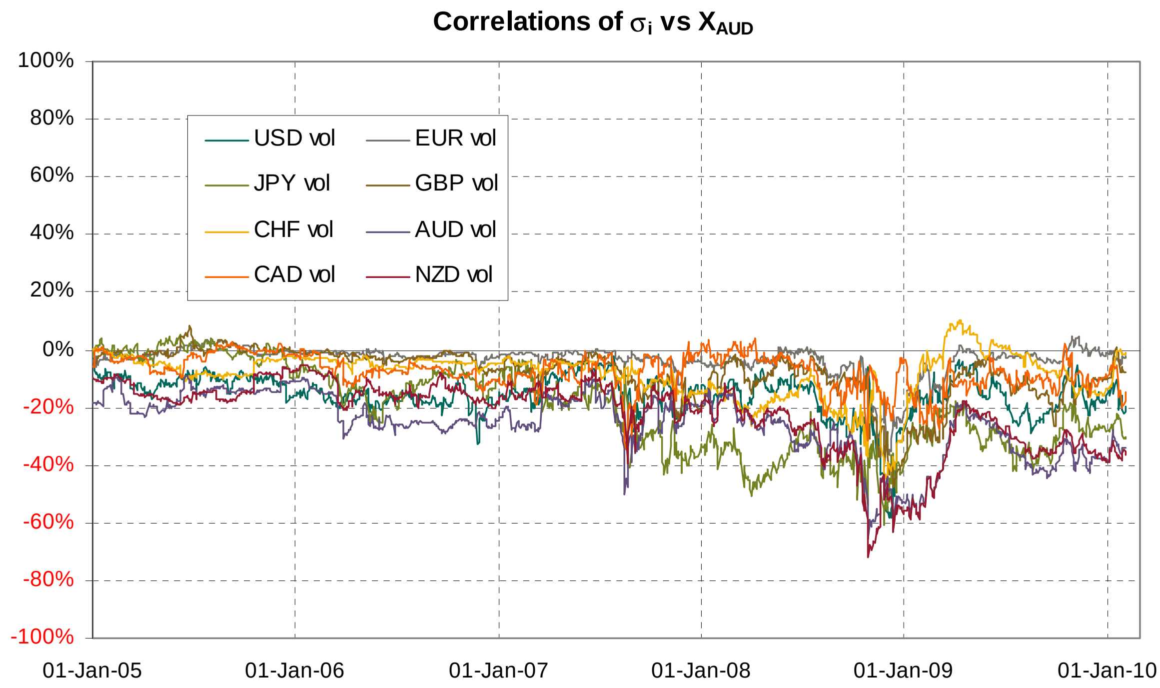


Figure 32: Historical implied correlations of $\sigma_i$ with $X_{AUD}$ for the $\upsilon_i^T = \upsilon^T$ model, from the correlation matrix $\tilde{\boldsymbol{\rho}}$. As with $NZD$, most correlations have been negative, so that any volatility increase is likely to be associated with $AUD$ weakness.

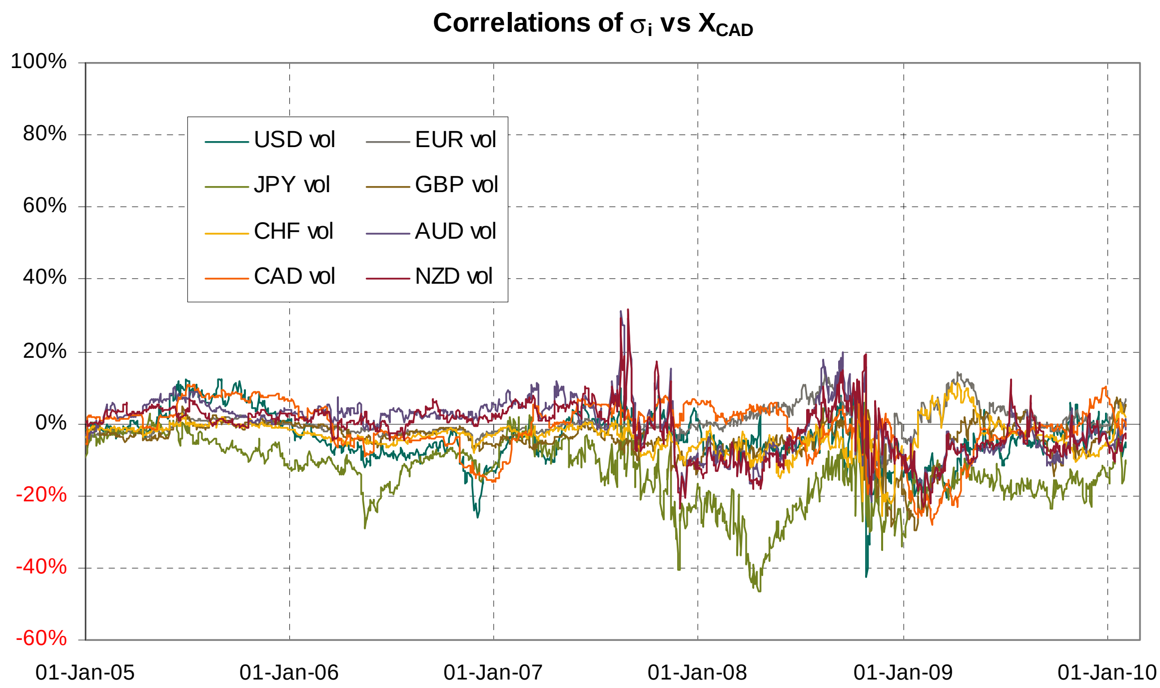


Figure 33: Historical implied correlations of $\sigma_i$ with $X_{CAD}$ for the $\upsilon_i^T = \upsilon^T$ model, from the correlation matrix $\tilde{\boldsymbol{\rho}}$. The correlation of $\sigma_{JPY}$ with $X_{CAD}$ has been consistently negative.

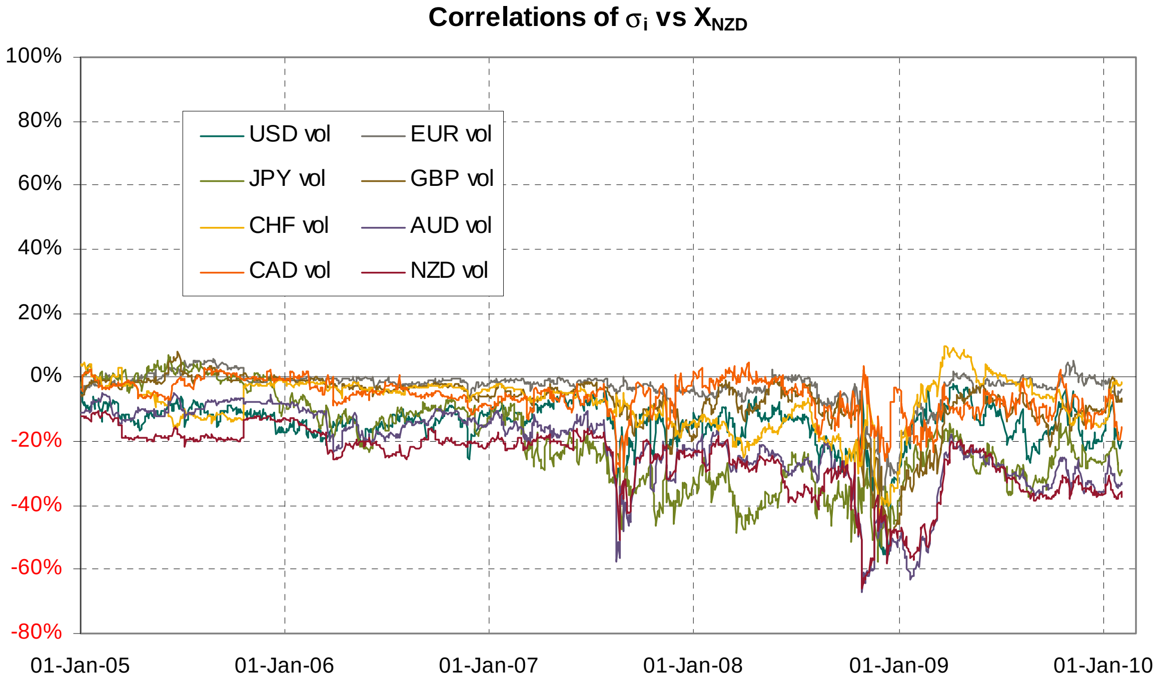


Figure 34: Historical implied correlations of $\sigma_i$ with $X_{NZD}$ for the $\upsilon_i^T = \upsilon^T$ model, from the correlation matrix $\tilde{\boldsymbol{\rho}}$. As with $AUD$, most correlations have been negative, so that any volatility increase is likely to be associated with $NZD$ weakness.

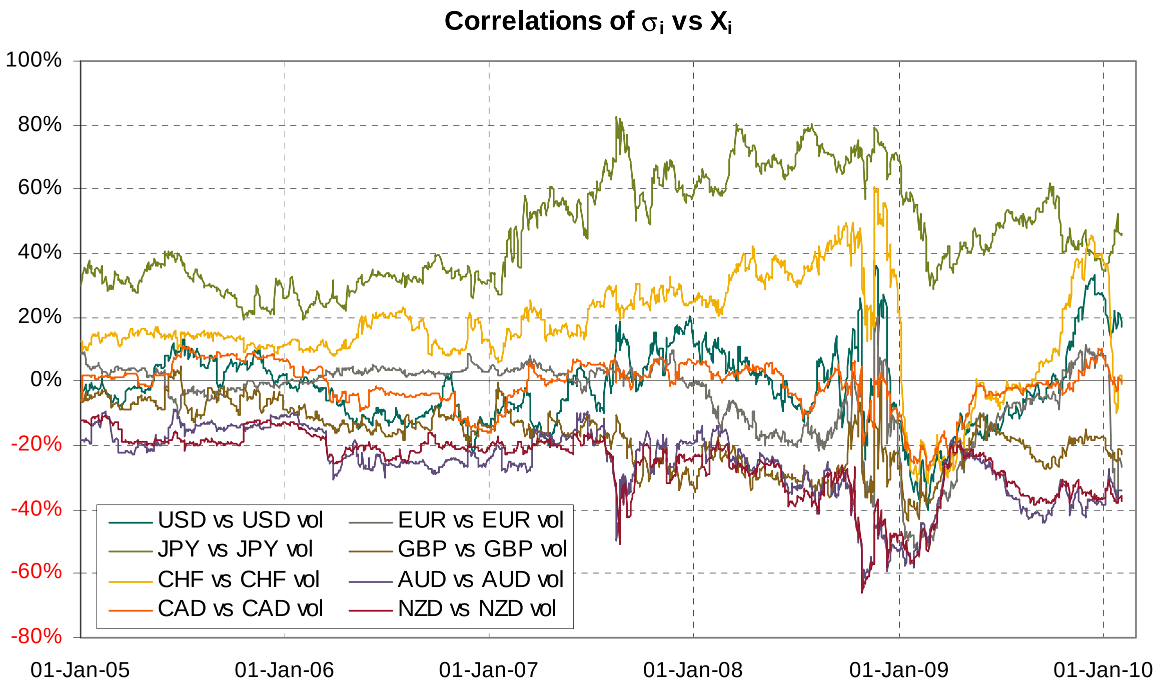


Figure 35: Historical implied correlations of $\sigma_i$ with $X_i$ (e.g. $\sigma_{USD}$ with $X_{USD}$ etc) for the $\upsilon_i^T = \upsilon^T$ model, from the correlation matrix $\tilde{\boldsymbol{\rho}}$. For the first 9 months of 2009, any increase in volatility in a currency was associated with weakness in that currency, apart from $JPY$ which has been significantly positive throughout.

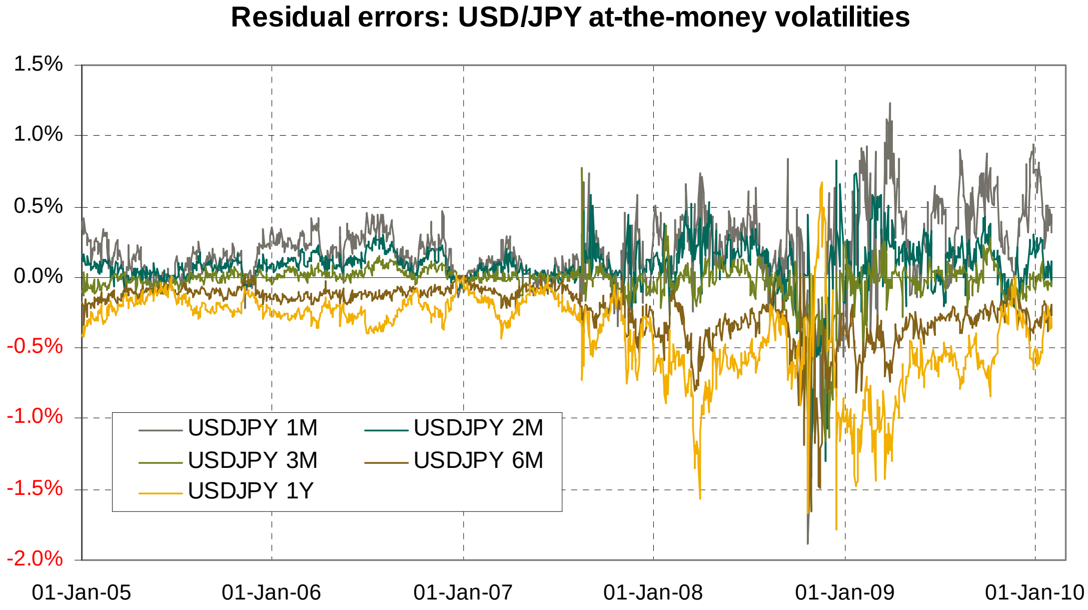


Figure 36: The residual at-the-money errors $[\varepsilon_\sigma]_{ij}^T$ for USD/JPY for the $\upsilon_i^T = \upsilon^T$ model, as defined by equation $(168)$ in appendix D.3. The 1M errors are usually positive, and the 1Y errors are usually negative, with the other tenors often lining up in between in an orderly fashion. This stongly suggests a persistent tenor dependency in the correlation matrix $\boldsymbol{\rho}$.

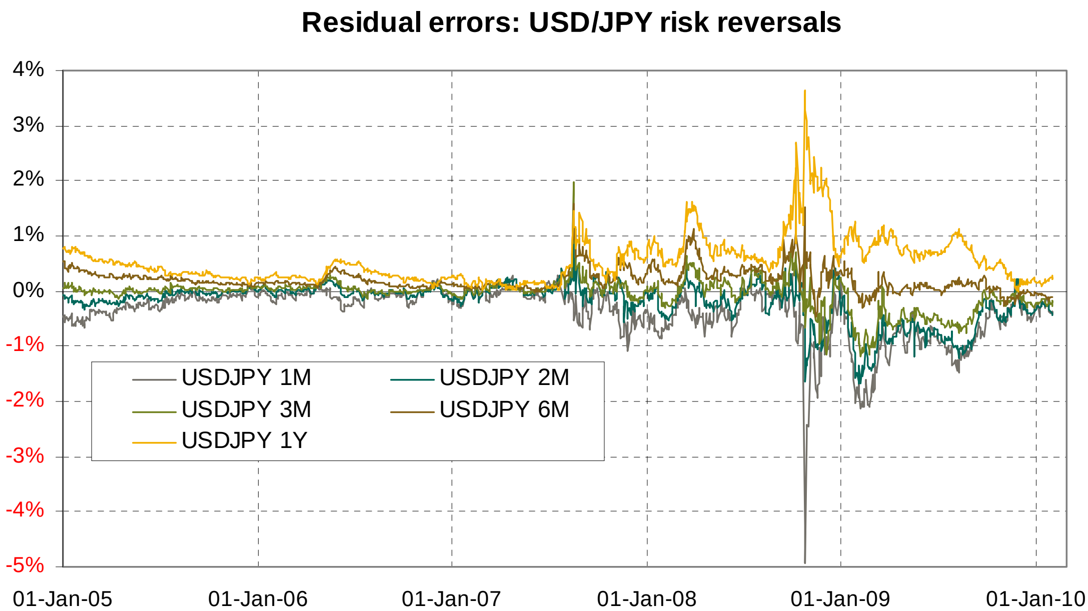


Figure 37: The residual errors in the risk reversal calibrations $[\varepsilon_{RR}]_{ij}^T$ for USD/JPY for the $\upsilon_i^T = \upsilon^T$ model, as defined by equation $(169)$ in appendix D.3. The 1M errors are often negative, and the 1Y errors are usually positive, with the other tenors often lining up in between in an orderly fashion. This stongly suggests a persistent tenor dependency in the correlation matrix $\tilde{\boldsymbol{\rho}}$.

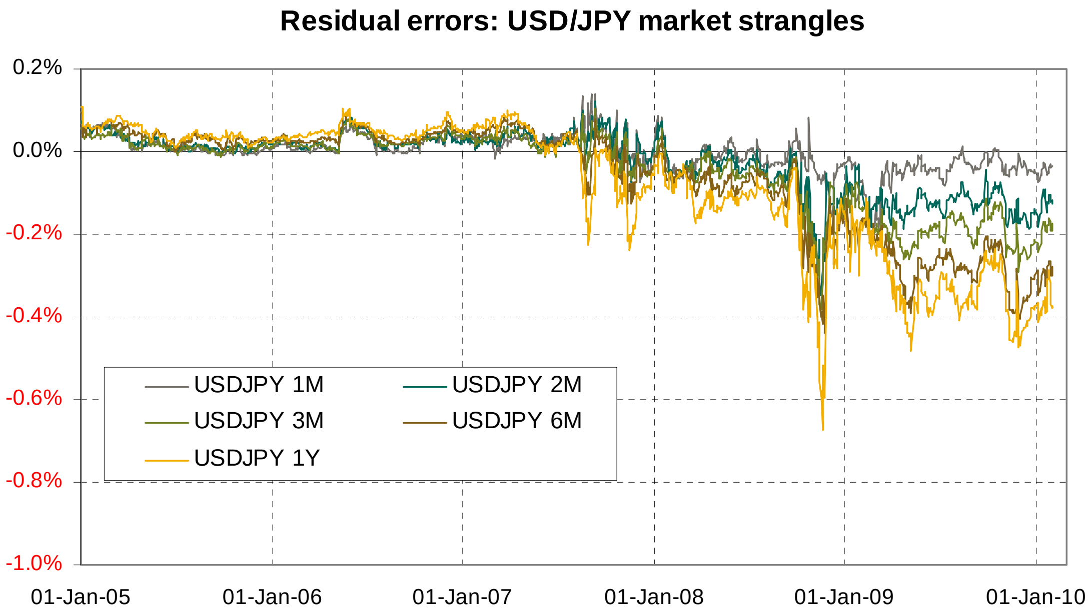


Figure 38: The residual errors in the market strangle calibrations $[\varepsilon_{MS}]_{ij}^{T}$ for USD/JPY for the $\upsilon_i^T = \upsilon^T$ model, as defined by equation $(170)$ in appendix D.3. The errors were tiny up until mid 2007 when the credit crunch started. As with the at-the-money and risk-reversal errors shown in figures 36 and 38, the fact that the errors are usually ordered from 1M to 1Y suggests tenor dependence in the correlation matrix.

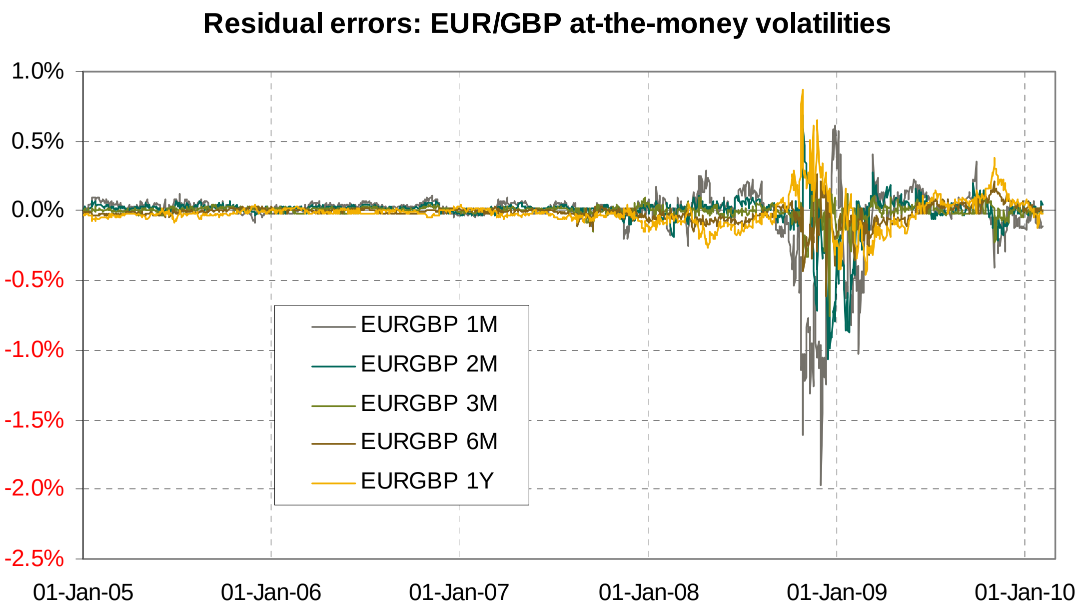


Figure 39: The residual at-the-money errors $[\varepsilon_{\sigma}]_{ij}^{T}$ for EUR/GBP for the $\upsilon_i^T = \upsilon^T$ model, as defined by equation $(168)$ in appendix D.3. Compared to the corresponding errors for USD/JPY in figure 36, there is much less order.

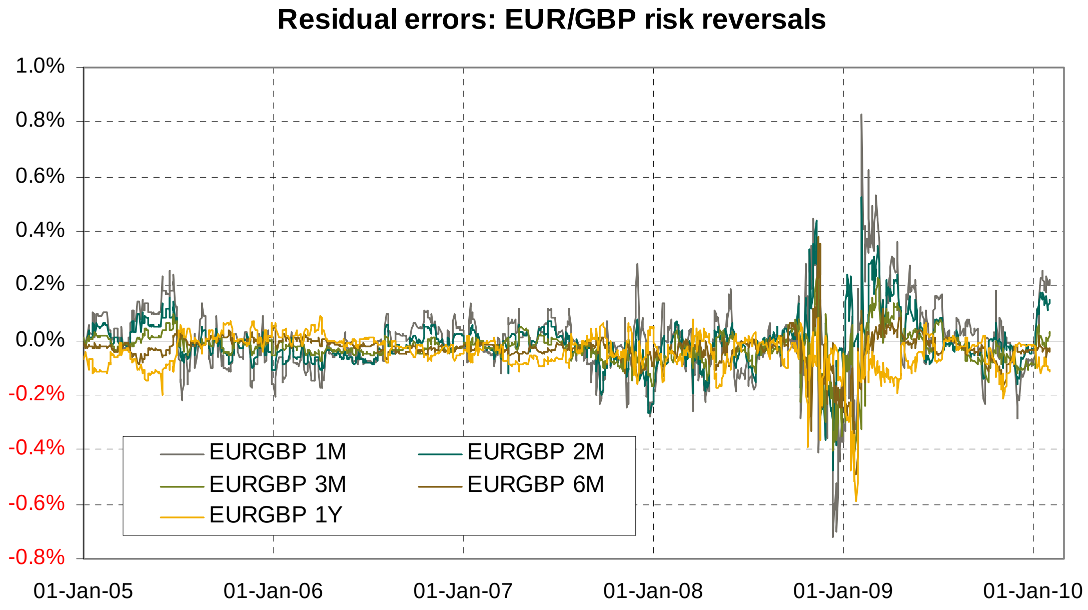


Figure 40: The residual errors in the risk reversal calibrations $[\varepsilon_{RR}]_{ij}^{T}$ for EUR/GBP for the $\upsilon_i^T = \upsilon^T$ model, as defined by equation $(169)$ in appendix D.3. Compared to the corresponding errors for USD/JPY in figure 37, there is much less order.

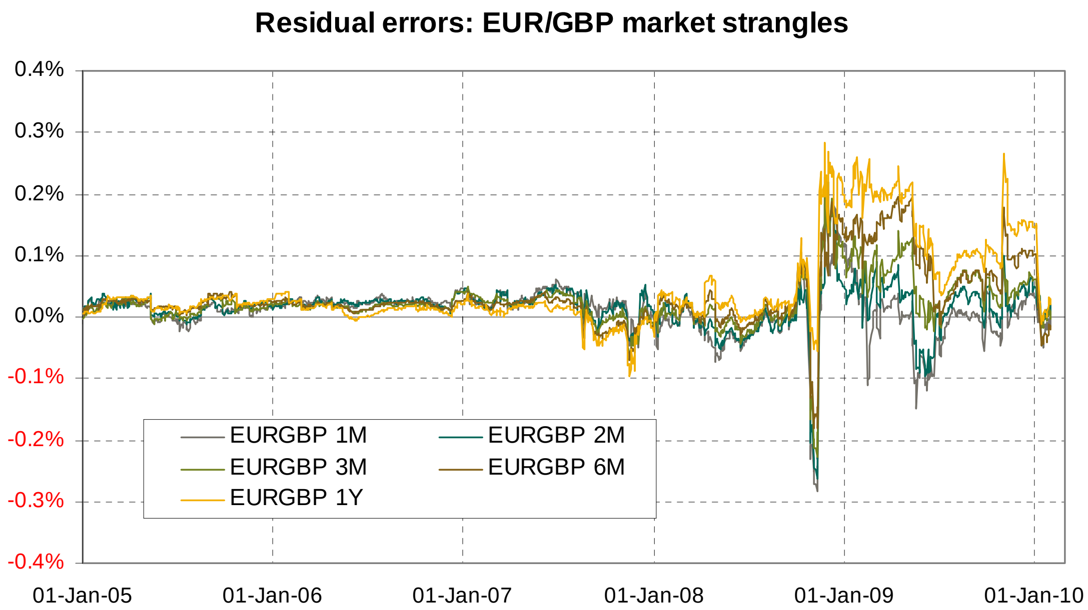


Figure 41: The residual errors in the market strangle calibrations $[\varepsilon_{MS}]_{ij}^{T}$ for EUR/GBP for the $\upsilon_i^T = \upsilon^T$ model, as defined by equation $(170)$ in appendix D.3. Compared to the corresponding errors for USD/JPY in figure 38, there is much less order.

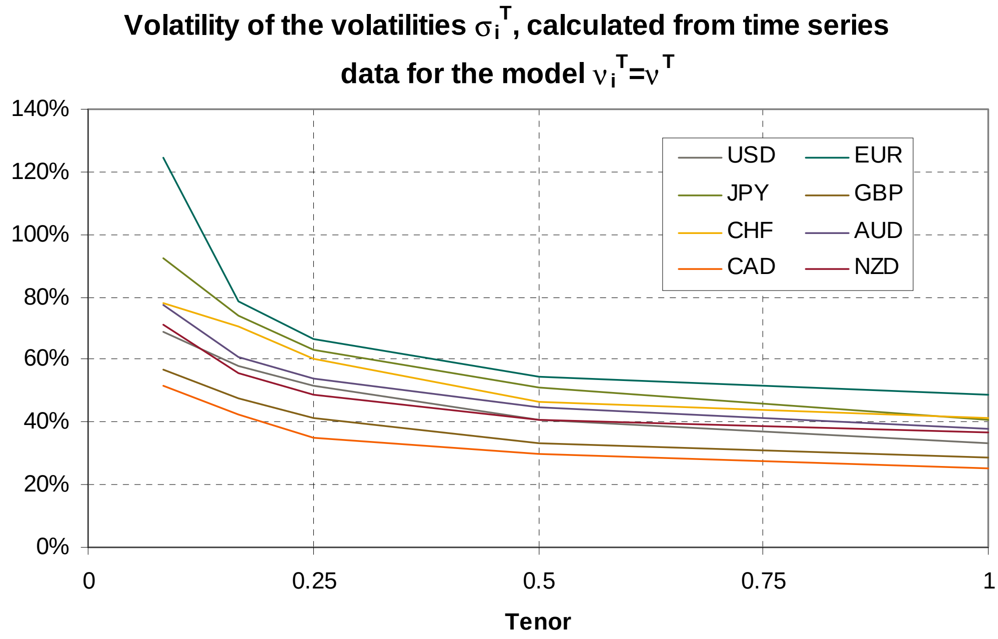


Figure 42: Realised volatilities of $\sigma_i^T$ calculated from time series data (such as the data shown in figures 10-13) for the $\upsilon_i^T = \upsilon^T$ model for the whole period from 1-Jan-2005 to 3-Feb-2010. These volatilities are significantly lower than the volatility of volatility parameters $\upsilon^T$ shown in figure 14.

| | Volatility |
|---|---|
| $X_{USD}$ | 8.2% |
| $X_{EUR}$ | 5.1% |
| $X_{JPY}$ | 12.5% |
| $X_{GBP}$ | 7.0% |
| $X_{CHF}$ | 8.7% |
| $X_{AUD}$ | 11.8% |
| $X_{CAD}$ | 9.2% |
| $X_{NZD}$ | 12.1% |

Table 6: Volatilities of $X_i$, calculated from time series data for the whole period from 1-Jan-2005 to 3-Feb-2010. These are comparable to the implied volatilities shown in figures 10-13.

## 5.4 Comparison to covariance matrix estimated from time series

As an independent way of assessing the model, the volatilities of the $X_i$ and $\sigma_i$ and the correlations between them were calculated from time series data. The time series for the $\sigma_i^T$ is already available, as shown in figures 10-13, and the time series for the $X_i$ was calculated using the methodology of [4].

Table 6 shows the realised volatilities of the $X_i$ over the period. Figure 42 shows the realised volatilities of the $\sigma_i^T$, and table 7 shows the realised correlation matrix between all the variables. In table 7, the 1M volatility $\sigma_i^{1M}$ was used as being representative of $\sigma_i$, because theoretically $\sigma_i$ is an instantaneous volatility.

Although these results are the averages realised over the period, it is instructive to compare them to the historical calibrations to implied volatility data which were presented in section 5.3. Firstly the volatilities of $X_i$ in table 6 look plausible given the graphs of implied volatilities shown in figures 10-13. Similarly, the correlations in table 7 have many of the features of the correlations seen in table 4 and in figures 16 to 35. For example, all the correlations $r_{ij}$ in table 4 are positive, which justifies including the term $(181)$ in the fitting procedure. The correlations between $X_i$ and $\sigma_{JPY}$ are all positive, as expected from figure 1, and similarly for the correlations

| | $X_{USD}$ | $X_{EUR}$ | $X_{JPY}$ | $X_{GBP}$ | $X_{CHF}$ | $X_{AUD}$ | $X_{CAD}$ | $X_{NZD}$ | $\sigma_{USD}$ | $\sigma_{EUR}$ | $\sigma_{JPY}$ | $\sigma_{GBP}$ | $\sigma_{CHF}$ | $\sigma_{AUD}$ | $\sigma_{CAD}$ | $\sigma_{NZD}$ |
|---|---|---|---|---|---|---|---|---|---|---|---|---|---|---|---|---|
| $X_{USD}$ | 1 | -0.20 | 0.44 | -0.08 | 0.12 | -0.29 | 0.10 | -0.25 | 0.14 | 0.11 | 0.17 | 0.15 | 0.12 | 0.20 | 0.12 | 0.17 |
| $X_{EUR}$ | -0.20 | 1 | 0.03 | -0.00 | 0.66 | 0.09 | 0.04 | 0.09 | 0.05 | 0.03 | 0.00 | 0.06 | 0.05 | 0.01 | -0.00 | -0.01 |
| $X_{JPY}$ | 0.44 | 0.03 | 1 | -0.20 | 0.40 | -0.51 | -0.23 | -0.45 | 0.34 | 0.16 | 0.44 | 0.24 | 0.20 | 0.28 | 0.12 | 0.25 |
| $X_{GBP}$ | -0.08 | -0.00 | -0.20 | 1 | -0.02 | 0.13 | 0.05 | 0.15 | -0.06 | -0.07 | -0.09 | -0.19 | -0.04 | -0.05 | 0.02 | -0.05 |
| $X_{CHF}$ | 0.12 | 0.66 | 0.40 | -0.02 | 1 | -0.12 | -0.01 | -0.07 | 0.20 | 0.16 | 0.19 | 0.16 | 0.20 | 0.14 | 0.06 | 0.10 |
| $X_{AUD}$ | -0.29 | 0.09 | -0.51 | 0.13 | -0.12 | 1 | 0.33 | 0.71 | -0.33 | -0.17 | -0.39 | -0.18 | -0.20 | -0.37 | -0.17 | -0.30 |
| $X_{CAD}$ | 0.10 | 0.04 | -0.23 | 0.05 | -0.01 | 0.33 | 1 | 0.26 | -0.05 | -0.04 | -0.11 | -0.03 | -0.02 | -0.09 | -0.00 | -0.05 |
| $X_{NZD}$ | -0.25 | 0.09 | -0.45 | 0.15 | -0.07 | 0.71 | 0.26 | 1 | -0.23 | -0.09 | -0.30 | -0.14 | -0.11 | -0.29 | -0.12 | -0.27 |
| $\sigma_{USD}$ | 0.14 | 0.05 | 0.34 | -0.06 | 0.20 | -0.33 | -0.05 | -0.23 | 1 | 0.24 | 0.55 | 0.45 | 0.40 | 0.42 | 0.30 | 0.36 |
| $\sigma_{EUR}$ | 0.11 | 0.03 | 0.16 | -0.07 | 0.16 | -0.17 | -0.04 | -0.09 | 0.24 | 1 | 0.30 | 0.22 | 0.56 | 0.19 | 0.09 | 0.19 |
| $\sigma_{JPY}$ | 0.17 | 0.00 | 0.44 | -0.09 | 0.19 | -0.39 | -0.11 | -0.30 | 0.55 | 0.30 | 1 | 0.44 | 0.47 | 0.57 | 0.29 | 0.50 |
| $\sigma_{GBP}$ | 0.15 | 0.06 | 0.24 | -0.19 | 0.16 | -0.18 | -0.03 | -0.14 | 0.45 | 0.22 | 0.44 | 1 | 0.33 | 0.40 | 0.26 | 0.39 |
| $\sigma_{CHF}$ | 0.12 | 0.05 | 0.20 | -0.04 | 0.20 | -0.20 | -0.02 | -0.11 | 0.40 | 0.56 | 0.47 | 0.33 | 1 | 0.35 | 0.19 | 0.33 |
| $\sigma_{AUD}$ | 0.20 | 0.01 | 0.28 | -0.05 | 0.14 | -0.37 | -0.09 | -0.29 | 0.42 | 0.19 | 0.57 | 0.40 | 0.35 | 1 | 0.36 | 0.76 |
| $\sigma_{CAD}$ | 0.12 | -0.00 | 0.12 | 0.02 | 0.06 | -0.17 | -0.00 | -0.12 | 0.30 | 0.09 | 0.29 | 0.26 | 0.19 | 0.36 | 1 | 0.35 |
| $\sigma_{NZD}$ | 0.17 | -0.01 | 0.25 | -0.05 | 0.10 | -0.30 | -0.05 | -0.27 | 0.36 | 0.19 | 0.50 | 0.39 | 0.33 | 0.76 | 0.35 | 1 |

Table 7: Correlation matrix calculated from time series data for the whole period from 1-Jan-2005 to 3-Feb-2010 for the $\upsilon_i^T = \upsilon^T$.model. Many of the broad characteristics which were present in the correlation matrix shown in table 4 are present in this correlation matrix as well.

between $X_i$ and $\sigma_{CHF}$ as seen in figure 31. The correlations $\rho_{ij}$ in the top right hand quadrant of table 7 also look like plausible averages of the correlations seen in figures 16 to 19, for example there is a large $X_{EUR}$-$X_{CHF}$ correlation and a large $X_{AUD}$-$X_{NZD}$ correlation.

The biggest discrepancy is in the comparison of figure 42 to figure 14, because the $\upsilon^T$ calibrated to a snapshot of market data from the forex option market are significantly larger than the realised volatilities of $\sigma_i^T$. One possible explanation is that the forex option market has high implied $\upsilon^T$ parameters because it's trying to cater for the possibility of unexpected jumps in the forex market, and since it's a pure diffusion model the stochastic intrinsic currency volatility model does not allow jumps.

# 6 Potential applications

The stochastic intrinsic currency volatility framework has many potential applications, which are the subject of current research:

- As mentioned in the introduction, one possible use of this model is in the calculation of volatility curves for less liquid currency pairs. The fitting procedure described in appendix D.3 involves minimising the errors between the model and market. The minimisation procedure takes all available data, so if e.g. only at-the-money volatilities are available for a particular currency pair, then the risk reversal and market strangle data can be omitted from the minimisation procedure. In that situation the maximum entropy principle that is incorporated into the fitting procedure will end up deriving values for the missing degrees of freedom, given all the other data that's available. Hence the model will output values for the missing market data. The same idea applies if at-the-money volatilities are also not available.

  An example of this was given in the previous work [5], in connection with the log-normal model calibrated to data for the same eight currencies that were considered here in section 5. Once the model had been calibrated to the eight currencies, market data for USD/SEK and EUR/SEK was then added, and the model then output values for at-the-money NZD/SEK volatilities. The main discrepancies occurred when the market was stressed, but in very stressed situations it's not clear that the market data for an illiquid currency pair like NZD/SEK is reliable, so the model values may have be reasonable after all.

- The original intrinsic currency valuation framework[3] suggested currency square trading strategies, to arbitrage inconsistencies between the at-the-money volatilities of related currency pairs. The basic idea was to look at the residual error terms, i.e. (model value) - (market values), and put on trades which bet that if there was a big discrepancy then the discrepancy will get eliminated over time. The same strategy can be applied to the discrepancies seen with the new model. Incorporating the risk reversal and market strangles creates a more realistic model of the forex market, so it may turn out that the trading ideas that come out of this model might be better than the trading ideas that arise from the original log-normal model.

- Beyond vanilla forex options, the model also has applications in the pricing of more complex multi-currency option structures. As mentioned in the introduction, for an option on a basket of currencies against one other currency, models are typically just calibrated to the volatility curves for all the currencies in the basket against the other currency. However, the stochastic intrinsic currency volatility framework also includes a calibration to the volatility curves of all the currency pairs between the currencies in the basket, so it should produce a more accurate result. The same would be true for other complex multi-currency derivatives. However, the approximation formula $(11)$ is no help in pricing such derivatives, because it just relates to vanilla options. Further work would be required to derive other approximation formulas, or to develop techniques to improve the efficiency of a Monte Carlo implementation of the underlying model $(6)$-$(8)$.

- As with the original work [3], one application is in the trading and risk management of forex option portfolios involving many currency pairs. For example, working out the sensitivity of a portfolio to e.g. $\sigma_{JPY}$ should give an accurate measure of the risks that the portfolio has in connection with a single currency.
- The model could be used to provide realistic simulations of the future movements of forex rates. The implied volatility curves in the forex market describe the multivariate probability distribution of the expected movements of all the currencies pairs, however this is probably the first model that can use all this information in a consistent way.
- The article [4] built on the original work [3] to produce a methodology for estimating intrinsic currency values themselves. The same will be possible with the new model described in this article. Given that incorporating risk reversals and market strangles into the intrinsic currency framework results in a more realistic description of the forex market, then associated estimates of intrinsic currency values should be more accurate as well.

# 7 Conclusion

This article has used the intrinsic currency concept to devise a stochastic volatility framework that, for a given set of currencies, can fit all the associated implied forex volatility curves simultaneously. The stochastic processes of the framework were defined to make the system symmetric with respect to a change in numéraire currency, which means that the processes for all forex rates, inverse forex rates and cross forex rates, have the same form as each other. Given this framework, the main result of this article is formula $(11)$, which are approximations for the implied volatility curves of forex rates in terms of the model parameters. All the mathematical details of the model are in the appendix.

The model was fitted historically to market data going back to the start of 2005. Section 5 discussed the calibration results, and showed that the fits are at least as good as the fits that were possible with the original log-normal intrinsic currency framework, but now fitting risk reversals and market strangles in addition to the at-the-money volatilities. The biggest discrepancy between the calibrated model and the market relates to the volatility of the observed stochastic volatilities, as presented in section 5.4. The volatilities of the time series of $\sigma_i$ seem to be significantly lower than the volatility of volatility parameters that are required to fit the market data. It is possible that the high volatility of volatility parameters that the calibrations produce are connected with the model's attempt to account for possible jumps in the underlying forex rates, which the model does not cater for explicitly.

Finally, section 6 discussed possible applications of this model, which are the subject of current research.

# Appendix

## A : Symmetrised SABR for modelling individual forex rates

Suppose that a forward forex rate $F$ follows a SABR process as specified by $(2)$-$(4)$. Then using Itô's lemma, it is straightforward to show that the inverse rate follows the process

$$\frac{dF^{-1}}{F^{-1}} = \varepsilon^2\sigma^2 dt - \varepsilon\sigma dW_1 \quad , \tag{27}$$

where $\sigma$ still follows the process $(3)$. The units of $F^{-1}$ are the inverse of the units of $F$, so to use $F^{-1}$ to analyse transactions, the natural thing to do is to make a measure change so that option values are calculated in the other currency of the currency pair. This measure change can be written

$$dW_1 \rightarrow dW_1' = -dW_1 + \varepsilon\sigma dt \quad . \tag{28}$$

To calculate the effect of this measure change on the stochastic process for $\sigma$, use the Bartlett decomposition on $dW_2$ and write

$$dW_2 = \rho dW_1 + \sqrt{1-\rho^2}dW_1^{\perp} \quad , \text{ where } \quad dW_1 dW_1^{\perp} = 0 \quad . \tag{29}$$

Then defining $dW_2'$ by

$$dW_2' = -\rho dW_1' + \sqrt{1-\rho^2}dW_1^{\perp} \quad , \tag{30}$$

it is clear that the measure change $(28)$ induces the change

$$dW_2 \rightarrow dW_2' = dW_2 - \varepsilon\rho\sigma dt \quad , \tag{31}$$

on $dW_2$. Hence that after the measure change, the stochastic differential equations for the system are

$$\frac{dF^{-1}}{F^{-1}} = \varepsilon\sigma dW_1' \quad , \tag{32}$$

$$\frac{d\sigma}{\sigma} = \varepsilon^2\rho\sigma\upsilon dt + \varepsilon\upsilon dW_2' \quad , \tag{33}$$

$$dW_1' dW_2' = -\rho dt \quad . \tag{34}$$

This means that instead of $(3)$, the process for $\sigma$ is now given by $(33)$, so the form of the stochastic processes for the inverse forex rate are different. However, if instead of using $(3)$ the stochastic processes for $\sigma$ is defined by

$$\frac{d\sigma}{\sigma} = -\frac{1}{2}\varepsilon^2\rho\sigma\upsilon dt + \varepsilon\upsilon dW_2 \quad , \tag{35}$$

then following the measure change the revised process for $\sigma$ becomes

$$\frac{d\sigma}{\sigma} = \frac{1}{2}\varepsilon^2\rho\sigma\upsilon dt + \varepsilon\upsilon dW_2' \quad . \tag{36}$$

This has the same form as $(35)$ because following the measure change the correlation between $dW_1'$ and $dW_2'$ is $-\rho$.

In terms of the implied volatility approximation formula, working through the full derivation of $(5)$ but using $(2)$, $(35)$ and $(4)$ as the starting point, the effect is a slight simplification of the formula. The result is

$$\sigma_B = \varepsilon\sigma\frac{z}{\tilde{x}(z)}\left(1 + \frac{2-3\rho^2}{24}\upsilon^2\varepsilon^2\tau_{ex}\right) \quad . \tag{37}$$

Even though this methodology restores symmetry between a forex rate and its inverse, if two forex rates with a common currency both follow these symmetrised SABR processes then the corresponding cross rate for the other two currencies will still follow a stochastic process with a different form. However, by describing the behaviour of the forex market in terms of intrinsic currency variables, the stochastic intrinsic currency volatility methodology presented in appendix B defines a fully consistent framework which circumvents these problems.

# B : Justification of the Stochastic Intrinsic Currency Volatility Framework

The purpose of this appendix is to show that the stochastic processes $(6)$-$(8)$ posses the right properties for modelling the forex rates $X_{ij}$, given by $(1)$.

The first thing to check is that the processes for $X_i$ in $(6)$ produce the correct risk-neutral processes for the $X_{ij}$. Using Itô's lemma shows that

$$\frac{dX_{ij}}{X_{ij}} = \left(r_j - r_i + \varepsilon^2\rho_{ik}\sigma_i\sigma_k - \varepsilon^2\rho_{jk}\sigma_j\sigma_k - \varepsilon^2\rho_{ij}\sigma_i\sigma_j + \varepsilon^2\sigma_j^2\right)dt + \varepsilon\sigma_i dW_i - \varepsilon\sigma_j dW_j \quad . \tag{38}$$

Recall that the forex rate $X_{ij}$ is the number of units of currency $j$ corresponding to one unit of currency $i$, so its natural units[3] are in currency $j$. Choosing the numéraire $k = j$, then it is easy to see that $(38)$ reduces to

$$\frac{dX_{ij}}{X_{ij}} = (r_j - r_i)\,dt + \varepsilon\sigma_i dW_i - \varepsilon\sigma_j dW_j \quad , \tag{39}$$

which is the correct risk-neutral processes for a forex rate $X_{ij}$ when using currency $j$ as numéraire. Hence $(6)$ produces the correct risk-neutral processes for $X_{ij}$.

The other thing to check is the drift term for the volatility process $(7)$. The important thing about the drift term is that it preserves symmetry with respect to change of numéraire currency. To see this, using the Bartlett decomposition then $\mathbf{dZ}$ can be written

$$\mathbf{dZ} = \tilde{\boldsymbol{\rho}}\boldsymbol{\rho}^{-1}\mathbf{dW} + \mathbf{A}\mathbf{dW}^{\perp} \tag{40}$$

where

$$\mathbf{A}\mathbf{A}' = \mathbf{r} - \tilde{\boldsymbol{\rho}}\boldsymbol{\rho}^{-1}\tilde{\boldsymbol{\rho}}' \quad , \quad \mathbf{dW}\mathbf{dW}^{\perp\prime} = 0 \quad , \quad \mathbf{dW}^{\perp}\mathbf{dW}^{\perp\prime} = \mathbf{I}dt \quad , \tag{41}$$

and where $\mathbf{I}$ is the identity matrix. The matrix $\mathbf{r} - \tilde{\boldsymbol{\rho}}\boldsymbol{\rho}^{-1}\tilde{\boldsymbol{\rho}}'$ is a Schur complement, and can be interpreted as the conditional variance of $\mathbf{dZ}$ given $\mathbf{dW}$. Hence it is guaranteed to be positive definite so the matrix $\mathbf{A}$ exists, for example, it could be the Cholesky decomposition of $\mathbf{r} - \tilde{\boldsymbol{\rho}}\boldsymbol{\rho}^{-1}\tilde{\boldsymbol{\rho}}'$.

Switching numéraire from currency $k$ to currency $l$ is accomplished with a measure change given by

$$dW_i = d\tilde{W}_i + \varepsilon\left(\rho_{il}\sigma_l - \rho_{ik}\sigma_k\right)dt \tag{42}$$

where $d\tilde{W}_i$ is the new Weiner process following the measure change. Substituting $(42)$ in $(6)$ shows that

$$\frac{dX_i}{X_i} = \left(\tilde{\lambda} - r_i + \varepsilon^2\rho_{il}\sigma_i\sigma_l\right)dt + \varepsilon\sigma_i d\tilde{W}_i \quad , \tag{43}$$

which has the same form as $(6)$ except that the index $k$ has been replaced by $l$. In vector notation, $(42)$ can be written

$$\mathbf{dW} = \mathbf{d\tilde{W}} + \varepsilon\left(\boldsymbol{\rho}\boldsymbol{\sigma}^{(l)} - \boldsymbol{\rho}\boldsymbol{\sigma}^{(k)}\right)dt \quad , \tag{44}$$

where $\boldsymbol{\sigma}^{(k)}$ is a column vector where the $k^{\text{th}}$ row is $\sigma_k$ and all other elements are zero. Then given $(40)$ which defines $\mathbf{dZ}$ in terms of $\mathbf{dW}$ and $\mathbf{dW}^{\perp}$, define the Weiner process $\mathbf{d\tilde{Z}}$ to have the same relationship to $\mathbf{d\tilde{W}}$ and $\mathbf{dW}^{\perp}$, i.e. define

$$\mathbf{d\tilde{Z}} = \tilde{\boldsymbol{\rho}}\boldsymbol{\rho}^{-1}\mathbf{d\tilde{W}} + \mathbf{A}\mathbf{dW}^{\perp} \quad . \tag{45}$$

Then substituting $(44)$ into $(40)$ and using $(45)$ shows that $\mathbf{dZ}$ can be written in terms of $\mathbf{d\tilde{Z}}$ by

$$\mathbf{dZ} = \mathbf{d\tilde{Z}} + \varepsilon\left(\tilde{\boldsymbol{\rho}}\boldsymbol{\sigma}^{(l)} - \tilde{\boldsymbol{\rho}}\boldsymbol{\sigma}^{(k)}\right)dt \quad . \tag{46}$$

[3] See [8] for a discussion of natural payoffs versus unnatural payoffs. That article shows that since the natural units of forex rate $X_{ij}$ are units of currency $j$, if one wants to regard it as being in different units (e.g. currency $i$) then a convexity correction applies when calculating its forward value.

Now substituting $(46)$ into $(7)$ shows that after the measure change the revised stochastic process for $\sigma_i$ is

$$\frac{d\sigma_i}{\sigma_i} = \varepsilon^2 \tilde{\rho}_{il} \upsilon_i \sigma_l dt + \varepsilon \upsilon_i d\tilde{Z}_i \quad . \tag{47}$$

Hence the new stochastic processes $(43)$ and $(47)$, where currency $l$ is the numéraire, have the same form as the original stochastic processes $(6)$ and $(7)$ when currency $k$ was the numéraire. Thus the processes $(6)$ and $(7)$ produce the correct risk-neutral process for $X_{ij}$, and possesses the correct symmetries with respect to changing the numéraire currency.

# C : Derivation of the main formulas

This appendix will use the same techniques that were used in Hagan et al [1] and in [2] to solve the backwards Kolmogorov equation for the stochastic processes $(6)$-$(8)$, and hence derive formula $(11)$ which is the main result of this article. Note that rather than working through the solution to the backwards Kolmogorov equation, an alternative way to verify the result is to differentiate $P(\tau, z, \sigma_i, \sigma_j)$ from $(121)$ with respect to $z$, $\sigma_i, \sigma_j$ and $\tau$. Then substituting the required derivatives[4] into $(69)$ below shows that $(121)$ satisfies $(69)$ up to and including $O(\varepsilon^2)$.

The stochastic processes $(6)$-$(8)$ for $X_i$ and $(38)$ for $X_{ij}$ are defined in terms of spot values, however it will be convenient to work with the forward values of instead. So given a fixed expiry time $T_{ex} > t$, define the forward values of $X_i$ and $X_{ij}$ by

$$X_i^F = X_i \exp\left(\left(\tilde{\lambda} - r_i\right)(T_{ex} - t)\right) \quad , \tag{48}$$

$$X_{ij}^F = \frac{X_i^F}{X_j^F} \quad , \tag{49}$$

and write

$$\tau_{ex} = T_{ex} - t \quad . \tag{50}$$

Then given $(6)$ and $(38)$, $X_i^F$ follows the stochastic process

$$\frac{dX_i^F}{X_i^F} = \varepsilon^2 \rho_{ik} \sigma_i \sigma_k dt + \varepsilon \sigma_i dW_i \quad , \tag{51}$$

[4]The required derivatives are

$$\frac{\partial P}{\partial \tau} = P\left(-\frac{1}{2\tau} + \frac{x^2}{2\tau^2} + \varepsilon^2 \kappa\right) \quad ,$$

$$\frac{\partial P}{\partial z} = P\left(\frac{n-\frac{3}{2}}{J}\frac{\partial J}{\partial z} + \frac{\varepsilon \sigma_{ij}}{2} + \varepsilon^2\left(\frac{a_1 \sigma_{ij}}{2} + a_3 + a_4 - \frac{a_5}{2}\right)\frac{z}{J^2} - \frac{1}{J}\frac{x}{\tau}\right) \quad ,$$

$$\frac{\partial^2 P}{\partial z^2} = P\left(\begin{array}{c} \frac{\left(n-\frac{3}{2}\right)\left(n-\frac{5}{2}\right)}{J^2}\left(\frac{\partial J}{\partial z}\right)^2 + \frac{\varepsilon^2 \sigma_{ij}^2}{4} + \varepsilon \sigma_{ij}\frac{n-\frac{3}{2}}{J}\frac{\partial J}{\partial z} + \frac{n-\frac{3}{2}}{J}\frac{\partial^2 J}{\partial z^2} + \varepsilon^2\left(\frac{a_1\sigma_{ij}}{2} + a_3 + a_4 - \frac{a_5}{2}\right)\frac{1}{J^2} \\ -\left(2\frac{n-2}{J^2}\frac{\partial J}{\partial z} + \varepsilon\sigma_{ij}\frac{1}{J} + 2\frac{\varepsilon^2 z}{J^3}\left(\frac{a_1\sigma_{ij}}{2} + a_3 + a_4 - \frac{a_5}{2}\right)\right)\frac{x}{\tau} \\ + \frac{x^2}{\tau^2 J^2} - \frac{1}{\tau J^2} + O\left(\varepsilon^2\right) \end{array}\right) \quad ,$$

$$\frac{\partial P}{\partial \sigma_k} = P\left(\frac{n-1}{\sigma_{ij}}\frac{\partial \sigma_{ij}}{\partial \sigma_k} + \frac{n-\frac{3}{2}}{J}\frac{\partial J}{\partial \sigma_k} + \frac{\varepsilon z}{2}\frac{\partial \sigma_{ij}}{\partial \sigma_k} - \frac{x}{\tau}\frac{\partial x}{\partial \sigma_k} + O\left(\varepsilon^2\right)\right) \quad \text{, where } k \text{ can be either } i \text{ or } j,$$

$$\frac{\partial^2 P}{\partial \sigma_i \partial \sigma_j} = P\left(\frac{(n-1)(n-2)}{\sigma_{ij}^2}\frac{\partial \sigma_{ij}}{\partial \sigma_i}\frac{\partial \sigma_{ij}}{\partial \sigma_j} + \frac{n-1}{\sigma_{ij}}\frac{\partial^2 \sigma_{ij}}{\partial \sigma_i \partial \sigma_j} + O(\varepsilon)\right) \quad ,$$

$$\frac{\partial^2 P}{\partial \sigma_k^2} = P\left(\frac{(n-1)(n-2)}{\sigma_{ij}^2}\left(\frac{\partial \sigma_{ij}}{\partial \sigma_k}\right)^2 + \frac{n-1}{\sigma_{ij}}\frac{\partial^2 \sigma_{ij}}{\partial \sigma_k^2} + O(\varepsilon)\right) \quad ,$$

$$\frac{\partial^2 P}{\partial z \partial \sigma_k} = P\left(\begin{array}{c} \frac{n-1}{\sigma_{ij}}\frac{n-\frac{3}{2}}{J}\frac{\partial \sigma_{ij}}{\partial \sigma_k}\frac{\partial J}{\partial z} + \varepsilon\frac{n}{2}\frac{\partial \sigma_{ij}}{\partial \sigma_k} + \frac{n-\frac{3}{2}}{J}\frac{\partial^2 J}{\partial z \partial \sigma_k} + \frac{x^2}{\tau^2}\frac{1}{J}\frac{\partial x}{\partial \sigma_k} - \frac{1}{\tau J}\frac{\partial x}{\partial \sigma_k} \\ -\left(\frac{n-1}{\sigma_{ij}}\frac{\partial \sigma_{ij}}{\partial \sigma_k}\frac{1}{J} + \frac{n-\frac{3}{2}}{J^2}\frac{\partial J}{\partial \sigma_k} + \frac{\varepsilon z}{2}\frac{\partial \sigma_{ij}}{\partial \sigma_k}\frac{1}{J} + \frac{\partial^2 x}{\partial z \partial \sigma_k}\right)\frac{x}{\tau} + O(\varepsilon) \end{array}\right) \quad ,$$

$$D_\sigma\left(\frac{\partial P}{\partial z}\right) = P\left(\begin{array}{c} (n-1)\left(n-\frac{3}{2}\right)\frac{a_1}{J}\frac{\partial J}{\partial z} + \varepsilon\frac{n}{2}\sigma_{ij}a_1 + \frac{n-\frac{3}{2}}{J}D_\sigma\left(\frac{\partial J}{\partial z}\right) + \frac{x^2}{\tau^2}\frac{D_\sigma(x)}{J} - \frac{1}{\tau}\frac{D_\sigma(x)}{J} \\ -\left((n-1)\frac{a_1}{J} + \frac{n-\frac{3}{2}}{J^2}D_\sigma(J) + \varepsilon\frac{z}{2}\sigma_{ij}\frac{a_1}{J} + \varepsilon\frac{1}{J^3}a_5 z\right)\frac{x}{\tau} + O(\varepsilon) \end{array}\right) \quad .$$

and $X_{ij}^F$ follows the stochastic process

$$\frac{dX_{ij}^F}{X_{ij}^F} = \varepsilon^2 \left(\rho_{ik}\sigma_i\sigma_k - \rho_{jk}\sigma_j\sigma_k - \rho_{ij}\sigma_i\sigma_j + \sigma_j^2\right) dt + \varepsilon\sigma_i dW_i - \varepsilon\sigma_j dW_j \quad . \tag{52}$$

To derive formula $(11)$, it is sufficient to focus on the case where the forward forex rate $X_{ij}^F$ is modelled using currency $j$ as numéraire. In what follows, the indices $i$ and $j$ will be regarded as referring to particular currency indices, and the index $k$ will be used whenever a formula is true for either $i$ or $j$. Hence with currency $j$ as numéraire, $(52)$ simplifies to

$$\frac{dX_{ij}^F}{X_{ij}^F} = \varepsilon\sigma_i dW_i - \varepsilon\sigma_j dW_j \quad , \tag{53}$$

and from $(7)$ the volatility processes are

$$\frac{d\sigma_k}{\sigma_k} = \varepsilon^2 \tilde{\rho}_{kj}\upsilon_k\sigma_j dt + \varepsilon\upsilon_k dZ_k \quad , \tag{54}$$

where $k$ is either $i$ or $j$, and with the correlations between the processes specified by $(8)$.

Let $p\left(t, X_{ij}^F, \sigma_i, \sigma_j; T_{ex}, \bar{X}_{ij}^F, \bar{\sigma}_i, \bar{\sigma}_j\right)$ be the transition probability density function from time $t$ to time $T_{ex} \geqslant t$, corresponding to the stochastic differential equations $(53)$ and $(54)$. Then $p$ will satisfy the forwards Kolmogorov equation with respect to the variables $T_{ex}$, $\bar{X}_{ij}^F$, $\bar{\sigma}_i$ and $\bar{\sigma}_j$, and the backwards Kolmogorov equation with respect to the variables $t$, $X_{ij}^F$, $\sigma_i$ and $\sigma_j$, in both cases with the boundary condition

$$p\left(t, X_{ij}^F, \sigma_i, \sigma_j; T_{ex}, \bar{X}_{ij}^F, \bar{\sigma}_i, \bar{\sigma}_j\right) = \delta\left(X_{ij}^F - \bar{X}_{ij}^F\right) \delta\left(\sigma_i - \bar{\sigma}_i\right) \delta\left(\sigma_j - \bar{\sigma}_j\right) \quad \text{when} \quad t = T_{ex} \quad . \tag{55}$$

Following the ideas in [2], one way to approach option pricing is to focus on the call option pricing formula

$$V\left(\tau, X_{ij}^F, \sigma_i, \sigma_j; K\right) = \int_0^\infty \left(\bar{X}_{ij}^F - K\right)^+ P\left(\tau, X_{ij}^F, \sigma_i, \sigma_j; \bar{X}_{ij}^F\right) d\bar{X}_{ij}^F \quad , \tag{56}$$

and aim to calculate $P\left(\tau, X_{ij}^F, \sigma_i, \sigma_j; \bar{X}_{ij}^F\right)$. The density $P\left(\tau, X_{ij}^F, \sigma_i, \sigma_j; \bar{X}_{ij}^F\right)$ is related to $p$ by

$$P\left(\tau, X_{ij}^F, \sigma_i, \sigma_j; \bar{X}_{ij}^F\right) = \int_0^\infty p\left(t, X_{ij}^F, \sigma_i, \sigma_j; t+\tau, \bar{X}_{ij}^F, \bar{\sigma}_i, \bar{\sigma}_j\right) d\bar{\sigma}_i d\bar{\sigma}_j \quad , \tag{57}$$

Differentiating under the integral sign in $(57)$ shows that $P$ must satisfy the backwards Kolmogorov equation, which is given by

$$\begin{aligned} \frac{\partial P}{\partial \tau} = \frac{1}{2}\varepsilon^2\sigma_{ij}^2 X_{ij}^{F2} \frac{\partial^2 P}{\partial X_{ij}^{F2}} + \frac{1}{2}\varepsilon^2\upsilon_i^2\sigma_i^2 \frac{\partial^2 P}{\partial \sigma_i^2} + \frac{1}{2}\varepsilon^2\upsilon_j^2\sigma_j^2 \frac{\partial^2 P}{\partial \sigma_j^2} + \varepsilon^2 X_{ij}^F \sigma_{ij} D_\sigma \left(\frac{\partial P}{\partial X_{ij}^F}\right) \\ + \varepsilon^2 r_{ij}\upsilon_i\upsilon_j\sigma_i\sigma_j \frac{\partial^2 P}{\partial\sigma_i\partial\sigma_j} + \varepsilon^2\tilde{\rho}_{ij}\upsilon_i\sigma_i\sigma_j \frac{\partial P}{\partial \sigma_i} + \varepsilon^2\tilde{\rho}_{jj}\upsilon_j\sigma_j^2 \frac{\partial P}{\partial \sigma_j} \quad , \end{aligned} \tag{58}$$

where $D_\sigma$ is the differential operator defined by

$$D_\sigma = \sigma_i\zeta_i \frac{\partial}{\partial\sigma_i} - \sigma_j\zeta_j \frac{\partial}{\partial\sigma_j} \quad , \tag{59}$$

where $\zeta_i$ and $\zeta_j$ were defined in $(21)$. Then substituting $(55)$ into $(57)$ shows that $P\left(\tau, X_{ij}^F, \sigma_i, \sigma_j; \bar{X}_{ij}^F\right)$ satisfies the boundary condition

$$P\left(\tau, X_{ij}^F, \sigma_i, \sigma_j; \bar{X}_{ij}^F\right) = \delta\left(X_{ij}^F - \bar{X}_{ij}^F\right) \quad \text{at} \quad \tau = 0 \quad . \tag{60}$$

Instead of focussing on $(56)$, an alternative idea is to follow Hagan et al [1]. Taking their approach, the forward value $V$ of a call option on $X_{ij}^F$ at a strike $K$ can be written

$$V\left(\tau, X_{ij}^F, \sigma_i, \sigma_j; K\right) = \int_0^\infty \left(\bar{X}_{ij}^F - K\right)^+ p\left(t, X_{ij}^F, \sigma_i, \sigma_j; t+\tau, \bar{X}_{ij}^F, \bar{\sigma}_i, \bar{\sigma}_j\right) d\bar{X}_{ij}^F d\bar{\sigma}_i d\bar{\sigma}_j \quad . \tag{61}$$

Then using the identity

$$p\left(t, X_{ij}^F, \sigma_i, \sigma_j; T_{ex}, \bar{X}_{ij}^F, \bar{\sigma}_i, \bar{\sigma}_j\right) = \delta\left(X_{ij}^F - \bar{X}_{ij}^F\right)\delta\left(\sigma_i - \bar{\sigma}_i\right)\delta\left(\sigma_j - \bar{\sigma}_j\right) + \int_t^{T_{ex}} \frac{\partial p}{\partial T} dT \quad , \tag{62}$$

the option price $(61)$ becomes

$$V\left(\tau, X_{ij}^F, \sigma_i, \sigma_j; K\right) = \left[X_{ij}^F - K\right]^+ + \int_0^\infty d\bar{X}_{ij}^F d\bar{\sigma}_i d\bar{\sigma}_j \left(\bar{X}_{ij}^F - K\right)^+ \int_t^{T_{ex}} \frac{\partial p}{\partial T} dT \quad . \tag{63}$$

Now use the fact that $p$ satisfies the forwards Kolmogorov equation to write $\partial p / \partial T$ in terms of derivatives with respect to $\bar{X}_{ij}^F$, $\bar{\sigma}_i$ and $\bar{\sigma}_j$. Then most of the terms disappear when integrated over $\bar{X}_{ij}^F$, $\bar{\sigma}_i$ and $\bar{\sigma}_j$, with the result that $(63)$ can be reduced to

$$V\left(\tau, X_{ij}^F, \sigma_i, \sigma_j; K\right) = \left[X_{ij}^F - K\right]^+ + \frac{1}{2}\varepsilon^2 K^2 \int_0^{\tau_{ex}} d\tau P_H\left(\tau, X_{ij}^F, \sigma_i, \sigma_j; K\right) \quad , \tag{64}$$

where $P_H\left(\tau, X_{ij}^F, \sigma_i, \sigma_j; K\right)$ is defined by

$$P_H\left(\tau, X_{ij}^F, \sigma_i, \sigma_j; K\right) = \int_0^\infty \left(\bar{\sigma}_i^2 - 2\rho_{ij}\bar{\sigma}_i\bar{\sigma}_j + \bar{\sigma}_j^2\right) p\left(t, X_{ij}^F, \sigma_i, \sigma_j; t+\tau, K, \bar{\sigma}_i, \bar{\sigma}_j\right) d\bar{\sigma}_i d\bar{\sigma}_j \quad . \tag{65}$$

Differentiating under the integral sign in $(65)$ shows that like $P$ in $(57)$, $P_H$ must also satisfy the backwards Kolmogorov equation $(58)$. However substituting $(55)$ into $(65)$ shows that instead of the boundary condition $(60)$, $P_H\left(\tau, X_{ij}^F, \sigma_i, \sigma_j; K\right)$ satisfies the boundary condition

$$P_H\left(\tau, X_{ij}^F, \sigma_i, \sigma_j; K\right) = \sigma_{ij}^2 \delta\left(X_{ij}^F - K\right) \quad \text{at} \quad \tau = 0 \quad , \tag{66}$$

where $\sigma_{ij}$ is defined in $(9)$. Since both $P_H\left(\tau, X_{ij}^F, \sigma_i, \sigma_j; K\right)$ and $P\left(\tau, X_{ij}^F, \sigma_i, \sigma_j; \bar{X}_{ij}^F\right)$ in $(57)$ depend on solving $(58)$, it is convenient to solve $(58)$ with the boundary condition

$$P\left(\tau, X_{ij}^F, \sigma_i, \sigma_j; K\right) = \sigma_{ij}^n \delta\left(X_{ij}^F - K\right) \quad \text{at} \quad \tau = 0 \quad , \tag{67}$$

so that choosing $n = 0$ gives $(60)$, and choosing $n = 2$ gives $(66)$. Hence the task is now to solve $(58)$ subject to the boundary condition $(67)$ up to and including $O\left(\varepsilon^2\right)$, assuming that $\varepsilon \ll 1$. Note that where $(60)$ involves $\bar{X}_{ij}^F$, $(66)$ involves $K$. Corresponding to this are different definitions of $z$. When $n = 0$, $z$ is defined by

$$z = \frac{1}{\varepsilon\sigma_{ij}} \ln\left(\frac{X_{ij}^F}{\bar{X}_{ij}^F}\right) \quad , \tag{68}$$

whereas when $n = 2$ then $z$ is defined by $(12)$. Without loss of generality, $K$ will be used in what follows instead of $\bar{X}_{ij}^F$, so $z$ will be defined by $(12)$ rather than $(68)$. This is the convention that was used in writing the common boundary condition $(67)$.

The first step is to change variables $X_{ij}^F \to z$ in $(58)$. The derivatives transform as

$$\begin{aligned}
\varepsilon X_{ij}^F \frac{\partial}{\partial X_{ij}^F} &\to \frac{1}{\sigma_{ij}} \frac{\partial}{\partial z} \\
\varepsilon^2 X_{ij}^{F2} \frac{\partial^2}{\partial X_{ij}^{F2}} &\to \frac{1}{\sigma_{ij}^2} \frac{\partial^2}{\partial z^2} - \frac{\varepsilon}{\sigma_{ij}} \frac{\partial}{\partial z} \\
\frac{\partial}{\partial \sigma_k} &\to -\frac{z}{\sigma_{ij}} \frac{\partial \sigma_{ij}}{\partial \sigma_k} \frac{\partial}{\partial z} + \frac{\partial}{\partial \sigma_k} \\
\varepsilon X_{ij}^F \frac{\partial^2}{\partial X_{ij}^F \partial \sigma_k} &\to -\frac{1}{\sigma_{ij}^2} \frac{\partial \sigma_{ij}}{\partial \sigma_k} \frac{\partial}{\partial z} - \frac{z}{\sigma_{ij}^2} \frac{\partial \sigma_{ij}}{\partial \sigma_k} \frac{\partial^2}{\partial z^2} + \frac{1}{\sigma_{ij}} \frac{\partial^2}{\partial z \partial \sigma_k} \\
\frac{\partial^2}{\partial \sigma_k^2} &\to \left(\frac{2}{\sigma_{ij}^2}\left(\frac{\partial \sigma_{ij}}{\partial \sigma_k}\right)^2 - \frac{1}{\sigma_{ij}} \frac{\partial^2 \sigma_{ij}}{\partial \sigma_k^2}\right) z \frac{\partial}{\partial z} + \frac{z^2}{\sigma_{ij}^2}\left(\frac{\partial \sigma_{ij}}{\partial \sigma_k}\right)^2 \frac{\partial^2}{\partial z^2} - \frac{2z}{\sigma_{ij}} \frac{\partial \sigma_{ij}}{\partial \sigma_k} \frac{\partial^2}{\partial z \partial \sigma_k} + \frac{\partial^2}{\partial \sigma_k^2} \\
\frac{\partial^2}{\partial \sigma_i \partial \sigma_j} &\to \left(\frac{2}{\sigma_{ij}^2} \frac{\partial \sigma_{ij}}{\partial \sigma_i} \frac{\partial \sigma_{ij}}{\partial \sigma_j} - \frac{1}{\sigma_{ij}} \frac{\partial^2 \sigma_{ij}}{\partial \sigma_i \partial \sigma_j}\right) z \frac{\partial}{\partial z} + z^2 \frac{1}{\sigma_{ij}^2} \frac{\partial \sigma_{ij}}{\partial \sigma_i} \frac{\partial \sigma_{ij}}{\partial \sigma_j} \frac{\partial^2}{\partial z^2} \\
&\quad - \frac{z}{\sigma_{ij}} \frac{\partial \sigma_{ij}}{\partial \sigma_j} \frac{\partial^2}{\partial z \partial \sigma_i} - \frac{z}{\sigma_{ij}} \frac{\partial \sigma_{ij}}{\partial \sigma_i} \frac{\partial^2}{\partial z \partial \sigma_j} + \frac{\partial^2}{\partial \sigma_i \partial \sigma_j} \quad .
\end{aligned}$$

Hence the change of variables $X_{ij}^F \to z$ means that $(58)$ becomes

$$\frac{\partial P}{\partial \tau} = \frac{1}{2}\left(1 - 2\varepsilon a_1 z + \varepsilon^2 a_2 z^2\right)\frac{\partial^2 P}{\partial z^2} + \left(-\frac{1}{2}\varepsilon\sigma_{ij} - \varepsilon a_1 + \varepsilon^2\left(a_2 - a_3 - a_4\right)z\right)\frac{\partial P}{\partial z} + \varepsilon D_\sigma\left(\frac{\partial P}{\partial z}\right)$$
$$- \varepsilon^2\frac{z}{\sigma_{ij}}\left(\upsilon_i^2\sigma_i^2\frac{\partial\sigma_{ij}}{\partial\sigma_i} + r_{ij}\upsilon_i\upsilon_j\sigma_i\sigma_j\frac{\partial\sigma_{ij}}{\partial\sigma_j}\right)\frac{\partial^2 P}{\partial z\partial\sigma_i} - \varepsilon^2\frac{z}{\sigma_{ij}}\left(\upsilon_j^2\sigma_j^2\frac{\partial\sigma_{ij}}{\partial\sigma_j} + r_{ij}\upsilon_i\upsilon_j\sigma_i\sigma_j\frac{\partial\sigma_{ij}}{\partial\sigma_i}\right)\frac{\partial^2 P}{\partial z\partial\sigma_j}$$
$$+ \frac{1}{2}\varepsilon^2\upsilon_i^2\sigma_i^2\frac{\partial^2 P}{\partial\sigma_i^2} + \varepsilon^2 r_{ij}\upsilon_i\upsilon_j\sigma_i\sigma_j\frac{\partial^2 P}{\partial\sigma_i\partial\sigma_j} + \frac{1}{2}\varepsilon^2\upsilon_j^2\sigma_j^2\frac{\partial^2 P}{\partial\sigma_j^2} + \varepsilon^2\tilde{\rho}_{ij}\upsilon_i\sigma_i\sigma_j\frac{\partial P}{\partial\sigma_i} + \varepsilon^2\tilde{\rho}_{jj}\upsilon_j\sigma_j^2\frac{\partial P}{\partial\sigma_j} \quad , \tag{69}$$

where the quantities $a_1$, $a_2$, $a_3$ and $a_4$ are the functions of $\sigma_i$ and $\sigma_j$ which were defined in $(16)$-$(19)$. Note that $a_1$ can be written in terms of $D_\sigma$ as

$$a_1 = \frac{1}{\sigma_{ij}}D_\sigma\sigma_{ij} \quad , \tag{70}$$

and that $a_4$ arises as

$$a_4 = \frac{\upsilon_i^2\sigma_i^2}{2\sigma_{ij}}\frac{\partial^2\sigma_{ij}}{\partial\sigma_i^2} + \frac{r_{ij}\upsilon_i\upsilon_j\sigma_i\sigma_j}{\sigma_{ij}}\frac{\partial^2\sigma_{ij}}{\partial\sigma_i\partial\sigma_j} + \frac{\upsilon_j^2\sigma_j^2}{2\sigma_{ij}}\frac{\partial^2\sigma_{ij}}{\partial\sigma_j^2} \quad . \tag{71}$$

Using $(9)$, $(10)$ and

$$\frac{\partial^2\sigma_{ij}}{\partial\sigma_i^2} = \frac{1}{\sigma_{ij}}\left(1 - \left(\frac{\partial\sigma_{ij}}{\partial\sigma_i}\right)^2\right), \quad \frac{\partial^2\sigma_{ij}}{\partial\sigma_j^2} = \frac{1}{\sigma_{ij}}\left(1 - \left(\frac{\partial\sigma_{ij}}{\partial\sigma_j}\right)^2\right), \quad \frac{\partial^2\sigma_{ij}}{\partial\sigma_i\partial\sigma_j} = -\frac{1}{\sigma_{ij}}\left(\rho_{ij} + \frac{\partial\sigma_{ij}}{\partial\sigma_i}\frac{\partial\sigma_{ij}}{\partial\sigma_j}\right) \tag{72}$$

shows that $(71)$ can be written as $(19)$. Then using the identity

$$\delta\left(X_{ij}^F - K\right) = \frac{1}{\varepsilon\sigma_{ij}K}\delta(z) \quad , \tag{73}$$

the boundary condition $(67)$ becomes

$$P(\tau, z, \sigma_i, \sigma_j) = \frac{\sigma_{ij}^{n-1}}{\varepsilon K}\delta(z) \quad \text{at} \quad \tau = 0 \quad . \tag{74}$$

The next step eliminates $\sigma_{ij}$ from the boundary condition $(74)$. To do this, define

$$\hat{P}(\tau, z, \sigma_i, \sigma_j) = \frac{\varepsilon K}{\sigma_{ij}^{n-1}}P(\tau, z, \sigma_i, \sigma_j) \quad . \tag{75}$$

Substituting $(75)$ into $(69)$ then the differential equation for $\hat{P}$ is

$$\frac{\partial\hat{P}}{\partial\tau} = \frac{1}{2}\left(1 - 2\varepsilon a_1 z + \varepsilon^2 a_2 z^2\right)\frac{\partial^2\hat{P}}{\partial z^2} - \left(\frac{1}{2}\varepsilon\sigma_{ij} - \varepsilon(n-2)a_1 + \varepsilon^2 z\left(a_3 + a_4 + (n-2)a_2\right)\right)\frac{\partial\hat{P}}{\partial z} + \varepsilon^2(n-1)a_3\hat{P}$$
$$+ \varepsilon D_\sigma\left(\frac{\partial\hat{P}}{\partial z}\right) - \varepsilon^2\frac{z}{\sigma_{ij}}\left(\upsilon_i^2\sigma_i^2\frac{\partial\sigma_{ij}}{\partial\sigma_i} + r_{ij}\upsilon_i\upsilon_j\sigma_i\sigma_j\frac{\partial\sigma_{ij}}{\partial\sigma_j}\right)\frac{\partial^2\hat{P}}{\partial z\partial\sigma_i} - \varepsilon^2\frac{z}{\sigma_{ij}}\left(\upsilon_j^2\sigma_j^2\frac{\partial\sigma_{ij}}{\partial\sigma_j} + r_{ij}\upsilon_i\upsilon_j\sigma_i\sigma_j\frac{\partial\sigma_{ij}}{\partial\sigma_i}\right)\frac{\partial^2\hat{P}}{\partial z\partial\sigma_j}$$
$$+ \frac{1}{2}\varepsilon^2\upsilon_i^2\sigma_i^2\frac{1}{\sigma_{ij}^{n-1}}\frac{\partial^2\left[\sigma_{ij}^{n-1}\hat{P}\right]}{\partial\sigma_i^2} + \varepsilon^2 r_{ij}\upsilon_i\upsilon_j\sigma_i\sigma_j\frac{1}{\sigma_{ij}^{n-1}}\frac{\partial^2\left[\sigma_{ij}^{n-1}\hat{P}\right]}{\partial\sigma_i\partial\sigma_j} + \frac{1}{2}\varepsilon^2\upsilon_j^2\sigma_j^2\frac{1}{\sigma_{ij}^{n-1}}\frac{\partial^2\left[\sigma_{ij}^{n-1}\hat{P}\right]}{\partial\sigma_j^2}$$
$$\varepsilon^2\tilde{\rho}_{ij}\upsilon_i\sigma_i\sigma_j\frac{\partial\hat{P}}{\partial\sigma_i} + \varepsilon^2\tilde{\rho}_{jj}\upsilon_j\sigma_j^2\frac{\partial\hat{P}}{\partial\sigma_j} \quad , \tag{76}$$

with boundary condition

$$\hat{P}(\tau, z, \sigma_i, \sigma_j) = \delta(z) \quad \text{at} \quad \tau = 0 \quad . \tag{77}$$

Looking at $(76)$, when $\varepsilon = 0$ the equation is independent of $\sigma_i$ and $\sigma_j$, so the solution must have the form

$$P(\tau, z, \sigma_i, \sigma_j) = P_0(\tau, z) + \varepsilon P_1(\tau, z, \sigma_i, \sigma_j) + O\left(\varepsilon^2\right) \quad . \tag{78}$$

This means that derivatives in $\sigma_i$ and $\sigma_j$ are $O(\varepsilon)$, so the $\varepsilon^2$ terms in $(69)$ which involve derivatives in $\sigma_i$ and $\sigma_j$ are thus $O(\varepsilon^3)$ and so to $O(\varepsilon^2)$ they can be ignored. Hence discarding terms of order $O(\varepsilon^3)$ and higher, the equation simplifies to

$$\frac{\partial \hat{P}}{\partial \tau} = \frac{1}{2}\left(1 - 2\varepsilon z a_1 + \varepsilon^2 z^2 a_2\right)\frac{\partial^2 \hat{P}}{\partial z^2} - \left(\frac{1}{2}\varepsilon\sigma_{ij} - \varepsilon(n-2)a_1 + \varepsilon^2 z\left(a_3 + a_4 + (n-2)a_2\right)\right)\frac{\partial \hat{P}}{\partial z}$$
$$+\varepsilon D_\sigma\left(\frac{\partial \hat{P}}{\partial z}\right) + \varepsilon^2(n-1)\left(\frac{1}{2}(n-2)a_2 + a_3 + a_4\right)\hat{P} \quad , \tag{79}$$

where the terms in $\varepsilon^2 a_2 \hat{P}$ and $\varepsilon^2 a_4 \hat{P}$ arise from the second order derivatives of $\sigma_{ij}^{n-1}\hat{P}$ with respect to $\sigma_i$ and $\sigma_j$.

The purpose of the next two steps is to eliminate dependence on $\sigma_i$ and $\sigma_j$ at $O(\varepsilon)$. First define the function $J(z, \sigma_i, \sigma_j)$ by

$$J(z, \sigma_i, \sigma_j) = \sqrt{\sum_{m=0}^{\infty} \varepsilon^m h_m(z, \sigma_i, \sigma_j)} \quad , \tag{80}$$

which is the same function that was given above in $(14)$. However $(14)$ only specified $J(z, \sigma_i, \sigma_j)$ up to and including $O(\varepsilon^2)$. Regarding the functions $h_m(z, \sigma_i, \sigma_j)$ in $(80)$, define

$$h_0(z, \sigma_i, \sigma_j) = 1 - 2\varepsilon a_1 z + \varepsilon^2 a_2 z^2 \quad , \tag{81}$$
$$h_m(z, \sigma_i, \sigma_j) = O(\varepsilon) \quad , \quad m \geqslant 1 \quad . \tag{82}$$

The full definition of $h_m(z, \sigma_i, \sigma_j)$ for $m \geqslant 1$ will be given later. For now, the only important property of $h_m$ for $m \geqslant 1$ is that all these terms are $O(\varepsilon)$, so that for $m \geqslant 1$ the terms $\varepsilon^m h_m$ are $O(\varepsilon^2)$ or smaller. Note that $h_0(z, \sigma_i, \sigma_j)$ is the coefficient of $\partial^2 P/\partial z^2$ in $(79)$. Also note that $h_0(z, \sigma_i, \sigma_j) \geqslant 0$ for all $z$, $\sigma_i$ and $\sigma_j$. The condition for $h_0(z, \sigma_i, \sigma_j) \geqslant 0$ is $a_2 \geqslant a_1^2$, and to show that this is always satisfied, consider two stochastic processes $d\xi_1$ and $d\xi_2$ defined by

$$d\xi_1 = \sigma_i dW_i - \sigma_j dW_j \quad ,$$
$$d\xi_2 = \sigma_i \upsilon_i \frac{\partial \sigma}{\partial \sigma_i} dZ_i + \sigma_j \upsilon_j \frac{\partial \sigma}{\partial \sigma_j} dZ_j \quad ,$$

where $(8)$ defines the correlations between the Wiener processes. Then the determinant of the covariance matrix of $(d\xi_1, d\xi_2)$ is given by $\left(a_2 - a_1^2\right)\sigma_{ij}^4$, so $a_2 \geqslant a_1^2$ because covariance matrices are positive semi-definite and thus have non-negative determinants.

Now make a change of variables $(z, \sigma_i, \sigma_j) \to \left(x, \sigma_i', \sigma_j'\right)$ where (as in $(13)$)

$$x(z, \sigma_i, \sigma_j) = \int_0^z \frac{d\xi}{J(\xi, \sigma_i, \sigma_j)} \quad , \tag{83}$$
$$\sigma_i' = \sigma_i \quad , \tag{84}$$
$$\sigma_j' = \sigma_j \quad . \tag{85}$$

For now it will be convenient to keep the distinction between $\sigma_i$, $\sigma_j$ and $\sigma_i', \sigma_j'$ so that when writing derivatives with respect to $\sigma_i$ and $\sigma_j$ it is $z$ which is being held constant, and when writing derivatives with respect to $\sigma_i'$ and $\sigma_j'$ it is $x$ which is being held constant. Then note that

$$\frac{\partial x}{\partial z} = \frac{1}{J} \quad , \quad \frac{\partial z}{\partial x} = J \quad , \quad \frac{\partial}{\partial x}\left(\frac{1}{J}\right) = -\frac{1}{J}\frac{\partial J}{\partial z} \quad , \tag{86}$$

and expanding in powers of $\varepsilon$, note that

$$J(z, \sigma_i, \sigma_j) = 1 - \varepsilon a_1 z + \frac{1}{2}\varepsilon^2\left(a_2 - a_1^2\right)z^2 + \frac{1}{2}\varepsilon h_1 + O\left(\varepsilon^3\right) \quad , \tag{87}$$
$$x(z, \sigma_i, \sigma_j) = z + \frac{1}{2}\varepsilon a_1 z^2 + O\left(\varepsilon^2\right) \quad , \tag{88}$$
$$z\left(x, \sigma_i', \sigma_j'\right) = x - \frac{1}{2}\varepsilon a_1 x^2 + O\left(\varepsilon^2\right) \quad , \tag{89}$$

so that the derivatives $\partial J/\partial z$, $\partial x/\partial\sigma_i$ and $\partial x/\partial\sigma_j$ are terms of order $O(\varepsilon)$. Then with the change of variables $(z, \sigma_i, \sigma_j) \to \left(x, \sigma'_i, \sigma'_j\right)$, the derivatives transform as

$$\begin{aligned}
\frac{\partial}{\partial z} &\longrightarrow \frac{1}{J}\frac{\partial}{\partial x} \quad , \\
\frac{\partial^2}{\partial z^2} &\longrightarrow \frac{1}{J^2}\left(\frac{\partial^2}{\partial x^2} - \frac{\partial J}{\partial z}\frac{\partial}{\partial x}\right) \quad , \\
\frac{\partial}{\partial\sigma_k} &\longrightarrow \frac{\partial x}{\partial\sigma_k}\frac{\partial}{\partial x} + \frac{\partial}{\partial\sigma'_k} \quad , \\
\frac{\partial^2}{\partial z\partial\sigma_k} &\longrightarrow \frac{\partial}{\partial z}\left(\frac{\partial x}{\partial\sigma_k}\right)\frac{\partial}{\partial x} + \frac{1}{J}\frac{\partial x}{\partial\sigma_k}\frac{\partial^2}{\partial x^2} + \frac{1}{J}\frac{\partial^2}{\partial x\partial\sigma'_k} \\
D_\sigma\frac{\partial}{\partial z} &\longrightarrow \frac{\partial}{\partial z}\left(D_\sigma x\right)\frac{\partial}{\partial x} + \frac{(D_\sigma x)}{J}\frac{\partial^2}{\partial x^2} + \frac{1}{J}D_{\sigma'}\frac{\partial}{\partial x}
\end{aligned}$$

where as usual, $k$ is either $i$ or $j$, and where $D_{\sigma'}$ is a differential operator like $D_\sigma$ except that it contains $\partial/\partial\sigma'_i$ and $\partial/\partial\sigma'_j$ in place of $\partial/\partial\sigma_i$ and $\partial/\partial\sigma_j$. Then using $(80)$, $(81)$ and $(86)$,

$$\frac{\partial}{\partial z}\left(D_\sigma x\right) = D_\sigma\left(\frac{\partial x}{\partial z}\right) = -\frac{1}{2J^3}D_\sigma\left(J^2\right) = \varepsilon\frac{1}{J^3}\left(D_\sigma a_1\right)z + O\left(\varepsilon^2\right) \quad , \tag{90}$$

so that up to and including $O(\varepsilon^2)$, $(79)$ becomes

$$\begin{aligned}
\frac{\partial\hat{P}}{\partial\tau} = \frac{1}{2}\left(\frac{h_0}{J^2} + 2\varepsilon\frac{(D_\sigma x)}{J}\right)\frac{\partial^2\hat{P}}{\partial x^2} + \left(-\frac{1}{2}\frac{\partial J}{\partial z} - \frac{1}{2}\varepsilon\sigma_{ij}\frac{1}{J} + \varepsilon(n-2)a_1\frac{1}{J} - \varepsilon^2 z\frac{1}{J}\left(a_3 + a_4 + (n-2)a_2\right) + \varepsilon^2 z\frac{1}{J^3}a_5\right)\frac{\partial\hat{P}}{\partial x} \\
+ \varepsilon\frac{1}{J}D_{\sigma'}\left(\frac{\partial\hat{P}}{\partial x}\right) + \varepsilon^2(n-1)\left(\frac{1}{2}(n-2)a_2 + a_3 + a_4\right)\hat{P} \quad ,
\end{aligned} \tag{91}$$

where $a_5$ is the function of $\sigma_i$ and $\sigma_j$ defined by $(20)$. In $(91)$ $a_5$ arises as

$$a_5 = D_\sigma a_1 \quad , \tag{92}$$

but using $(10)$, $(72)$ and $(21)$ to show that

$$D_\sigma\sigma_i = \sigma_i\zeta_i \quad , \quad D_\sigma\sigma_j = -\sigma_j\zeta_j \quad , \tag{93}$$

$$D_\sigma\left(\frac{\partial\sigma_{ij}}{\partial\sigma_i}\right) = -a_1\frac{\partial\sigma_{ij}}{\partial\sigma_i} + \frac{\sigma_i\zeta_i + \rho_{ij}\sigma_j\zeta_j}{\sigma_{ij}} \quad , \quad D_\sigma\left(\frac{\partial\sigma_{ij}}{\partial\sigma_j}\right) = -a_1\frac{\partial\sigma_{ij}}{\partial\sigma_j} - \frac{\sigma_j\zeta_j + \rho_{ij}\sigma_i\zeta_i}{\sigma_{ij}} \quad , \tag{94}$$

$$D_\sigma\zeta_i = -a_1\zeta_i + \frac{\upsilon_i\left(\tilde{\rho}_{ii}\sigma_i\zeta_i + \tilde{\rho}_{ij}\sigma_j\zeta_j\right)}{\sigma_{ij}} \quad , \quad D_\sigma\zeta_j = -a_1\zeta_j - \frac{\upsilon_j\left(\tilde{\rho}_{jj}\sigma_j\zeta_j + \tilde{\rho}_{ji}\sigma_i\zeta_i\right)}{\sigma_{ij}} \quad , \tag{95}$$

coupled with $(16)$ it is straightforward to derive the more explicit formula for $a_5$ given in $(20)$.

In the original definition of $J(z, \sigma_i, \sigma_j)$ given in $(80)$-$(82)$, only $h_0$ was defined. Now, choose the $h_m$ for $m \geqslant 1$ so that the coefficient of $\partial^2\hat{P}/\partial x^2$ in $(91)$ equals $\frac{1}{2}$, i.e. require

$$\frac{h_0}{J^2} + 2\varepsilon\frac{(D_\sigma x)}{J} = 1 \quad . \tag{96}$$

The following sub-section C.1 shows how to solve $(96)$ to determine the $h_m$ for all $m \geqslant 1$, however for now it is sufficient just to determine $h_1(z)$ up to and including $O\left(\varepsilon^2\right)$. Using $(88)$ in $(96)$ shows that

$$h_1(z) = \varepsilon a_5 z^2 + O\left(\varepsilon^2\right) \quad . \tag{97}$$

Note that for the solution to make sense, it is important that $\sum_{m=0}^{\infty}\varepsilon^m h_m(z, \sigma_i, \sigma_j) > 0$ so that $J(z, \sigma_i, \sigma_j)$ in $(80)$ is well defined. Using $(97)$ then up to and including $O\left(\varepsilon^2\right)$ the approximation for $J(z, \sigma_i, \sigma_j)$ is $\sqrt{h_0 + \varepsilon^2 a_5 z^2}$, so the condition for $J(z, \sigma_i, \sigma_j)$ to be well defined is $a_2 + a_5 > a_1^2$. Although this is not guaranteed, in practise this condition was comfortably satisfied for all the fits to market data that were discussed in section 5.

Given $(96)$, then $(91)$ simplifies to

$$\frac{\partial \hat{P}}{\partial \tau}=\frac{1}{2}\frac{\partial^2 \hat{P}}{\partial x^2}+\left(-\frac{1}{2}\frac{\partial J}{\partial z}-\frac{1}{2}\varepsilon\sigma_{ij}\frac{1}{J}+\varepsilon\left(n-2\right)a_1\frac{1}{J}-\varepsilon^2 z\frac{1}{J}\left(a_3+a_4+\left(n-2\right)a_2\right)+\varepsilon^2 z\frac{1}{J^3}a_5\right)\frac{\partial \hat{P}}{\partial x}$$
$$+\varepsilon\frac{1}{J}D_{\sigma'}\left(\frac{\partial \hat{P}}{\partial x}\right)+\varepsilon^2\left(n-1\right)\left(\frac{1}{2}\left(n-2\right)a_2+a_3+a_4\right)\hat{P} \quad . \tag{98}$$

Since $\partial x/\partial z=1$ at $z=0$, the boundary condition is

$$\hat{P}\left(\tau,x,\sigma_i',\sigma_j'\right)=\delta\left(x\right) \quad \text{at} \quad \tau=0 \quad . \tag{99}$$

The last remaining dependence on $\sigma_i$ and $\sigma_j$ at $O\left(\varepsilon\right)$ is in the term $\partial\hat{P}/\partial x$. To eliminate this, define $H\left(\tau,x,\sigma_i',\sigma_j'\right)$ by

$$\hat{P}\left(\tau,x,\sigma_i',\sigma_j'\right)=e^{\frac{1}{2}\varepsilon\sigma_{ij}z(x)}J\left(z\left(x\right)\right)^{n-\frac{3}{2}}H\left(\tau,x,\sigma_i',\sigma_j'\right) \quad . \tag{100}$$

Then in terms of derivatives of $H$, the derivatives of $\hat{P}$ are

$$\frac{\partial \hat{P}}{\partial x}=e^{\frac{1}{2}\varepsilon\sigma_{ij}z}J\left(z\right)^{n-\frac{3}{2}}\left(\frac{1}{2}\varepsilon\sigma_{ij}JH+\left(n-\frac{3}{2}\right)\frac{\partial J}{\partial z}H+\frac{\partial H}{\partial x}\right) \tag{101}$$

$$\begin{aligned}\frac{\partial^2 \hat{P}}{\partial x^2}&=e^{\frac{1}{2}\varepsilon\sigma_{ij}z}J\left(z\right)^{n-\frac{3}{2}}\left(\begin{array}{r}\left[\frac{1}{2}\varepsilon\sigma_{ij}J+\left(n-\frac{3}{2}\right)\frac{\partial J}{\partial z}\right]\left[\frac{1}{2}\varepsilon\sigma_{ij}JH+\left(n-\frac{3}{2}\right)\frac{\partial J}{\partial z}H+\frac{\partial H}{\partial x}\right]\\+\frac{1}{2}\varepsilon\sigma_{ij}\frac{\partial J}{\partial z}JH+\frac{1}{2}\varepsilon\sigma_{ij}J\frac{\partial H}{\partial x}+\left(n-\frac{3}{2}\right)J\frac{\partial^2 J}{\partial z^2}H+\left(n-\frac{3}{2}\right)\frac{\partial J}{\partial z}\frac{\partial H}{\partial x}+\frac{\partial^2 H}{\partial x^2}\end{array}\right)\\&=e^{\frac{1}{2}\varepsilon\sigma_{ij}z}J\left(z\right)^{n-\frac{3}{2}}\left(\begin{array}{r}\frac{\partial^2 H}{\partial x^2}+\varepsilon\sigma_{ij}J\frac{\partial H}{\partial x}+2\left(n-\frac{3}{2}\right)\frac{\partial J}{\partial z}\frac{\partial H}{\partial x}+\frac{1}{4}\varepsilon^2\sigma_{ij}^2J^2H+\varepsilon\sigma_{ij}J\left(n-1\right)\frac{\partial J}{\partial z}H\\+\left(n-\frac{3}{2}\right)^2\left(\frac{\partial J}{\partial z}\right)^2H+\left(n-\frac{3}{2}\right)J\frac{\partial^2 J}{\partial z^2}H\end{array}\right)\end{aligned} \tag{102}$$

$$\begin{aligned}\frac{\partial^2 \hat{P}}{\partial x\partial\sigma_k'}&=e^{\frac{1}{2}\varepsilon\sigma_{ij}z}J\left(z\right)^{n-\frac{3}{2}}\left(\begin{array}{r}\left[\frac{1}{2}\varepsilon z\frac{\partial\sigma_{ij}}{\partial\sigma_k}+\left(n-\frac{3}{2}\right)\frac{1}{J}\frac{\partial J}{\partial\sigma_k'}\right]\left[\frac{1}{2}\varepsilon\sigma_{ij}JH+\left(n-\frac{3}{2}\right)\frac{\partial J}{\partial z}H+\frac{\partial H}{\partial x}\right]\\+\frac{1}{2}\varepsilon\frac{\partial\sigma_{ij}}{\partial\sigma_k}JH+\frac{1}{2}\varepsilon\sigma_{ij}\frac{\partial J}{\partial\sigma_k}H+\frac{1}{2}\varepsilon\sigma_{ij}J\frac{\partial H}{\partial\sigma_k'}\\+\left(n-\frac{3}{2}\right)\frac{\partial^2 J}{\partial z\partial\sigma_k'}H+\left(n-\frac{3}{2}\right)\frac{\partial J}{\partial z}\frac{\partial H}{\partial\sigma_k'}+\frac{\partial^2 H}{\partial x\partial\sigma_k'}\end{array}\right)\\&=e^{\frac{1}{2}\varepsilon\sigma_{ij}z}J\left(z\right)^{n-\frac{3}{2}}\left(\begin{array}{r}\frac{1}{2}\varepsilon\frac{\partial\sigma_{ij}}{\partial\sigma_k}\left(z\frac{\partial H}{\partial x}+JH\right)+\left(n-\frac{3}{2}\right)\left(\frac{1}{J}\frac{\partial J}{\partial\sigma_k'}\frac{\partial H}{\partial x}+\frac{\partial^2 J}{\partial z\partial\sigma_k'}H\right)\\+\left(\frac{1}{2}\varepsilon\sigma_{ij}J+\left(n-\frac{3}{2}\right)\frac{\partial J}{\partial z}\right)\frac{\partial H}{\partial\sigma_k'}+\frac{\partial^2 H}{\partial x\partial\sigma_k'}+O\left(\varepsilon^2\right)\end{array}\right)\end{aligned} \tag{103}$$

$$D_{\sigma'}\left(\frac{\partial \hat{P}}{\partial x}\right)=e^{\frac{1}{2}\varepsilon\sigma_{ij}z}J\left(z\right)^{n-\frac{3}{2}}\left(\begin{array}{r}\frac{1}{2}\varepsilon a_1\sigma_{ij}\left(z\frac{\partial H}{\partial x}+JH\right)+\left(n-\frac{3}{2}\right)\left(\frac{1}{J}\left(D_{\sigma'}J\right)\frac{\partial H}{\partial x}+D_{\sigma'}\left(\frac{\partial J}{\partial z}\right)H\right)\\+\left(\frac{1}{2}\varepsilon\sigma_{ij}J+\left(n-\frac{3}{2}\right)\frac{\partial J}{\partial z}\right)D_{\sigma'}H+D_{\sigma'}\left(\frac{\partial H}{\partial x}\right)+O\left(\varepsilon^2\right)\end{array}\right) . \tag{104}$$

Substituting these into $(98)$, using

$$J^2=1-2\varepsilon a_1 z+\varepsilon^2\left(a_2+a_5\right)z^2+O\left(\varepsilon^3\right) \quad , \tag{105}$$

and ignoring all terms of order $O\left(\varepsilon^3\right)$ and higher produces

$$\frac{\partial H}{\partial \tau}=\frac{1}{2}\frac{\partial^2 H}{\partial x^2}+\varepsilon^2 z\frac{1}{J}\left(\frac{1}{2}a_5-\frac{1}{2}a_1\sigma_{ij}-a_3-a_4\right)\frac{\partial H}{\partial x}$$
$$+\frac{1}{2}\left(n-\frac{3}{2}\right)J\frac{\partial^2 J}{\partial z^2}H+\frac{1}{2}\left(n-\frac{3}{2}\right)\left(n-\frac{5}{2}\right)\left(\frac{\partial J}{\partial z}\right)^2H-\frac{1}{8}\varepsilon^2\sigma_{ij}^2H$$
$$+\varepsilon^2\left(-\left(n-2\right)\left(n-\frac{3}{2}\right)a_1^2+\left(n-1\right)\left(\frac{1}{2}\left(n-2\right)a_2+\frac{1}{2}a_1\sigma_{ij}+a_3+a_4\right)-\left(n-\frac{3}{2}\right)a_5\right)H$$
$$+\varepsilon\frac{1}{J}\left[\left(\frac{1}{2}\varepsilon\sigma_{ij}J+\left(n-\frac{3}{2}\right)\frac{\partial J}{\partial z}\right)D_{\sigma'}H+D_{\sigma'}\left(\frac{\partial H}{\partial x}\right)\right] \quad . \tag{106}$$

As argued before in connection with $(78)$, derivatives with respect to $\sigma_i'$ and $\sigma_j'$ must be $O\left(\varepsilon\right)$. But now this means that $(106)$ has no dependence on $\sigma_i'$ and $\sigma_j'$ until $O\left(\varepsilon^2\right)$, so in fact derivatives with respect to $\sigma_i'$ and $\sigma_j'$ must in fact be $O\left(\varepsilon^2\right)$. Hence up to and including $O\left(\varepsilon^2\right)$ the terms with derivatives with respect to $\sigma_i'$ and $\sigma_j'$

can be dropped, and since the boundary condition is independent of $\sigma_i$ and $\sigma_j$ as well, then $\sigma_i$ and $\sigma_j$ can be regarded as constants. Hence dropping the $D_{\sigma'}$ terms and using $(105)$ again, the equation becomes

$$\frac{\partial H}{\partial \tau} = \frac{1}{2}\frac{\partial^2 H}{\partial x^2} + \varepsilon^2 z \frac{1}{J}\left(\frac{1}{2}a_5 - \frac{1}{2}a_1\sigma_{ij} - a_3 - a_4\right)\frac{\partial H}{\partial x}$$
$$+\varepsilon^2\left(\frac{n^2-2n+\frac{1}{2}}{2}a_2 - \frac{1}{2}\left(n-\frac{1}{2}\right)\left(n-\frac{3}{2}\right)a_1^2 - \frac{1}{8}\sigma_{ij}^2 + (n-1)\left(\frac{1}{2}a_1\sigma_{ij}+a_3+a_4\right) - \frac{1}{2}\left(n-\frac{3}{2}\right)a_5\right)H \tag{107}$$

with boundary condition

$$H(\tau,x) = \delta(x) \quad \text{at} \quad \tau = 0 \quad . \tag{108}$$

To solve $(107)$, look for a solution to $(107)$ of the form

$$H(\tau,x) = \frac{g(z(x))\exp\left(-\frac{x^2}{2\tau}+\varepsilon^2\kappa\tau\right)}{\sqrt{2\pi\tau}} \quad , \tag{109}$$

where $\kappa$ is a constant which will be determined below, and where the boundary condition $(108)$ corresponds to

$$g(0) = 1 \quad . \tag{110}$$

Substituting $(109)$ into $(107)$ produces three categories of terms, namely terms in $\tau^{-2}$, $\tau^{-1}$ and $\tau^0$. It will now be shown that it is possible to match the terms up to and including $O\left(\varepsilon^2\right)$. Then taking care because $g(z)$ in $(109)$ is defined as a function of $z$ rather than $x$, the derivatives of $H$ are

$$\frac{\partial H}{\partial \tau} = H\left(-\frac{1}{2\tau}+\frac{x^2}{2\tau^2}+\varepsilon^2\kappa\right) \quad , \tag{111}$$
$$\frac{\partial H}{\partial x} = H\left(\frac{1}{g}\frac{dg}{dz}J - \frac{x}{\tau}\right) \quad , \tag{112}$$
$$\frac{\partial^2 H}{\partial x^2} = H\left[-2\frac{1}{g}\frac{dg}{dz}J\frac{x}{\tau} + \frac{x^2}{\tau^2} + \frac{1}{g}\frac{d^2g}{dz^2}J^2 + \frac{1}{g}\frac{dg}{dz}\frac{\partial J}{\partial z}J - \frac{1}{\tau}\right] \quad . \tag{113}$$

Substituting into $(107)$, by construction the terms in $\tau^{-2}$ match immediately. Note that if $(96)$ is satisfied to all orders in $\varepsilon$ then the $\tau^{-2}$ also match to all orders in $\varepsilon$. The conditions to match the terms in $\tau^{-1}$ and $\tau^0$ are

$$\tau^{-1}: 0 = -\frac{1}{g}\frac{dg}{dz}J - \varepsilon^2 z\frac{1}{J}\left(\frac{1}{2}a_5 - \frac{1}{2}a_1\sigma_{ij} - a_3 - a_4\right) \quad , \tag{114}$$
$$\tau^0: \varepsilon^2\kappa = \frac{1}{2g}\frac{d^2g}{dz^2}J^2 + \frac{1}{2g}\frac{dg}{dz}\frac{\partial J}{\partial z}J + \varepsilon^2 z\left(\frac{1}{2}a_5 - \frac{1}{2}a_1\sigma_{ij} - a_3 - a_4\right)\frac{1}{g}\frac{dg}{dz}$$
$$+\varepsilon^2\left(\frac{n^2-2n+\frac{1}{2}}{2}a_2 - \frac{1}{2}\left(n-\frac{1}{2}\right)\left(n-\frac{3}{2}\right)a_1^2 - \frac{1}{8}\sigma_{ij}^2 + (n-1)\left(\frac{1}{2}a_1\sigma_{ij}+a_3+a_4\right) - \frac{1}{2}\left(n-\frac{3}{2}\right)a_5\right) \quad . \tag{115}$$

Then the $\tau^{-1}$ terms match if

$$\frac{1}{g}\frac{dg}{dz} = -\varepsilon^2\left(\frac{1}{2}a_5 - \frac{1}{2}a_1\sigma_{ij} - a_3 - a_4\right)\frac{z}{J^2} \quad , \tag{116}$$

so

$$g(z) = \exp\left(\varepsilon^2\left(\frac{1}{2}a_1\sigma_{ij}+a_3+a_4-\frac{1}{2}a_5\right)\int_0^z \frac{\xi}{J(\xi)^2}d\xi\right) \quad . \tag{117}$$

To match the terms in $\tau^0$, the derivatives of $g(z)$ are needed. From $(116)$, the derivatives are given by

$$\frac{dg}{dz} = \varepsilon^2 g\left(\frac{1}{2}a_1\sigma_{ij}+a_3+a_4-\frac{1}{2}a_5\right)z + O\left(\varepsilon^3\right) \tag{118}$$
$$\frac{d^2g}{dz^2} = \varepsilon^2 g\left(\frac{1}{2}a_1\sigma_{ij}+a_3+a_4-\frac{1}{2}a_5\right) + O\left(\varepsilon^3\right) \quad . \tag{119}$$

Substituting these into $(115)$ shows that

$$\kappa = \frac{n^2 - 2n + \frac{1}{2}}{2} a_2 - \frac{1}{2}\left(n - \frac{1}{2}\right)\left(n - \frac{3}{2}\right) a_1^2 - \frac{1}{8}\sigma_{ij}^2 + \frac{1}{2}\left(n - \frac{1}{2}\right)\left(a_1\sigma_{ij} + 2a_3 + 2a_4\right) - \frac{1}{2}\left(n-1\right) a_5 \quad . \tag{120}$$

Then using $(75)$, $(100)$ and $(109)$ to reverse back through the transformations, the density function which satisfies $(69)$ and $(74)$ up to and including $O\left(\varepsilon^2\right)$ is given by

$$P\left(\tau, z, \sigma_i, \sigma_j\right) = \frac{\sigma_{ij}^{n-1}}{\varepsilon K} J\left(z\right)^{n-\frac{3}{2}} \frac{\exp\left(\frac{\varepsilon\sigma_{ij} z}{2} + \varepsilon^2\left(\frac{a_1\sigma_{ij}}{2} + a_3 + a_4 - \frac{a_5}{2}\right)\int_0^z \frac{\xi}{J(\xi)^2} d\xi\right)\exp\left(-\frac{x(z)^2}{2\tau} + \varepsilon^2\kappa\tau\right)}{\sqrt{2\pi\tau}} \quad . \tag{121}$$

It is important to note that $P\left(\tau, z, \sigma_i, \sigma_j\right)$ has the correct symmetries under the transformation $i \to j$ and $z \to -z$. This transformation corresponds to using $i$ as the numéraire currency instead of $j$. In $(121)$ $a_3$ only occurs in via the expression $a_1\sigma + 2a_3$ which is given by

$$a_1\sigma_{ij} + 2a_3 = \frac{1}{\sigma_{ij}^2}\left[\left(\sigma_i\upsilon_i\left(\tilde\rho_{ii}\sigma_i + \tilde\rho_{ij}\sigma_j\right)\left(\sigma_i - \rho_{ij}\sigma_j\right) + \sigma_j\upsilon_j\left(\tilde\rho_{jj}\sigma_j + \tilde\rho_{ji}\sigma_i\right)\left(\sigma_j - \rho_{ij}\sigma_i\right)\right)\right] \quad , \tag{122}$$

so under the transformation $i \to j$ and $z \to -z$ the various quantities transform as

$$\begin{aligned} a_1 &\to -a_1 \\ a_2 &\to a_2 \\ a_1\sigma_{ij} + 2a_3 &\to a_1\sigma_{ij} + 2a_3 \\ a_4 &\to a_4 \\ a_5 &\to a_5 \\ J\left(z, \sigma_i, \sigma_j\right) &\to J\left(-z, \sigma_j, \sigma_i\right) \\ x\left(z\right) &\to -x\left(-z\right) \end{aligned}$$

with the result that

$$P\left(\tau, z, \sigma_i, \sigma_j\right) = P\left(\tau, -z, \sigma_j, \sigma_i\right)\frac{X_{ij}^F}{K} \quad . \tag{123}$$

This guarantees the same physical option prices for options between currency $i$ and currency $j$, independent of whether currency $i$ or currency $j$ is chosen as numéraire.

To prove $(11)$, the last steps are to use $(121)$ with $n = 2$ to derive an expression for the Black volatility. Substituting $(121)$ into $(64)$ and using

$$\int_0^z \frac{\xi}{J\left(\xi\right)^2} = \frac{1}{2}z^2 + O\left(\varepsilon\right) \tag{124}$$

shows that the option price is given by

$$\begin{aligned} V\left(\tau, X_{ij}^F, \sigma_i, \sigma_j; K\right) &= \left[X_{ij}^F - K\right]^+ \\ &+ \frac{1}{2}\varepsilon\sigma_{ij} K\sqrt{J\left(z\right)}\exp\left(\frac{1}{2}\varepsilon\sigma_{ij} z + \frac{1}{4}\varepsilon^2\left(a_1\sigma_{ij} + 2a_3 + 2a_4 - a_5\right)z^2\right)\int_0^{\tau_{ex}} d\tau \frac{\exp\left(-\frac{x(z)^2}{2\tau} + \varepsilon^2\kappa\tau\right)}{\sqrt{2\pi\tau}} \quad . \end{aligned} \tag{125}$$

To make sense of this, first use

$$\frac{X_{ij}^F - K}{\sqrt{X_{ij}^F K}} = e^{\frac{1}{2}\ln\left(\frac{X_{ij}^F}{K}\right)} - e^{-\frac{1}{2}\ln\left(\frac{X_{ij}^F}{K}\right)} = \ln\left(\frac{X_{ij}^F}{K}\right) + \frac{1}{24}\ln^3\left(\frac{X_{ij}^F}{K}\right) + \cdots \tag{126}$$

to show that

$$\ln\left(\frac{\varepsilon\sigma_{ij} z\sqrt{X_{ij}^F K}}{X_{ij}^F - K}\right) = -\frac{1}{24}\varepsilon^2\sigma_{ij}^2 z^2 + \cdots \quad . \tag{127}$$

Then using $(97)$, note that up to and including $O\left(\varepsilon^2\right)$ $(87)$ and $(88)$ are

$$J\left(z,\sigma_i,\sigma_j\right) = 1 - \varepsilon a_1 z + \frac{1}{2}\varepsilon^2\left(a_2 + a_5 - a_1^2\right)z^2 + O\left(\varepsilon^3\right) \tag{128}$$

$$x\left(z,\sigma_i,\sigma_j\right) = z + \frac{1}{2}\varepsilon a_1 z^2 - \frac{1}{6}\varepsilon^2\left(a_2 + a_5 - 3a_1^2\right)z^3 + O\left(\varepsilon^3\right) \quad . \tag{129}$$

It is then straightforward to show that

$$\ln\left(\frac{x\sqrt{J\left(z,\sigma_i,\sigma_j\right)}}{z}\right) = \varepsilon^2\left(\frac{2\left(a_2+a_5\right) - 3a_1^2}{24}\right)z^2 \quad . \tag{130}$$

Then, quite amazingly, $(127)$ and $(130)$ together with $(12)$ and $(120)$ show that

$$\begin{aligned} &\varepsilon\sigma_{ij}K\sqrt{J\left(z\right)}\exp\left(\frac{1}{2}\varepsilon\sigma_{ij}z + \frac{1}{4}\varepsilon^2\left(a_1\sigma_{ij} + 2a_3 + 2a_4 - a_5\right)z^2\right) \\ &= \frac{X_{ij}^F - K}{x}\exp\left(\frac{\varepsilon^2}{24}\left(-\sigma_{ij}^2 + 2\left(a_2+a_5\right) - 3a_1^2\right)z^2 + \frac{\varepsilon^2}{4}\left(a_1\sigma_{ij} + 2a_3 + 2a_4 - a_5\right)z^2\right) \\ &= \frac{X_{ij}^F - K}{x}\exp\left(\frac{1}{3}\varepsilon^2\kappa z^2\right) \quad . \end{aligned} \tag{131}$$

At $O\left(\varepsilon^2\right)$, $z^2$ in $(131)$ can be replaced by $x^2$, so using

$$\exp\left(\varepsilon^2\kappa\tau\right) = \frac{1}{\left(1 - \frac{2}{3}\varepsilon^2\kappa\tau\right)^{3/2}} + O\left(\varepsilon^4\right) \quad , \tag{132}$$

the option price $(125)$ becomes

$$V\left(t, X_{ij}^F, \sigma_i, \sigma_j\right) = \left(X_{ij}^F - K\right)^+ + \frac{1}{2}\frac{X_{ij}^F - K}{x}\int_0^{\tau_{ex}} d\tau \frac{\exp\left(-\frac{x(z)^2}{2\tau} + \frac{1}{3}\varepsilon^2\kappa x^2\right)}{\sqrt{2\pi\tau}\left(1 - \frac{2}{3}\varepsilon^2\kappa\tau\right)^{3/2}} \quad . \tag{133}$$

Now change integration variables to

$$q = \frac{x^2}{2\tau} - \frac{1}{3}\varepsilon^2\kappa x^2 \quad \text{so that} \quad d\tau = -\frac{x^2}{2\left(q + \frac{1}{3}\varepsilon^2\kappa x^2\right)^2}dq \quad .$$

The result is

$$V\left(t, X_{ij}^F, \sigma_i, \sigma_j\right) = \left(X_{ij}^F - K\right)^+ + \frac{X_{ij}^F - K}{4\sqrt{\pi}}\int_{\frac{x^2}{2\tau_{ex}}\left(1 - \frac{2}{3}\varepsilon^2\kappa\tau_{ex}\right)}^{\infty} \frac{\exp\left(-q\right)}{q^{3/2}}dq \quad . \tag{134}$$

In the case where $\upsilon_i = \upsilon_j = 0$ this reduces to the standard log-normal forex option pricing. In that case, volatility is the standard log-normal volatility $\sigma_B$, i.e. one can substitute $\sigma_B$ for $\varepsilon\sigma_{ij}$ wherever it occurs in $\kappa$, in the lower bound of the integral in $(134)$. So with $\upsilon_i = \upsilon_j = 0$, then $a_1 = a_2 = a_3 = a_4 = a_5 = 0$ so $\kappa = -\sigma_B^2/8$ and $x = z = \ln\left(X_{ij}^F/K\right)/\sigma_B$. Hence focusing on the lower bound of the integration, the condition to match the log-normal volatility $\sigma_B$ to the option price in $(134)$ is

$$\left(\frac{\ln\left(X_{ij}^F/K\right)}{\sigma_B}\right)^2\left(1 + \frac{1}{12}\sigma_B^2\tau_{ex}\right) = x^2\left(1 - \frac{2}{3}\varepsilon^2\kappa\tau_{ex}\right) \quad . \tag{135}$$

Then using $(12)$, taking the square root and re-arranging produces the final result shown in $(11)$.

## C.1 : Series solution to equation $(96)$

The equation to solve is

$$\frac{h_0}{J^2} + 2\varepsilon\frac{\left(D_\sigma x\right)}{J} = 1 \quad . \tag{136}$$

Although this is an implicit definition of $J$ because $x$ is an integral which depends on the function $J$, it is possible to solve this equation. From $(83)$,

$$\frac{\partial x}{\partial\sigma_k} = -\int_0^z \frac{d\xi}{J\left(\xi\right)^2}\frac{\partial J\left(\xi\right)}{\partial\sigma_k} \quad , \quad \text{so} \quad D_\sigma x = -\int_0^z \frac{d\xi}{J\left(\xi\right)^2}D_\sigma J\left(\xi\right) \quad . \tag{137}$$

Hence $(136)$ can be written as

$$J=\frac{h_0}{J}-2\varepsilon\int_0^z\frac{d\xi}{J(\xi)^2}D_\sigma J(\xi)\quad, \tag{138}$$

and differentiating with respect to $z$ produces

$$\frac{\partial J}{\partial z}=\frac{1}{J}\frac{\partial h_0}{\partial z}-\frac{h_0}{J^2}\frac{\partial J}{\partial z}-2\varepsilon\frac{D_\sigma J}{J^2}\quad. \tag{139}$$

Then multiplying by $J^3$ and writing the equation in terms of derivatives of $J^2$ results in

$$\frac{1}{2}\left(J^2+h_0\right)\frac{\partial J^2}{\partial z}=J^2\frac{\partial h_0}{\partial z}-\varepsilon D_\sigma J^2\quad. \tag{140}$$

To solve this, substitute $(80)$ into $(140)$. Then the terms in $\varepsilon^0$ match immediately, and for $m\geqslant 1$, matching the terms in $\varepsilon^m$ shows that

$$\frac{1}{2}\sum_{k=0}^{m-1}h_{m-k}\frac{\partial h_k}{\partial z}+h_0\frac{\partial h_m}{\partial z}=h_m\frac{\partial h_0}{\partial z}-D_\sigma h_{m-1}\quad. \tag{141}$$

This can be re-arranged to show that

$$\frac{\partial\left(h_m h_0^{-1/2}\right)}{\partial z}=-h_0^{-3/2}\left(\frac{1}{2}\sum_{k=1}^{m-1}h_{m-k}\frac{\partial h_k}{\partial z}+D_\sigma h_{m-1}\right)\quad, \tag{142}$$

and integrating produces the result

$$h_m(z)=-\sqrt{h_0(z)}\int_0^z\frac{d\xi}{\left(h_0(\xi)\right)^{3/2}}\left(\frac{1}{2}\sum_{k=1}^{m-1}h_{m-k}(\xi)\frac{\partial h_k(\xi)}{\partial z}+D_\sigma h_{m-1}(\xi)\right)\text{ , for }\ m\geqslant 1\quad. \tag{143}$$

In particular, the first two terms are given by

$$h_1(z)=-\sqrt{h_0(z)}\int_0^z\frac{d\xi}{\left(h_0(\xi)\right)^{3/2}}D_\sigma h_0(\xi)\quad, \tag{144}$$

$$h_2(z)=-\sqrt{h_0(z)}\int_0^z\frac{d\xi}{\left(h_0(\xi)\right)^{3/2}}\left(\frac{1}{2}h_1(\xi)\frac{\partial h_1(\xi)}{\partial z}+D_\sigma h_1(\xi)\right)\quad. \tag{145}$$

As an example, to calculate $h_1(z)$ note that

$$\int_0^z\frac{\xi}{\sqrt{\left(1-2\varepsilon a_1\xi+\varepsilon^2 a_2\xi^2\right)^3}}d\xi=\frac{1}{\varepsilon\left(a_2-a_1^2\right)}\left(\frac{\left(\varepsilon a_1 z-1\right)}{\sqrt{1-2\varepsilon a_1 z+\varepsilon^2 a_2 z^2}}+1\right)\quad,\text{ and} \tag{146}$$

$$\int_0^z\frac{\xi^2}{\sqrt{\left(1-2\varepsilon a_1\xi+\varepsilon^2 a_2\xi^2\right)^3}}d\xi=\frac{1}{\varepsilon^2 a_2}\left(\begin{array}{c}\frac{1}{\left(a_2-a_1^2\right)}\left(\frac{\varepsilon\left(2a_1^2-a_2\right)z-a_1}{\sqrt{1-2\varepsilon a_1 z+\varepsilon^2 a_2 z^2}}+a_1\right)\\+\frac{1}{\sqrt{a_2}}\ln\left(\frac{\sqrt{1-2\varepsilon a_1 z+\varepsilon^2 a_2 z^2}-\frac{a_1}{\sqrt{a_2}}+\varepsilon\sqrt{a_2}z}{1-\frac{a_1}{\sqrt{a_2}}}\right)\end{array}\right)\quad. \tag{147}$$

Then

$$\begin{aligned}h_1(z)&=\sqrt{1-2\varepsilon a_1 z+\varepsilon^2 a_2 z^2}\int_0^z\frac{2\varepsilon a_5 z'-\varepsilon^2\left(D_\sigma a_2\right)z'^2}{\sqrt{\left(1-2\varepsilon a_1 z'+\varepsilon^2 a_2 z'^2\right)^3}}dz'\\&=2a_5\frac{1}{\left(a_2-a_1^2\right)}\left(\left(\varepsilon a_1 z-1\right)+\sqrt{h_0}\right)-\frac{\left(D_\sigma a_2\right)}{a_2}\frac{1}{\left(a_2-a_1^2\right)}\left(\varepsilon\left(2a_1^2-a_2\right)z-a_1+a_1\sqrt{h_0}\right)\\&\qquad-\frac{\left(D_\sigma a_2\right)\sqrt{h_0}}{a_2\sqrt{a_2}}\ln\left(\frac{\sqrt{h_0}-\frac{a_1}{\sqrt{a_2}}+\varepsilon\sqrt{a_2}z}{1-\frac{a_1}{\sqrt{a_2}}}\right)\quad,\end{aligned} \tag{148}$$

and using $(93)$-$(95)$ it is straightforward to show that

$$\begin{aligned}D_\sigma a_2=-4a_2a_1+\frac{2}{\sigma_{ij}^2}&\left(\upsilon_i^2\sigma_i^2\zeta_i\left(\frac{\partial\sigma_{ij}}{\partial\sigma_i}\right)^2+r_{ij}\upsilon_i\upsilon_j\left(\zeta_i-\zeta_j\right)\sigma_i\sigma_j\frac{\partial\sigma_{ij}}{\partial\sigma_i}\frac{\partial\sigma_{ij}}{\partial\sigma_j}-\upsilon_j^2\sigma_j^2\zeta_j\left(\frac{\partial\sigma_{ij}}{\partial\sigma_j}\right)^2\right.\\&+\upsilon_i^2\sigma_i^2\left(\frac{\sigma_i\zeta_i+\rho_{ij}\sigma_j\zeta_j}{\sigma_{ij}}\right)\frac{\partial\sigma_{ij}}{\partial\sigma_i}+r_{ij}\upsilon_i\upsilon_j\sigma_i\sigma_j\left(\frac{\sigma_i\zeta_i+\rho_{ij}\sigma_j\zeta_j}{\sigma_{ij}}\right)\frac{\partial\sigma_{ij}}{\partial\sigma_j}\\&\left.-r_{ij}\upsilon_i\upsilon_j\sigma_i\sigma_j\frac{\partial\sigma_{ij}}{\partial\sigma_i}\left(\frac{\sigma_j\zeta_j+\rho_{ij}\sigma_i\zeta_i}{\sigma_{ij}}\right)-\upsilon_j^2\sigma_j^2\left(\frac{\sigma_j\zeta_j+\rho_{ij}\sigma_i\zeta_i}{\sigma_{ij}}\right)\frac{\partial\sigma_{ij}}{\partial\sigma_j}\right)\end{aligned} \tag{149}$$

Note that to leading order $D_\sigma h_0(\xi) = -2\varepsilon a_5 \xi + O(\varepsilon^2)$, which is consistent with $(97)$. Also note that $(143)$ shows that for $m \geqslant 1$ the terms $h_m$ are $O(\varepsilon)$, as originally required in $(82)$.

As discussed above, for the approximations $(14)$ and $(13)$ to be well defined, $a_2 + a_5 > a_1^2$ is required, however it is possible to find situations where $a_2 + a_5 < a_1^2$. Simulation of random correlation matrices for $(8)$ suggests that this only tends to occur when $\rho_{ij}$ gets close to $1$. One possible solution to this problem is to use the methodology of this section to calculate higher orders of the approximation for $J$, because intuitively it seems plausible that when higher orders are taking into account then $J^2$ will always be positive.

To test the effect of using higher order approximations, the results of section 5.1 were re-calculated using $J(z, \sigma_i, \sigma_j) = \sqrt{h_0 + \varepsilon h_1}$ where $h_1$ was defined by $(148)$ instead of $(97)$. Gaussian quadrature was used to calculate the integral in $(83)$. However, for the market data used in section 5.1 the difference turned out to be negligible, i.e. typically less less than 0.01% in the calibration errors shown in table 5.

# D : Fitting the model to market data

This appendix describes how snapshots of forex option market data were fitted to the stochastic intrinsic volatility model to produce the results discussed in section 5 above. The market data consists of at-the-money volatilities, risk reversals and market strangles, for multiple currency pairs and multiple tenors. The basic idea is to use conjugate gradient techniques to force the square of the errors to a minimum.

This appendix is organised as follows. Sub-section D.1 introduces a trick which can be useful for making the calibration faster. Sub-section D.2 defines smooth versions of the maximum and minimum functions, which are needed in connection with defining the function of market data to be minimised. Finally, sub-section D.3 describes how all the fits were done, including full details of the function that was minimised.

## D.1 At-the-money volatilities, and the connection with the single variable SABR approximation formula

As discussed in [2], a slightly improved single variable SABR approximation formula can be derived by avoiding approximations in the final stages of the calculation. Instead of $(5)$, the formula is

$$\sigma_B = \varepsilon\sigma\left(\frac{z}{\tilde{x}(z)}\right)\frac{1}{\sqrt{1 - \frac{\varepsilon^2}{12}\left(\left[6\rho\sigma\upsilon - \sigma^2 + \left(2 - 3\rho^2\right)\upsilon^2\right] + \sigma^2\left(\frac{z}{\tilde{x}(z)}\right)^2\right)\tau_{ex}}} \quad . \tag{150}$$

Using $(22)$ and $(23)$, it is straightforward to show that $(150)$ reduces to $(5)$.

For at-the-money options $z = x(z) = \tilde{x}(z) = 1$, so denoting the market at-the-money volatility by $\sigma_B^{ATM}$, for this case $(11)$ reduces to

$$\sigma_B^{ATM} = \varepsilon\sigma_{ij}\frac{1}{\sqrt{1 - \frac{2\varepsilon^2}{3}\left(\kappa_1 + \frac{1}{8}\sigma_{ij}^2\right)\tau_{ex}}} \quad , \tag{151}$$

and $(150)$ reduces to

$$\sigma_B^{ATM} = \varepsilon\sigma\frac{1}{\sqrt{1 - \frac{\varepsilon^2}{12}\left(6\rho\sigma\upsilon + \left(2 - 3\rho^2\right)\upsilon^2\right)\tau_{ex}}} \quad . \tag{152}$$

Then using $(151)$ in $(11)$ and $(152)$ in $(150)$, the implied volatility approximation formulas can be written in terms of $\sigma_B^{ATM}$, producing

$$\sigma_B = \sigma_B^{ATM}\frac{z}{x(z)}\frac{1}{\sqrt{1 + \frac{\left(\sigma_B^{ATM}\right)^2}{12}\left(1 - \left(\frac{z}{x(z)}\right)^2\right)\tau_{ex}}} \quad \text{instead of } (11) \quad , \tag{153}$$

$$\text{and} \quad \sigma_B = \sigma_B^{ATM}\frac{z}{\tilde{x}(z)}\frac{1}{\sqrt{1 + \frac{\left(\sigma_B^{ATM}\right)^2}{12}\left(1 - \left(\frac{z}{\tilde{x}(z)}\right)^2\right)\tau_{ex}}} \quad \text{instead of } (150) \quad . \tag{154}$$

Thus if both $(11)$ and $(150)$ are calibrated to produce the same at-the-money volatility $\sigma_B^{ATM}$, then the two formulas will produce the same implied volatility curves for all strikes if $x(z) = \tilde{x}(z)$. The conditions for $x(z) = \tilde{x}(z)$ are

$$a_1 = \upsilon\rho \quad , \quad \text{and} \quad a_2 + a_5 = \upsilon^2 \quad . \tag{155}$$

This result is useful when calibrating $(11)$ to market data. Each currency pair can first be calibrated to the single variable formula $(150)$ to determine $\rho$ and $\upsilon$, and then the task is to fit $(151)$ and $(155)$. This can be an efficient way of organising the calibration to market data, because using $(11)$ to calculate the risk reversals and market strangles involves quite intensive calculations, so taking this route those calculations can be by-passed.

## D.2 Smooth functions for $\max(x, y)$ and $\min(x, y)$

As discussed in the introduction to this appendix, the main idea for fitting the model to the market data is to use conjugate gradient techniques to force the square of the errors to a minimum. However, as will be described in the following sub-section, additional terms are included in the function which is being minimised which try to ensure that the fit has various desirable characteristics. A crude definition of these additional terms would involve maximum and minimum functions, however although $\max(x, y)$ and $\min(x, y)$ are continuous functions of $x$ and $y$, their derivatives are discontinuous and that leads to problems given that conjugate gradient techniques are being used. The solution to this problem is to use functions which will be denoted by $\psi_{\max}(x, y; \sigma)$ and $\psi_{\min}(x, y; \sigma)$[5], where

$$\psi_{\max}(x, y; \sigma) = xN\left(\frac{x-y}{\sigma}\right) + yN\left(\frac{y-x}{\sigma}\right) + \frac{\sigma}{\sqrt{2\pi}}\exp\left(-\frac{1}{2}\left(\frac{x-y}{\sigma}\right)^2\right) \quad , \text{ and} \tag{156}$$

$$\psi_{\min}(x, y; \sigma) = xN\left(\frac{y-x}{\sigma}\right) + yN\left(\frac{x-y}{\sigma}\right) - \frac{\sigma}{\sqrt{2\pi}}\exp\left(-\frac{1}{2}\left(\frac{x-y}{\sigma}\right)^2\right) \quad , \tag{157}$$

where $N(x)$ is the cumulative univariate normal distribution function. These functions are continuous versions of $\max(x, y)$ and $\min(x, y)$, because in the limit that $\sigma \to 0$,

$$\lim_{\sigma\to 0} \psi_{\max}(x, y; \sigma) = \max(x, y) \quad , \text{ and} \tag{158}$$

$$\lim_{\sigma\to 0} \psi_{\min}(x, y; \sigma) = \min(x, y) \quad . \tag{159}$$

The parameter $\sigma$ sets the scale that determines how quickly $\psi_{\max}(x, y; \sigma)$ and $\psi_{\min}(x, y; \sigma)$ switch between $x$ and $y$ as $x$ and $y$ vary. In terms of their derivatives, they have the useful properties

$$\frac{\partial\psi_{\max}}{\partial x} = N\left(\frac{x-y}{\sigma}\right) \quad , \quad \frac{\partial\psi_{\max}}{\partial y} = N\left(\frac{y-x}{\sigma}\right) \quad , \tag{160}$$

$$\frac{\partial\psi_{\min}}{\partial x} = N\left(\frac{y-x}{\sigma}\right) \quad , \quad \frac{\partial\psi_{\min}}{\partial y} = N\left(\frac{x-y}{\sigma}\right) \quad . \tag{161}$$

## D.3 Procedure for fitting market data to the stochastic intrinsic currency volatility model

The heart of the methodology for fitting market data to the parameters $\sigma_i$, $\upsilon_i$, $\rho_{ij}$, $r_{ij}$ and $\tilde{\rho}_{ij}$ is to minimise the difference between the model values and the market values for all the available market data points, subject to certain additional conditions which will now be described.

To be specific, and adopting notation similar to the notation used in [3, 5], the idea is to determine the parameters by minimising the function $F$ defined by

$$F(\sigma_i, \upsilon_i, \rho_{ij}, \tilde{\rho}_{ij}, r_{ij}) = Z_1(\sigma_i, \upsilon_i, \rho_{ij}, \tilde{\rho}_{ij}, r_{ij}) + Z_2(\rho_{ij}, \tilde{\rho}_{ij}, r_{ij}) + Z_3(\sigma_i, \upsilon_i, \rho_{ij}, \tilde{\rho}_{ij}, r_{ij}) \quad , \tag{162}$$

where $Z_1$ is the $\chi^2$ statistic for the model, $Z_2$ is the maximum entropy term, and $Z_3$ is designed to encourage various desirable characteristics. Given $F$, the minimisation was done using a Polak-Ribière conjugate gradient methodology, where the derivatives of $F$ were calculated analytically for maximum speed.

[5] The functions $\psi_{\max}(x, y; \sigma)$ and $\psi_{\min}(x, y; \sigma)$ are inspired by option pricing where the underlying variables are normally distributed.

To help the numerical algorithms find plausible values of the volatility parameters $\sigma_i^T$, the $\sigma_i^T$ were calculated from parameters $x_i^T$ via the function

$$\sigma_i^T\left(x_i^T\right) = \frac{\sigma_{\max}}{1+e^{-x_i^T}} \tag{163}$$

where $\sigma_{\max} = 80\%$, because this enforces the condition $0 < \sigma_i^T < \sigma_{\max}$ which makes the fitting procedure more stable. Similarly the volatility of volatility parameters $\upsilon^T$ were calculated from parameters $y^T$ via the function

$$\upsilon^T\left(y^T\right) = \frac{\upsilon_{\max}}{1+e^{-y^T}} \quad , \tag{164}$$

where $\upsilon_{\max} = 500\%$. Additionally, the correlation matrix $(8)$ has to be positive definite, so this was enforced by parameterising the Cholesky decomposition of the correlation matrix.

To complete the definition of the methodology, full details of the three terms $Z_1$, $Z_2$ and $Z_3$ are given below.

### D.3.1 Definition of $Z_1$: the $\chi^2$ statistic

In the context of fitting market data to a model, a $\chi^2$ statistic is defined by

$$\chi^2 = \sum_{\text{data points}} \left[\frac{(\text{market-value}) - (\text{model-value})}{\Delta\left[(\text{market-value}) - (\text{model-value})\right]}\right]^2 \tag{165}$$

where $\Delta\left[(\text{market-value}) - (\text{model-value})\right]$ means the standard deviation of $(\text{market-value}) - (\text{model-value})$. Hence each error term is normalised by its standard deviation, which corresponds to how accurately each data point is known.

If the trick described in section D.1 is being used, then for each currency pair $ij$ and tenor $T$ there are three market data points, namely the at-the-money volatility $\left[\sigma^{ATM}_{\text{Market}}\right]^T_{ij}$, the SABR $\rho$ parameter $\left[\rho_{\text{Market}}\right]^T_{ij}$, and the SABR $\upsilon$ parameter $\left[\upsilon_{\text{Market}}\right]^T_{ij}$. Hence since $Z_1$ is defined to be the $\chi^2$ statistic for the model, it will be the sum of three terms, i.e.

$$Z_1 = \chi^2_{ATM} + \chi^2_\rho + \chi^2_\upsilon \quad , \tag{166}$$

where $\chi^2_{ATM}$ is the $\chi^2$ statistic composed of the terms involving $\left[\sigma^{ATM}_{\text{Market}}\right]^T_{ij}$, $\chi^2_\rho$ is the $\chi^2$ statistic composed of the terms involving $\left[\rho_{\text{Market}}\right]^T_{ij}$, and where $\chi^2_\upsilon$ is the $\chi^2$ statistic composed of the terms involving $\left[\upsilon_{\text{Market}}\right]^T_{ij}$. Alternatively, $Z_1$ can be defined directly as

$$Z_1 = \chi^2_{ATM} + \chi^2_{RR} + \chi^2_{MS} \quad , \tag{167}$$

where $\chi^2_{RR}$ is the $\chi^2$ statistic composed of the terms involving the risk reversal data points which will be written $\left[RR_{\text{Market}}\right]^T_{ij}$, and where $\chi^2_{MS}$ is the $\chi^2$ statistic composed of the terms involving the market strangle data points which will be written $\left[MS_{\text{Market}}\right]^T_{ij}$.

The term $\chi^2_{ATM}$ is straightforward to define. As in the previous work [3, 5], define the standard deviation $\left[\Delta_\sigma\right]^T_{ij}$ of $\left[\sigma^{ATM}_{\text{Market}}\right]^T_{ij}$ to be half the bid-offer spread[6]. Then $\chi^2_{ATM}$ is given by

$$\chi^2_{ATM} = \sum_{ij,T}\left(\frac{\left[\varepsilon_\sigma\right]^T_{ij}}{\left[\Delta_\sigma\right]^T_{ij}}\right)^2 \quad , \quad \text{where} \quad \left[\varepsilon_\sigma\right]^T_{ij} = \left[\sigma^{ATM}_{\text{Market}}\right]^T_{ij} - \left[\sigma^{ATM}_B\right]^T_{ij} \quad , \tag{168}$$

and where $\sigma^{ATM}_B$ is defined by $(151)$.

Similarly to define $\chi^2_{RR}$ and $\chi^2_{MS}$, the standard deviations $\left[\Delta_{RR}\right]^T_{ij}$ and $\left[\Delta_{MS}\right]^T_{ij}$ of the risk reversals and market strangles need to be determined. Risk reversals and market strangles are structures which involve vega netting. In that situation the individual options in the structure are organised into two groups, those with positive vega and those with negative vega, and then the group of options with the lowest absolute value of vega are

[6] Note that when fitting the model to historical market data, the bid-offer spread needs to be calculated dynamically, because it changes as market conditions change. As discussed in [5], a good assumption is that the bid-offer spread of a volatility should be proportional to the volatility itself. This was used in doing all the historical fits to market data in section 5.

traded at mid-market. Hence the bid-offer for a risk reversal is determined by the 25-delta option with the highest absolute value of vega, and in price terms the bid-offer for a market strangle is the same as the corresponding at-the-money options. These bid-offers specifications must be translated into bid-offers for the numbers that are traded in the market, i.e. the risk-reversal and market strangle quotes. Then $[\Delta_{RR}]_{ij}^T$ and $[\Delta_{MS}]_{ij}^T$ are defined to be half the bid-offer spreads in the risk-reversal and market strangle quotes, so that $\chi_{RR}^2$ and $\chi_{MS}^2$ are given by

$$\chi_{RR}^2 = \sum_{ij,T} \left( \frac{[\varepsilon_{RR}]_{ij}^T}{[\Delta_{RR}]_{ij}^T} \right)^2 \quad , \text{ where } \quad [\varepsilon_{RR}]_{ij}^T = [RR_{\text{Market}}]_{ij}^T - [RR_{\text{Model}}]_{ij}^T \quad , \tag{169}$$

$$\chi_{MS}^2 = \sum_{ij,T} \left( \frac{[\varepsilon_{MS}]_{ij}^T}{[\Delta_{MS}]_{ij}^T} \right)^2 \quad , \text{ where } \quad [\varepsilon_{MS}]_{ij}^T = [MS_{\text{Market}}]_{ij}^T - [MS_{\text{Model}}]_{ij}^T \quad , \tag{170}$$

where $[RR_{\text{Model}}]_{ij}^T$ and $[MS_{\text{Model}}]_{ij}^T$ are the model values for the risk reversals and market strangles.

Lastly to define $\chi_\rho^2$ and $\chi_\upsilon^2$, the standard deviations $[\Delta_\rho]_{ij}^T$ and $[\Delta_\upsilon]_{ij}^T$ of the SABR parameters $[\rho_{\text{Market}}]_{ij}^T$ and $[\upsilon_{\text{Market}}]_{ij}^T$ need to be determined. These are defined as the biggest change in each parameter that produces risk reversal and market strangle prices within their bid-offer values, keeping all other parameters the same. Hence, given $(155)$ and $(165)$, $\chi_\rho^2$ and $\chi_\upsilon^2$ are given by

$$\chi_\rho^2 = \sum_{ij,T} \left( \frac{[\varepsilon_\rho]_{ij}^T}{[\Delta_\rho]_{ij}^T} \right)^2 \quad , \text{ where } \quad [\varepsilon_\rho]_{ij}^T = [\rho_{\text{Market}}]_{ij}^T - \left[ \frac{a_1}{\sqrt{a_2 + a_5}} \right]_{ij}^T \quad , \text{ and} \tag{171}$$

$$\chi_\upsilon^2 = \sum_{ij,T} \left( \frac{[\varepsilon_\upsilon]_{ij}^T}{[\Delta_\upsilon]_{ij}^T} \right)^2 \quad , \text{ where } \quad [\varepsilon_\upsilon]_{ij}^T = [\upsilon_{\text{Market}}]_{ij}^T - \left[ \sqrt{a_2 + a_5} \right]_{ij}^T \quad . \tag{172}$$

In practice, using $(166)$ in the preliminary iterations of the minimisation and $(167)$ in the later iterations to home in on the final answer seems to work best.

#### D.3.2 Definition of $Z_2$: the maximum entropy term

As discussed in section 2 on page 8, the information entropy idea that was used in [5] in connection with the correlation matrix $\boldsymbol{\rho}$ will be used here as well in connection with the correlation matrix $(8)$. Maximising entropy loosely corresponds to minimising the correlations between the variables being modelled, and results in a correlation matrix which contains the least amount of information given the other constraints (see [5] for more details).

Because there are so many parameters to determine, there is a danger that minimising the single function $F$ in $(162)$ will make inappropriate trade-offs between all the different parameters. This is the reason for including the term $Z_3$ which will be defined below. The same is true in connection with information entropy, and here maximising the information entropy in the correlation matrix $\boldsymbol{\rho}$ in the top left hand corner of the full correlation matrix $(8)$ is particularly important, because that corresponds to ensuring that the basic variables $X_i$ correspond to the intrinsic currency values of the corresponding currency. Hence $Z_2$ will consist of two terms, one relating to the information entropy of $\boldsymbol{\rho}$, and the other relating to the information entropy of the full correlation matrix.

The information entropy in a correlation matrix is proportional to the log of the determinant, so given that $F$ in $(162)$ is to be minimised, then information entropy will be maximised by defining $Z_2$ to be

$$Z_2 = -\omega_{\text{TL}} \ln\left(\det\left(\boldsymbol{\rho}\right)\right) - \omega_{\text{FULL}} \ln\left(\det\begin{pmatrix} \boldsymbol{\rho} & \tilde{\boldsymbol{\rho}}' \\ \tilde{\boldsymbol{\rho}} & \mathbf{r} \end{pmatrix}\right) \quad , \tag{173}$$

where $\omega_{\text{TL}}$ and $\omega_{\text{FULL}}$ control the influence that each term has in the minimisation. The results which were discussed in section 5 were calculated using $\omega_{\text{TL}} = 2$ and $\omega_{\text{FULL}} = 80$.

### D.3.3 Definition of $Z_3$: the term which encourages desirable characteristics

As discussed in the previous section, because there are so many parameters to determine, there is a danger that minimising the single function $F$ defined by $Z_1 + Z_2$ in $(162)$ will make inappropriate trade-offs between all the different parameters. The purpose of the $Z_3$ term is to correct the inappropriate trade-offs that were identified as a result of the experience gained in fitting the model to market data without $Z_3$, and hence impose desirable characteristics which were missing. To be explicit, when the trick described in section D.1 is being used, $Z_3$ was defined by

$$Z_3 = \omega_\sigma^{PM} Z_\sigma^{PM} + \omega_\rho^{PM} Z_\rho^{PM} + \omega_\upsilon^{PM} Z_\upsilon^{PM} + \omega_{r>0} Z_{r>0} + \sum_T \omega_\upsilon^T Z_\upsilon^T \quad , \tag{174}$$

and without the trick of section D.1 $Z_3$, was defined by

$$Z_3 = \omega_\sigma^{PM} Z_\sigma^{PM} + \omega_{RR}^{PM} Z_{RR}^{PM} + \omega_{MS}^{PM} Z_{MS}^{PM} + \omega_{r>0} Z_{r>0} + \omega_S Z_S + \sum_T \omega_{MS}^T Z_{MS}^T \quad . \tag{175}$$

Taking the terms in turn, the crude definitions of $Z_\sigma^{PM}$, $Z_\rho^{PM}$, $Z_\upsilon^{PM}$, $Z_{RR}^{PM}$ and $Z_{MS}^{PM}$ would be

$$Z_\sigma^{PM} = \sum_{ij} \left( \min\left[0, \max_T \left( [\varepsilon_\sigma]_{ij}^T \right)\right] - \max\left[0, \min_T \left( [\varepsilon_\sigma]_{ij}^T \right)\right] \right)^2 \quad , \tag{176}$$

$$Z_\rho^{PM} = \sum_{ij} \left( \min\left[0, \max_T \left( [\varepsilon_\rho]_{ij}^T \right)\right] - \max\left[0, \min_T \left( [\varepsilon_\rho]_{ij}^T \right)\right] \right)^2 \quad , \tag{177}$$

$$Z_\upsilon^{PM} = \sum_{ij} \left( \min\left[0, \max_T \left( [\varepsilon_\upsilon]_{ij}^T \right)\right] - \max\left[0, \min_T \left( [\varepsilon_\upsilon]_{ij}^T \right)\right] \right)^2 \quad , \tag{178}$$

$$Z_{RR}^{PM} = \sum_{ij} \left( \min\left[0, \max_T \left( [\varepsilon_{RR}]_{ij}^T \right)\right] - \max\left[0, \min_T \left( [\varepsilon_{RR}]_{ij}^T \right)\right] \right)^2 \quad , \tag{179}$$

$$Z_{MS}^{PM} = \sum_{ij} \left( \min\left[0, \max_T \left( [\varepsilon_{MS}]_{ij}^T \right)\right] - \max\left[0, \min_T \left( [\varepsilon_{MS}]_{ij}^T \right)\right] \right)^2 \quad , \tag{180}$$

The purpose of these terms is to ensure that when looking across the errors for different tenors with each currency pair, some of the errors are positive and other errors are negative. When some errors are positive and some are negative for a particular currency pair $ij$, it suggests that the fit to market data from multiple tenors is doing a reasonable job at matching the market data for that currency pair, so that the tenor independent correlation matrices $\boldsymbol{\rho}$, $\mathbf{r}$ and $\tilde{\boldsymbol{\rho}}$ are indeed suitable average correlations As discussed in section D.2, using conjugate gradient techniques to minimise a function containing $\max(x, y)$ and $\min(x, y)$ functions doesn't work well, because the derivatives aren't smooth. So in practice, the above crude definitions are implemented using $\psi_{\min}$ and $\psi_{\max}$. However, since the $\max$ and $\min$ over the tenor $T$ involve more than two arguments, $\psi_{\max}$ is used instead of $\max_T$ by taking the largest two error terms, and $\psi_{\min}$ is used instead of $\min_T$ by taking the two most negative error terms. Regarding the results which were discussed in section 5, the $\sigma$ parameter in $(156)$ and $(157)$ was set to $0.01\%$ in connection with $Z_\sigma^{PM}$, $Z_{RR}^{PM}$ and $Z_{MS}^{PM}$, and the same parameter was set to $0.01$ in connection with $Z_\rho^{PM}$ and $Z_\upsilon^{PM}$. The weights were $\omega_\sigma^{PM} = 10^9$, $\omega_{RR}^{PM} = 10^6$, $\omega_{MS}^{PM} = 10^7$, $\omega_\rho^{PM} = 10^4$ and $\omega_\upsilon^{PM} = 400$.

The term $Z_{r>0}$ is designed to ensure that all the correlations $r_{ij}$ are positive. This condition is intuitively sensible, and was justified by the time series analysis in section 5.4. Positive $r_{ij}$ are usually found anyway without the $Z_{r>0}$ term, but sometimes the minimisation scheme can produce negative values of $r_{ij}$ which is inappropriate, so the $Z_{r>0}$ term discourages that. The definition is

$$Z_{r>0} = \sum_{ij} \left( \psi_{\min}\left(r_{ij}, 0; \sigma_{r>0}\right) \right)^2 \tag{181}$$

The results which were discussed in section 5 were calculated using $\omega_{r>0} = 200$ and $\sigma_{r>0} = 0.004$.

The term $Z_S$ encourages the $\sigma_i^T$ to have a similar volatility slope $\sigma_i^{1Y} - \sigma_i^{1M}$ as the slopes seen in the at-the-money volatilities for currency pairs. Typically the slope of the intrinsic currency volatilities naturally correspond to the slope of the at-the-money currency pair volatilities without using this term, but in some circumstances when the market is under stress, the fitting procedure can produce unintuitive results which don't follow that rule. This term helps correct that. The term $Z_S$ is defined by

$$Z_S = \sum_i \left(\psi_{\max}\left(S_i - 0.75\%, 0; 0.075\%\right) - \psi_{\min}\left(S_i + 0.75\%, 0; 0.075\%\right)\right)^2 \quad \text{, where} \tag{182}$$

$$S_i = \sigma_i^{1Y} - \sigma_i^{1M} - \frac{1}{n_{j\neq i}} \sum_{j\neq i} \left(\sigma_{ij}^{1Y} - \sigma_{ij}^{1M}\right) \quad , \tag{183}$$

where $\sigma_{ij}^{1M}$ and $\sigma_{ij}^{1Y}$ are the at-the-money 1M and 1Y currency pair volatilities between currencies $i$ and $j$, and where $n_{j\neq i}$ are the number of currency pairs $ij$ for a given currency $i$. The use of $\psi_{\min}$ and $\psi_{\max}$ means that the $Z_S$ term has little effect when $-0.75\% < S_i < 0.75\%$. The results which were discussed in section 5 were calculated using $\omega_S = 10^4$.

Lastly, the terms $Z_\upsilon^T$ and $Z_{MS}^T$were introduced because there was often structure in the corresponding error terms $[\varepsilon_\upsilon]_{ij}^T$ and $[\varepsilon_{MS}]_{ij}^T$, whereby most 1M terms would have one sign, and most 1Y terms would have the other sign. Ideally there should be no structure, but worse than that, when processing the historical data the solution would sometimes jump from one state to the other and with corresponding jumps in the $\upsilon^T$. These terms solve that problem, and are defined by

$$Z_\upsilon^T = \left(\sum_{ij} \left([\varepsilon_\upsilon]_{ij}^T\right)\right)^2 \quad , \tag{184}$$

$$Z_{MS}^T = \left(\sum_{ij} \left([\varepsilon_{MS}]_{ij}^T\right)\right)^2 \quad . \tag{185}$$

The results which were discussed in section 5 were calculated using $\omega_\upsilon^T = 25$, $\omega_{RR}^T = 2 \times 10^5$ and $\omega_{MS}^T = 4 \times 10^4$ for all $T$.

# References


[1] P. S. Hagan, D. Kumar, A. S. Lesniewski, and D. E. Woodward, "Managing smile risk", *Wilmott Magazine*, pages 84–108, July 2002.

[2] Paul Doust, "Modelling option volatility: An improved SABR model", *RBS research article*, 14th August 2009.

[3] Paul Doust, "The intrinsic currency valuation framework", *RISK magazine*, March 2007.

[4] Jian Chen and Paul Doust, "Estimating Intrinsic Currency Values", *RISK magazine*, July 2008.

[5] Jian Chen and Paul Doust, "Improving intrinsic currency analysis: using information entropy and beyond", *RBS research article*, 12th November 2009.

[6] Fischer Black, Myron Scholes, "The pricing of options and corporate liabilities", *Journal of political economy*, 1973.

[7] Fischer Black, "The pricing of commodity contracts", *Journal of Financial Economics*, 1976.

[8] Paul Doust, "Relative pricing techniques in the swaps and options markets", The Journal of financial engineering, Vol 4 No 1, March 1995, pp 11-46.

The Royal Bank of Scotland